UC Berkeley
Research Reports

Title

Longitudinal Control Development For IVHS Fully Automated And Semi-automated Systems: Phase II

Permalink

https://escholarship.org/uc/item/4k559099

Authors

Hedrick, J. K.
Garg, V.
Gerdes, J. C.
et al.

Publication Date

1996

eScholarship.org Powered by the California Digital Library
University of California

This paper has been mechanically scanned. Some errors may have been inadvertently introduced.

CALIFORNIA PATH PROGRAM
INSTITUTE OF TRANSPORTATION STUDIES
UNIVERSITY OF CALIFORNIA, BERKELEY

Longitudinal Control Development for IVHS Fully Automated and Semi-Automated Systems: Phase II

J.K. Hedrick, V. Garg, J.C. Gerdes,

D.B. Maciuca, D. Swaroop

California PATH Research Report
UCB-ITS-PRR-96-1

This work was performed as part of the California PATH Program of the University of California, in cooperation with the State of California Business, Transportation, and Housing Agency, Department of Transportation; and the United States Department of Transportation, Federal Highway Administration.

The contents of this report reflect the views of the authors who are responsible for the facts and the accuracy of the data presented herein. The contents do not necessarily reflect the official views or policies of the State of California. This report does not constitute a standard, specification, or regulation.

January 1996

ISSN 1055-1425

LONGITUDINAL CONTROL DEVELOPMENT

FOR IVHS FULLY AUTOMATED AND SEMI-AUTOMATED SYSTEMS PHASE II

FINAL REPORT - JANUARY 31, 1995

Submitted to : PATH (MOU 101)

J. K. Hedrick, P. I
V. Garg
J. C. Gerdes
D. B. Maciuca
D. Swaroop

Department of Mechanical Engineering,
University of California, Berkeley

Acknowledgements

The authors would like to thank Mr. Peter Develin for his help with the hardware development, Dr.Sei-hum Choi and Mr. Leon Chen for their help with the real-time vehicle control code. The authors acknowledge PATH engineers, Mr. Scott Baysinger and Mr. Erik Johnson, Cal Trans Engineers Mr. Randy Woolley and Mr. Bob Battersby, for their help in organizing and conducting the four vehicle experiments at the California Highway Patrol Academy in Sacramento.

Abstract

This report is concerned with performance issues in Automated Vehicle Control Systems (AVCS). Specifically, this report addresses the braking controller design issues, effects of braking on IVHS Lane capacity, performance of platoons with various information structures, fault detection filter design for AVCS.

This report deals with the issues of Automatic Brake Controller Design. Simulation Results show good speed tracking between two vehicles. Although controlling the retrofitted brake system in AVCS Longitudinal Control is feasible, the ride quality is not upto the mark.

The effect of braking on the capacity of the IVHS Lane is also discussed. Vehicle Model considered for analysis includes engine dynamics, brake, aerodynamic drag, rolling resistance, brake dynamics, ABS and tire road interaction. Emergency braking maneuvers are considered with such a vehicle model, since it reveals the basic limitations of deployable IVHS system.

Experimental testing of a pedal actuation system (incorporating vacuum booster) revealed deterioration in passenger comfort. Unfortunately, owing to the complexity of the dynamic model and the controller, the exact cause of the deterioration is not clear. Question then arises whether pedal actuation presents a feasible solution for platooning and, if not, what requirements a suitable actuation system should possess. Addressing this, however, requires some notion of the desired characteristics of the brake system and the interactions between hardware choice and platform performance. This report offers a control perspective on the issue of brake performance. Taking the sliding controller framework, we highlight the critical areas in which the brake system dynamics affect platoon performance. Since maneuvers, tracking accuracy and comfort required by an automated highway are not firmly defined, we adopt a limiting approach. The analysis in this chapter, therefore, may be viewed as specifying the performance of a brake system capable of attaining tracking and robustness properties demonstrated by a multiple surface controller in simulation.

String stability performance is defined for a platoon and characterised in terms of guaranteed spacing error attenuation from vehicle to vehicle. In this chapter, various spacing strategies are considered and their limitations/advantages in terms of guaranteed spacing error attenuation is analyzed.

The effects of sensor and actuator faults on system performance are also discuseed. Analysis of these effects is done by approximate feedback linearized transfer function relationships between the fault error term and the resulting error in tracking. Redundancy relations among longitudinal sensors are identified and exploited for fault detection purposes. A feedback linearizing filter is designed to detect actuator faults and results of experimental verification of the filter are also presented. Variable Threshold Algorithm is applied to ensure a fixed false alarm rate and minimum detection delay in detection of signal changes. This algorithm is applied to residuals obtained from redundancy relations between speed sensors and the radar closing rate. Finally, detection filters are applied to the longitudinal platooning problem.

Key words: IVHS, AHS, AVCS, Longitudinal Control, Brake control, String/Platoon Stability, Fault Detection, Isolation and Tolerance.

Executive Summary

In this report, a nonlinear brake controller was developed. The controller takes advantage of the operating mode of the vacuum booster present in the brake system. The controller is robust to modeling errors and input disturbances. However, it was theoretically shown and experimentally confirmed that there is a significant trade-off between tracking and passenger comfort.

Necessity of lead vehicle information is theoretically demonstrated in this report. The tradeoffs associated with different platoon schemes utilizing different communicated information are characterized in terms of string stability performance parameter and robustness to actuator lags.

The emphasis of the fault management work in this report is towards design of a fault tolerant control system architecture for the automated highway systems problem. The contribution of this work is mostly in the area of fault detection. Specifically, actuator fault detection was achieved by a feedback linearizing filter. Detection filter theory was extended to the class of nonlinear systems in which nonlinearities are Lipschitz bounded. It was shown that directionality properties of the detection filters in linear systems can be ensured even in the presence of Lipschitz nonlinearities in the early stages of detection as well as stability of the nonlinear observer can be guaranteed. Detection filters were designed for the longitudinal vehicle model for detecting actuator faults using a modified observer scheme.

A computationally efficient detection logic algorithm was developed. Salient features of this algorithm are on-line threshold determination ensuring a fixed false alarm rate and minimizing detection delay. This algorithm was implemented on residuals obtained from sensor redundancy relations. It can be applied to detection filter residuals also.

Observer design was extended to systems with no linear part. One of the advantages of the scheme used is that it is a fully nonlinear observer, i.e. no linear approximations are done. It can be used even when the Taylor expansion of the nonlinearities does not have a linear part. The observer gains used by this method can be high.

Feasibility of redundancy based and observer based state reconstruction techniques in event of sensor faults was demonstrated. Nonlinear observers were employed to estimate states in absence of the entire state information and were used as back up states in the system in case of sensor failures.

Contents

List of Figures

Chapter 1

Introduction

This report is concerned with performance issues in Automated Vehicle Control Systems (AVCS). Specifically, this report addresses the braking controller design issues, effects of braking on IVHS Lane capacity, performance of platoons with various information structures, fault detection filter design for AVCS.

Chapter 1 of this report deals with the issues of Automatic Brake Controller Design. Simulation Results show good speed tracking between two vehicles. Although controlling the retrofitted brake system in AVCS Longitudinal Control is feasible, the ride quality is not upto the mark.

Chapter 2 discusses the effect of braking on the capacity of the IVHS Lane. Vehicle Model considered for analysis includes engine dynamics, brake, aerodynamic drag, rolling resistance, brake dynamics, ABS and tire road interaction. Emergency braking maneuvers are considered with such a vehicle model, since it reveals the basic limitations of deployable IVHS system.

Experimental testing of a pedal actuation system (incorporating vacuum booster) revealed deterioration in passenger comfort. Unfortunately, owing to the complexity of the dynamic model and the controller, the exact cause of the deterioration is not clear. Question then arises whether pedal actuation presents a feasible solution for platooning and, if not, what requirements a suitable actuation system should possess. Addressing this, however, requires some notion of the desired characteristics of the brake system and the interactions between hardware choice and platform performance. Chapter 3 offers a control perspective on the issue of brake performance. Taking the sliding controller framework, we highlight the critical areas in which the

brake system dynamics affect platoon performance. Since maneuvers, tracking accuracy and comfort required by an automated highway are not firmly defined, we adopt a limiting approach. The analysis in this chapter, therefore, may be viewed as specifying the performance of a brake system capable of attaining tracking and robustness properties demonstrated by a multiple surface controller in simulation.

In Chapter 4, string stability performance is defined for a platoon and characterised in terms of guaranteed spacing error attenuation from vehicle to vehicle. In this chapter, various spacing strategies are considered and their limitations/advantages in terms of guaranteed spacing error attenuation is analyzed.

Chapter 5 discusses the effects of sensor and actuator faults on system performance. Analysis of these effects is done by approximate feedback linearized transfer function relationships between the fault error term and the resulting error in tracking. Redundancy relations among longitudinal sensors are identified and exploited for fault detection purposes. A feedback linearizing filter is designed to detect actuator faults and results of experimental verification of the filter are also presented. Variable Threshold Algorithm is applied to ensure a fixed false alarm rate and minimum detection delay in detection of signal changes. This algorithm is applied to residuals obtained from redundancy relations between speed sensors and the radar closing rate. Finally, detection filters are applied to the longitudinal platooning problem.

Chapter 6 summarizes the results of this report.

Chapter 2

Automatic Braking Control for IVHS

2.1 Introduction

The concept of IVHS and automatic brake control are not new. These topics have seen a lot of research in the 60's and 70's. Unfortunately, most of the early attempts have fallen short of the desired goal to automatically control the brakes smoothly and safely in an AHS environment. However, due to a need to increase capacity, reduce pollution and improve safety on the major highways, the topics have seen renewed interest in the recent years.

Partners for Advanced Transit and Highways (PATH) and CalTrans have supported IVHS research since 1988. This particular study emphasizes the development of an automatic brake controller for IVHS. The controller was developed for a Lincoln Town Car retrofitted for IVHS use, but it can be easily modified for other cars. Although retrofitting provides an easy, reliable and liability-free way to actuate the brakes, it also make the job of controlling them more difficult.

Recent analysis of the brake system shows that it contains a series of non-linearities. First, the vacuum booster, which is an integral part of the brake system, contains deadzones, spring preloads, and nonlinear fluid flow dynamics. Second, the dynamics of vacuum booster are dependent on the engine manifold dynamics which are nonlinear. The third source of nonlinearities is the actuation system. Composed of a solenoid valve and a hydraulic piston,

this actuation system has a high order dynamic response.

Due to these nonlinearities, the linear control methods have failed to meet the necessary requirements. The controller must also ensure good performance and reliability over a large range of operating points. Therefore, a nonlinear controller was used for this study.

Section 2.2 describes the mathematical model used to design and simulate the controller. The model includes a simplified powertrain. The brake system relies on a model complex enough to capture the important dynamics, and yet simple enough to facilitate the controller design and reduce computation time.

The actual brake controller is developed in section 2.3. The methodology used was the Lyapunov-based technique of Sliding Control. In order to accommodate implementation issues, a multiple surface sliding controller was used. Also, modifications were made to accommodate the discrete type input present in the vacuum booster.

The controller provided good tracking even under the presence of modeling errors and noise. This kind of performance was obtained both in simulation and experiments. These results are presented in section 2.4.

2.2 Mathematical Model

The powertrain model was adapted form Cho and Hedrick (1989) and McMahon, Hedrick and Shladover (1990). Since the emphasis of this study is brake control, a simplified model of the powertrain is used. The model is complete enough though to capture the dynamics of the vehicle. The brake model was developed by Gerdes, et. al.(1993) specifically for the task of brake control in an IVHS environment.

2.2.1 Powertrain

A simplified three state model of an automotive powertrain was used. For a more complex model see Gerdes, et.al.(1993). For this model the following assumptions are made:

1. Time delays associated with power generation in the engine are negligible.

2. The torque converter is locked.

3. No torsion of the drive axle.

4. No slip at the wheels.

Figure 2.1 shows a free body diagram of this simplified model.

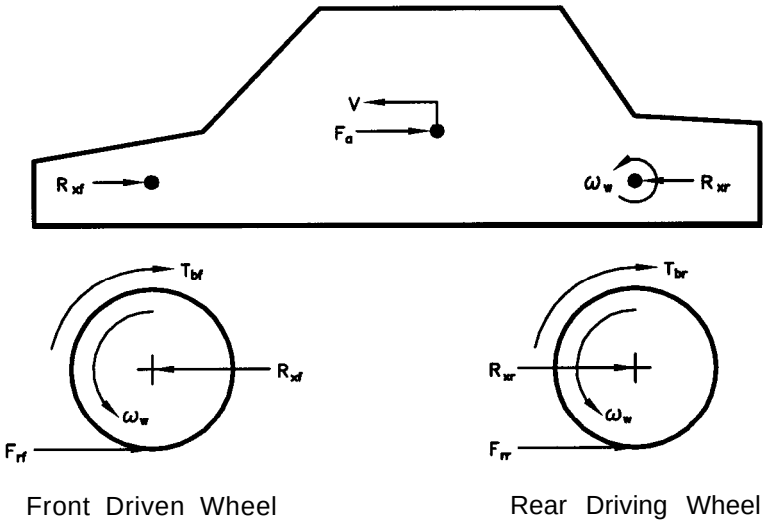

Figure 2.1: Vehicle Free Body Diagram

The two state equations for the engine are:

$$\dot{m}_a = c_1 TC(\alpha) - c_2 w_e m_a \tag{2.1}$$

$$\dot{w}_e = \frac{1}{J_e}[T_i - T_f - T_r - T_d - T_b] \tag{2.2}$$

where

m_a - mass of air in the intake manifold.
w_e - engine speed.
TC - Throttle Characteristic.
J_e - Effective vehicle inertia.
$T_i = c_3 m_a$ - Indicated torque.
$T_f = c_4 w_e$ - Indicated torque.

$T_r = hF_r$ - Rolling resistance.
$T_d = c_5 v^2$ - aerodynamic drag.
T_b - total brake torque.
h - effective tire radius.

The third and final state is the combined brake torque. In the past it has been modeled as a first order linear system. The new model is discussed in detail in the following sections.

2.2.2 Retrofitted Brake System

This study revolves around a Lincoln Town Car retrofitted for IVHS studies. There are several reasons why a retrofitted brake system was chosen over a system specifically designed for IVHS. Most importantly, such a system is easy to design and implement. The time frame and financial cost are considerably reduced. Furthermore, such a system is more reliable since it relies heavily on the existing brake system.

Figure 2.2 is a schematic of the brake system present in the test vehicle.

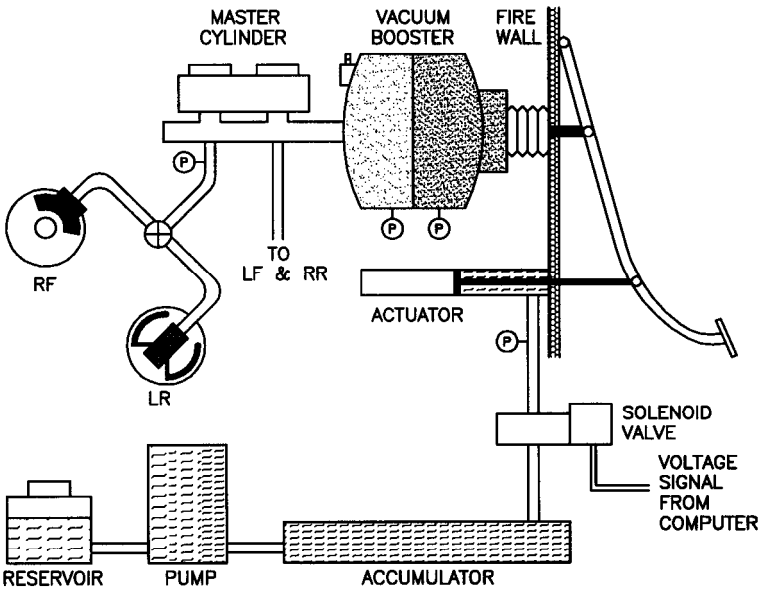

Figure 2.2: Brake System Diagram

As it can be seen from the above diagram, the voltage signal from a

computer controls the flow of hydraulic fluid to the actuator through the use of a solenoid valve. Once the actuator starts pulling on the brake pedal through the fire wall, the system operates in the same manner as if a human driver would apply the brakes. The only significant difference over a stock brake system is that in this system the brake pressure, the pressure in the two chambers of vacuum booster and the pressure in the actuator can be measured.

One disadvantage that a retrofitted brake system is that it is a lot more difficult to control. First, the current hydraulic actuation system has a high order dynamic response which is difficult to model. Further downstream, the vacuum booster is an integral part of any modern brake system. Its purpose is to amplify the operator's input by a factor of approximately 10 and thus reduce the operator fatigue and provide the higher braking pressure required for the operation of disc brakes.

The vacuum booster though adds to the complexity of controlling the brakes by introducing a series of nonlinearities. One key difficulty is the fact that the booster has a low bandwidth internal feedback loop. Another problem is that the available input is virtually a three stage discrete input: apply, hold and release. This makes a fast, accurate operation difficult.

The operation of vacuum booster is documented in literature (see Puhn, 1985 and Gerdes, et. al., 1993). However, what is important to notice in figure 2.3 is the source of nonlinearities. Both the valve springs and the return spring have preloads that must be overcome before any motion can take place. This gives rise to several deadzones. The air flow dynamics from atmosphere to the apply chamber (in the *apply* mode) and from the apply to vacuum chamber (in the release mode) is also a phenomenon that presents nonlinear dynamics. Important to notice is also the fact that the power piston has three discrete modes of operation. In the *apply* mode air is allowed into the apply chamber from the atmosphere while the two chambers are sealed from each other. In the *hold* mode the chambers remain sealed but no air is admitted. In the release mode air is still not admitted in the apply chamber and the two chambers are connected thus equalizing the pressure across the diaphragm. As long as the pressure in the vacuum chamber is greater than the manifold pressure, the air drains to the manifold through a check valve.

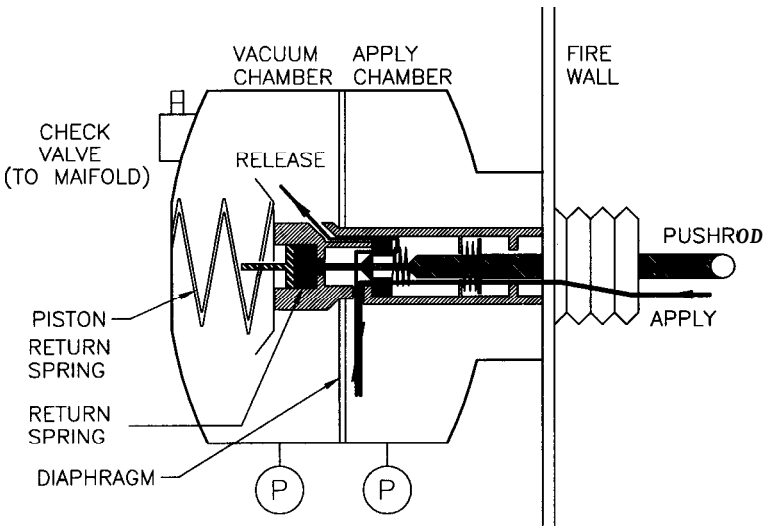

Figure 2.3: Vacuum Booster Diagram

2.2.3 Brake Model

Based on recent experimental data and analysis of the brake system a mathematical model was developed (Gerdes, et. al., 1993). As mentioned earlier, the automatic brake system is composed of the actuation system, the brake booster and the master cylinder and brake lines.

Due to the solenoid valve behavior, the actuator presents a high order dynamic response to a step input. Furthermore, this response is very difficult to model. It is however possible, for control purposes, to bound it. This will be the topic of section 2.3.5.

The vacuum booster dynamics have been modeled in two sections: force balance equations are presented below:

$$F_{in} - F_{vs} - r \,.\, F_{mc} = 0 \tag{2.3}$$

$$F_{vs} + F_d - F_{rs} - (1 - r) \,.\, F_{mc} = 0 \tag{2.4}$$

where
F_{in} = pushrod input force
F_{vs} = valve springs force
F_{mc} = master cylinder force

F_d = booster diaphragm force
F_{rs} = return spring force
r = pushrod/master cylinder reaction washer ratio.

The booster diaphragm force can be approximated as the pressure difference over the area of the diaphragm

$$F_d = (P_a - P_v) \cdot A_d = \Delta P \cdot A_d \tag{2.5}$$

For the air dynamics, the ideal gas law dictates that

$$P = \frac{m}{V} RT \tag{2.6}$$

And therefore, the pressure change at constant temperature is

$$\dot{P} = \dot{m} \frac{RT}{\dot{V}} \tag{2.7}$$

The temperature is assumed constant since the engine compartment temperature is constant under steady state operating conditions and the vacuum booster is located in the engine compartment.

From the booster operation it is also known the check valve from the vacuum chamber pressure is higher than the manifold pressure. Also, the booster valve air ports open and close in about lms and therefore, it can be assumed that they have only discrete orifice areas. The booster valve operation is summarized in table 2.1.

Mode	Atmosphere to Apply	Apply to Vacuum
APPLY	OPEN	CLOSED
HOLD	CLOSED	CLOSED
RELEASE	CLOSED	OPEN

Table 2.1: Booster Valve Operation

Based on the air flow equations and the booster valve operation, the change in pressure difference over the booster diaphragm can be represented as

Mode	u_1	u_2
APPLY	1	0
HOLD	0	0
RELEASE	0	1

Table 2.2: Booster Input

$$\Delta\dot{P} = \dot{m}_{aA}\frac{RT}{\dot{V}_A}u_1 - \dot{m}_{AV}RT[\frac{1}{\dot{V}_A} + \frac{1}{\dot{V}_V}]u_2 + \dot{m}_{Vm}\frac{RT}{\dot{V}_V} \tag{2.8}$$

where the subscripts
a = atmosphere
A = apply chamber
V = vacuum chamber
m = manifold
and u_1 and u_2 are described by table 2.2.

Lastly, from experimental results, it was determined that there is a linear relationship between brake torque (Nm) and the force applied to the master cylinder (N). Its empirical solution is :

$$T_{br} = 2.94F_{mc} - 535.1 \tag{2.9}$$

2.3 Controller Development

2.3.1 Introduction

The development of a simplified powertrain and a retrofitted brake models were discussed in section 2.2. A detailed discussion of a control methodology is presented in this section. Since the longitudinal control using throttle angle has been investigated in the past, the focus of this study will be concentrated on the longitudinal control using brakes. For this specific purpose, the control task is to track the velocity of the preceding vehicle while maintaining a constant spacing.

2.3.2 Application to Advanced Highway Systems

Due to the operation of the brake system, a natural approach is to use a multiple surface sliding controller. A sliding controller forces a system to a surface and then tracks along that surface. The first surface of this system is based on the engine speed error. The second surface is based on the brake torque error and it dictates the mode in which the power piston should be in (apply, hold or release). Finally, the third surface is based on the actuator force error and the resulting input is the voltage signal to the solenoid valve.

2.3.3 Brake Torque Controller

By observation, from Equation 2.2, the brake torque appears in the first derivative of the engine speed. Therefore, the first sliding surface is defined as

$$S_1 \equiv w_e - w_{edes} \tag{2.10}$$

Its first time derivative is then

$$\dot{S}_1 = \dot{w}_e - \dot{w}_{edes} = \frac{1}{J_e}[T_i - T_f - T_d - T_r - T_{br}] - \dot{w}_{edes} \tag{2.11}$$

Therefore,

$$T_{brdes} = J_e[\frac{1}{J_e}(T_i - T_f - T_d - T_r) - \dot{w}_{edes} + K_{br}S_1] \tag{2.12}$$

In order for the controller to operate under parameter uncertainties, K_{br} was designed to tolerate a 20 % error in J_e and 10 % error in T_i, T_f, T_d and T_r.

Therefore, K_{br} is of the form (Slotine and Li, 1991):

$$K_{br} = \frac{(1-\beta_{min})|\hat{\tilde{f}}| + \alpha + \eta}{\beta_{min}} \tag{2.13}$$

where

$\alpha = (0.377 + 0.0011w_e + 0.000027w_e^2|$

$\hat{\tilde{f}} = \frac{1}{J_e}(T_i - T_f - T_d - T_r) - \dot{w}_{edes}$

$\eta = 1.0$

$\beta_{min} = 0.82$

2.3.4 Booster Controller

In this section it will be assumed that the available pressure difference in vacuum booster is high enough so that, in the apply mode, the booster has the potential to provide the required force without additional input force from the actuator. In this case, the actuator force need only be large enough to open the booster valve to atmosphere. Since the actuator can only provide a "pull" action, in release mode the actuator cannot help reduce the brake torque faster than the booster can purge the air to vacuum.

Under these conditions, a linear relationship between the desired pressure difference over the booster diaphragm and brake torque under specific operating conditions can be derived:

$$\Delta P_{des} = 8031 + 5.6T_{brdes} \tag{2.14}$$

By inspection, it can be seen that the controller appears after the first derivative, therefore

$$S_2 \equiv \Delta P - \Delta P_{des} \tag{2.15}$$

$$\dot{S}_2 = \Delta\dot{P} - \Delta\dot{P}_{des} = \dot{m}_{aA}\frac{RT}{\dot{V}_A}u_1 - \dot{m}_{AV}RT[\dot{1}\dot{V}_A + \dot{1}\dot{V}_V]u_2 + \dot{m}_{Vm}\frac{RT}{\dot{V}_V} - \Delta\dot{P}_{des}$$

As it can be seen, it would be very difficult to obtain the values for u_1 and u_2 from the above equations. Furthermore, a large number of parameter uncertainties would be introduced since the flows are highly dependent on the effective orifice areas which are difficult to calculated accurately. However, since u_1 and u_2 can only take the values described previously, the problem simplifies significantly. It is also important to notice that in the apply mode, for example, $\dot{V}_A$ is positive or zero, $\dot{V}_V$ is negative or zero, $\dot{m}_{AV}$ is zero and $\dot{m}_{Vm}$ is positive or zero. The objective is to have $S_2\dot{S}_2 < 0$. Therefore, when $S_2 < 0$, $\dot{S}_2 > 0$ which can only be achieved when $u_1 = 1$ and up = 0 or apply mode. The opposite is true when $S_2 > 0$. This statement is also physically intuitive. It says that if the pressure difference is too low, more pressure is needed in the apply chamber, and so the brakes should be applied. The significance of this statement is even more far reaching. It implies that this control scheme can be used with any vacuum booster that operates in this manner as long as the pressure difference measurement is available.

The booster valve position, in turn, correlates with the valve spring force F_{VS}. The above statements can be summarized in table 2.3.

S_2	Mode	u_1	u_2	F_{VS}
$S_2 < 0$	APPLY	1	0	89.0
$S_2 = 0$	HOLD	0	0	75.0
$S_2 > 0$	RELEASE	0	1	62.0

Table 2.3: Booster Control

2.3.5 Actuator Control

The assumption made in the previous section will be revisited here. There will be cases when the air in the vacuum chamber would not have had enough time to drain to the manifold and the desired pressure difference in the booster will not be available fast enough. In such cases, the booster will not be able to provide the entire braking force. However, the hydraulic system present in the Lincoln Town Car is able to provide forces large enough to provide braking even in the absence of the vacuum booster. Therefore, the actuator control should take advantage of this availability in order to provide faster and safer braking. Therefore, the desired actuator force is

$$F_{indes} = (F_{vs}des + r \cdot F_{mc} - \frac{r \cdot S_2}{1 - r} p)/L_r \tag{2.16}$$

where

$$p = \begin{cases} 0 \text{ if } S_2 > 0 \text{ (cannot push on the pedal)} \\ 1 \quad \text{if } S_2 \leq 0 \text{ (can pull on the pedal)} \end{cases}$$

and L_r = brake pedal linkage ratio.

In the above equation, the first two terms represent the amount of force required to obtain the desired F_{VS} and the third term represents the compensation for not having enough pressure differential of the booster diaphragm.

At this point, the solenoid valve currently in operation cannot provide the actuator with a "clean" input. A step input on the valve reveals high order dynamics. The solution suggested to solve this problem is to bound the dynamics between two first order responses and to treat the difference in the two gains and time constants as parameter uncertainties which can be bounded. A typical step response for the valve along with the first order

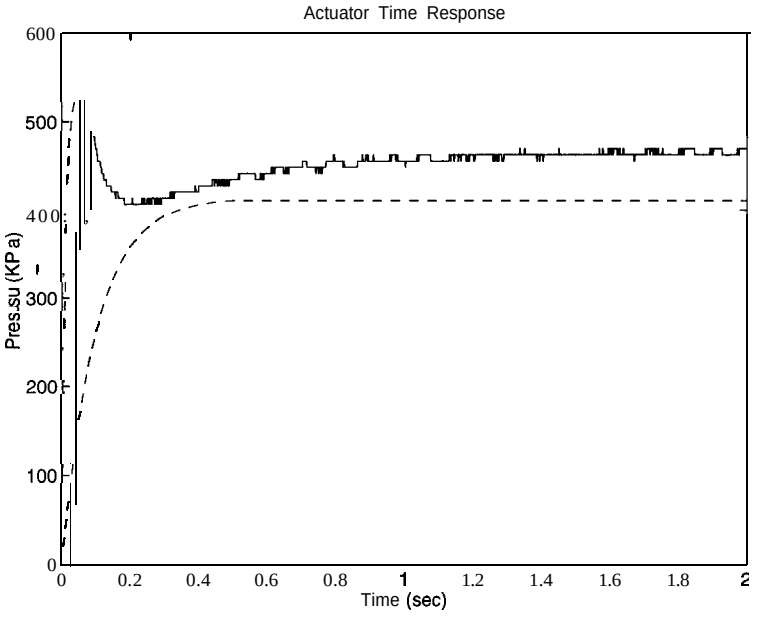

Figure 2.4: Brake Actuator Step Response

dynamics bounding it are shown in figure 2.4. Consider the above concepts, the brake actuator dynamics can be estimated as:

$$\dot{F}_{in} = \frac{(v - v_{off}) \cdot k \cdot A_{act} - F_{in}}{\tau} \tag{2.17}$$

where
v = input voltage
v_{off} = voltage offset
A_{act} = actuator area
k = proportionality constant between voltage and actuator pressure.

Since the voltage is the input, by inspection, the input appears after the first differentiation. Therefore:

$$S_3 \equiv En - F_{indes} \tag{2.18}$$

$$\dot{S}_3 = \dot{F}_{in} - \dot{F}_{indes} = \frac{(v - v_{off}) \cdot k \cdot A_{act} - F_{in}}{\tau} - \dot{F}_{indes} \tag{2.19}$$

and so

$$v = \frac{\tau}{k \cdot A_{act}}\left(\frac{v_{off} \cdot k \cdot A_{act}}{\tau} + \frac{F_{in}}{\tau} + \dot{F}_{indes} - K_{act}S_3\right) \tag{2.20}$$

In ***implementation,*** $\dot{F}_{indes}$ is approximated as $\frac{F_{indes}(t+\Delta t)-F_{indes}(t)}{\Delta t}$ since it is difficult and computationally intensive to calculate it analytically. K_{act} must be designed so that the higher dynamics fit in the bounds determined by the first order responses. Therefore (Slotine and Li, 1991):

$$K_{act} = \frac{(1-\beta_{min})|\hat{\dot{f}}| + \alpha + \eta}{\beta_{min}} \tag{2.21}$$

where

$$\hat{\dot{f}} = \frac{v \cdot k \cdot A_{act}}{\tau} + \frac{F_{in}}{\tau} + \dot{F}_{indes} \tag{2.22}$$

Allowing for 20 % error in k and τ and 10 % error in A_{act} and v_{off}, the following expressions were obtained for α and β_{min}:

$$\alpha = 12.24 + 26.41F_{VS} + 0.0033P_{br}| \tag{2.23}$$

$$\beta_{min} = 0.73 \tag{2.24}$$

$$\eta = 10.0 \tag{2.25}$$

However, since F_{VS} is not a measurable state, its largest can be used to calculate α. Therefore,

$$\alpha = 15265.1 + 0.0033P_{br}| \tag{2.26}$$

2.4 Brake Controller Performance

2.4.1 Simulation Results

A speed trajectory was designed for simulation purposes. It represents a typical acceleration/deceleration maneuver performed at highway speeds under "normal" conditions. Figures 2.5 and 2.6 show simulation results of the desired and actual speed trajectories and the speed error associated with them.

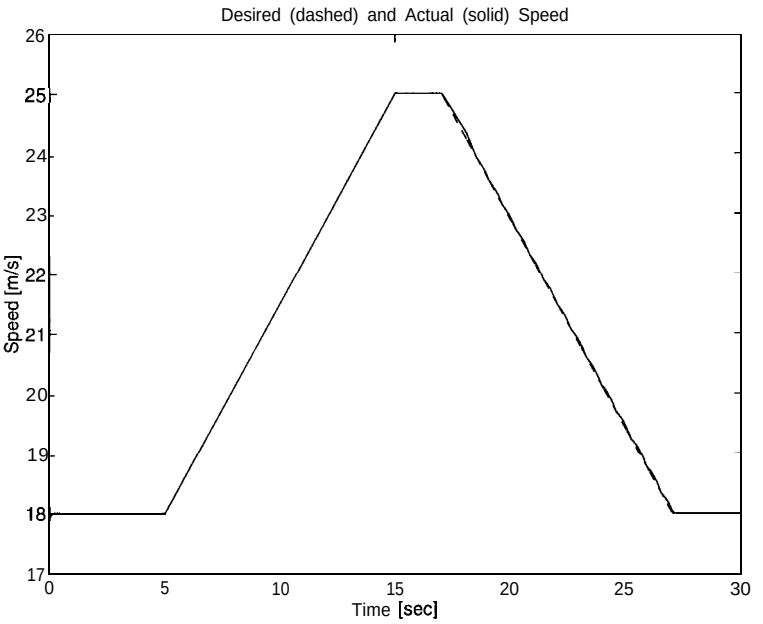

Figure 2.5: Desired and Actual Speed (Simulation)

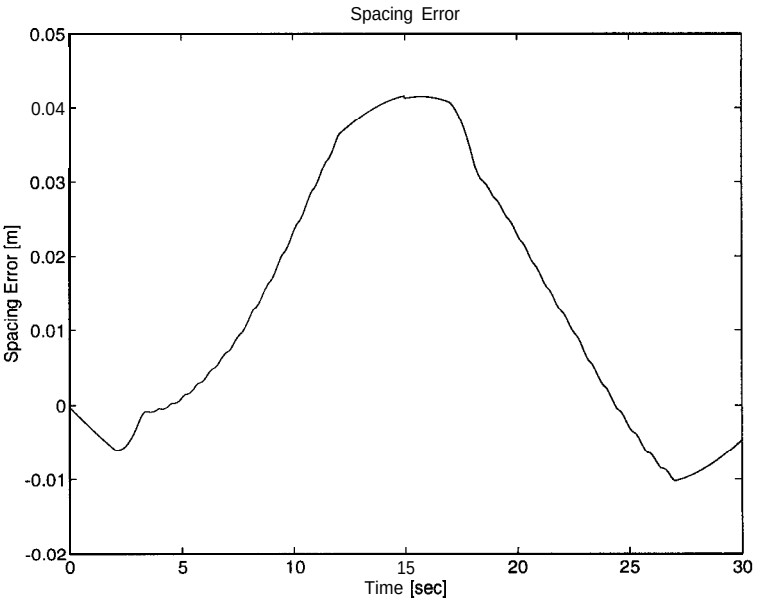

Figure 2.6: Spacing Error (Simulation)

2.4.2 Experimental Results

The experiments conducted concentrated on the ability of the controller to maintain a constant spacing from the lead vehicle. For this purpose, a ramp speed profile was used in simulating an idealized lead vehicle. Figure 2.7 shows the desired and actual speed used in these tests. More importantly, however, is the ability of the controller to maintain a constant space from the lead vehicle or any other desired trajectory. As figure 2.8 shows, the largest spacing error is less than $0.2\mathrm{m}$. Although the control algorithm provided good

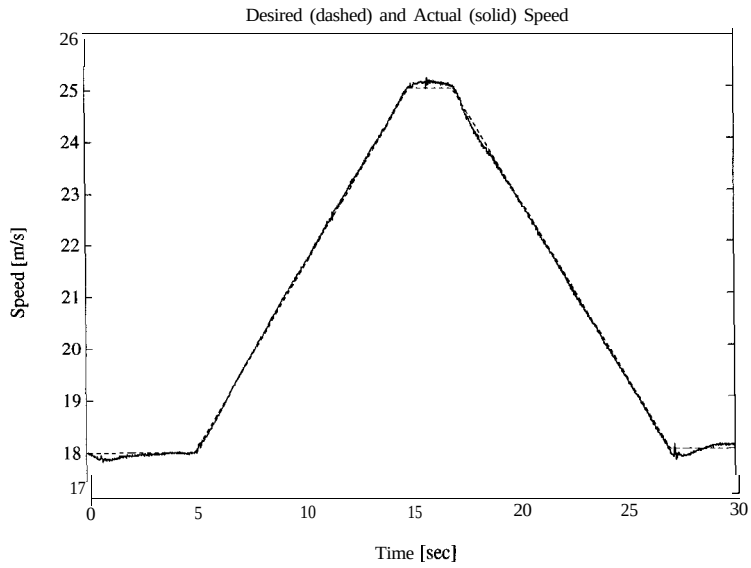

Figure 2.7: Desired and Actual Speed (Experimental)

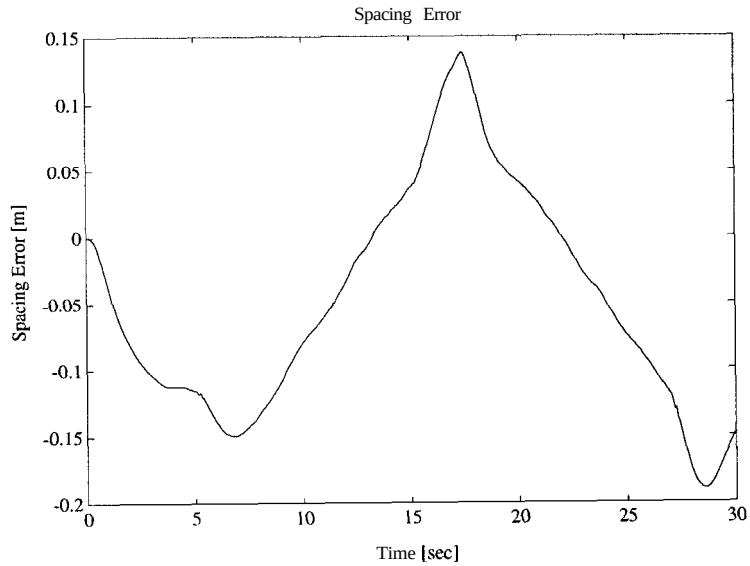

Figure 2.8: Spacing Error (Experimental)

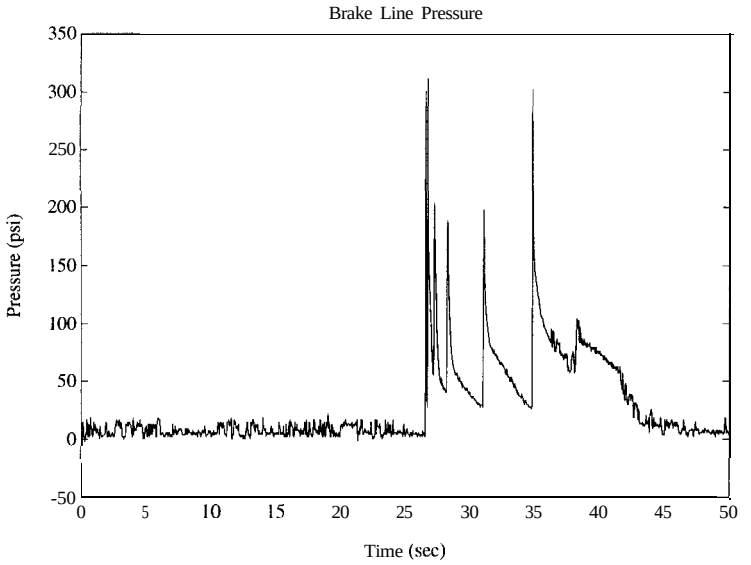

Figure 2.9: Brake pressure during braking maneuver

speed tracking, the passenger comfort was deemed suboptimal. As figure 2.9 indicates, “spikes” are present in the brake pressure which translates in unacceptable jerk levels in the vehicle. It was determined that the major cause of this behavior is the presence of the vacuum booster in the brake system. Its low bandwidth, deadzones and spring preloads contribute to this undesirable dynamics. It is therefore suggested to redesign the brake actuation system so that the vacuum booster can be eliminated. It is thus expected that the faster and simpler dynamics will provide excellent speed tracking while maintaining a great level of comfort.

2.5 Conclusions

An automotive brake system model was developed and used in designing an automatic brake controller. A powertrain model was also adapted for this purpose. Due to the nonlinear nature of both models, a nonlinear control methodology was chosen. Due to its robustness in the presence of model errors and input disturbances, the method of Sliding Control was used. A multiple sliding surface was used since the relative degree of the system was greater than one.

This study showed that it is possible to control a retrofitted brake system in the frame of AHS longitudinal control. Simulation results show good speed tracking for a platoon of two vehicles. The experimental results corroborated the simulation predictions. The three surface controller shows a good tracking even in the presence of modeling errors.

However, there was a significant degradation in the passenger comfort due to the very slow dynamics of the vacuum booster. Therefore emphasis must be placed on developing a new brake actuator that eliminates the vacuum booster. Consequently, a new controller must be developed for said actuator.

Chapter 3

Brake Dynamics Effect on IVHS Lane Capacity

3.1 Introduction

Over the last two decades, the urban and suburban traffic in the United States has experienced a continued growth while there has been a slowdown in the construction of new highways and the expansion of the existing ones. The result of this situation is increased highway congestion and an associated increase in operating cost for shipping companies and increase in stress and fatigue for all drivers.

An obvious idea to reduce congestion would be to expand the existing highway system. However, in most urban areas, this is not feasible due to lack of suitable land, increase in pollution and noise. As a result, the Federal Highway Administration (FHWA) and various state agencies and private companies have embarked on a research effort to better utilize the existing highway miles. The research area known as Intelligent Vehicle and Highway Systems (IVHS) proposes to use electronics, control and communication technologies to increase the efficiency of current highways.

A major component of the local IVHS agency, Partners for Advanced Transit and Highways (PATH), is to develop an Automated Highway System (AHS). In the present concept, an AHS would be able to increase the capacity of conventional highways by allowing vehicles to travel with very short spacings using automated control techniques.

One of the issues in AHS research is estimating the capacity increase in order to determine whether the IVHS concept is a cost-effective investment. Such an estimate must be based on theoretical vehicle models since the capacity increase must be estimated before an AHS is implemented and actual measurements are available. It is also important to know how the performance of each individual vehicle affects the capacity of the IVHS lane.

This study will concentrate on the effect of the brake performance on the capacity of the IVHS lane. The model is designed to take into account the engine dynamics, engine brake, aerodynamic drag, rolling resistance and brake dynamics. Also taken into account is the effect of Anti-lock Brake System (ABS) and the tire-road interaction. To illustrate the fundamental principles, the model is used to analyze an emergency braking maneuver, since such a condition will reveal the basic limitations of the system.

3.2 Longitudinal Vehicle Model

The powertrain model was adapted from Cho and Hedrick (1989) and McMahon, Hedrick and Shladover (1990). Since the emphasis of this study is the brake control, a simplified model of the powertrain described in the previous chapter is used. With automatic transmission locked in overdrive, and the "NO-SLIP" assumption, there is a linear relationship between engine speed, $w_e\,(\mathrm{rad/s})$, and the vehicle speed, v(Km/h):

$$v = 5.55 w_e$$

Due to this relationship, it can be assumed that a change in the vehicle speed will be directly reflected in a change in engine speed. Therefore, a change in the throttle angle, α, will change the engine speed, which, in turn, will change the vehicle speed, while a change in the brake torque, T_b, will change the vehicle speed, which, in turn, will affect the engine speed.

Although the brake dynamics are complex, as we have seen in the last chapter, it will be assumed that the brake torque dynamics is a pure time delay followed by a first order dynamic time response for this analysis. A typical brake response is shown in figure 3.1. The maximum brake torque is limited to 10,000 Nm to account for the capabilities of the current brake systems. Furthermore, the deceleration is limited to 6.7 m/s^2. This is to

account for the limitation of the tire-road interaction and the activation of the ABS.

3.3 IVHS and Human Drivers

In order to evaluate the efficiency of an AHS, it is critical to determine the effect of vehicle dynamics on the capacity. In this paper, the emphasis will be placed on the effects of brake dynamics during an emergency braking on the capacity of the AHS.

As illustrated in figure 3.1, an idealized brake dynamic response can be divided in two separate sections. The first one is the pure time delay. In turn, the pure time delay has two components. The first component is due to the recognition of the emergency brake mode, which is dependent on the communication protocol and hardware. In the current system, a token protocol involving a voting scheme is used, making the pure time delay associated with the communication approach a duration of 60 msec. The second component of the pure time delay is due to the delay in the brake hardware. It generally depends on the type of valves, hydraulic system and design of the brake system. The duration of this pure time delay can range from 10 to 100 msec. Therefore, the lumped length of the pure time delay varies from 70 to 160 msec. The second component of the idealized brake dynamic response is the first order response. The critical element of this part is the time constant of the response. Again, the time constant varies with the brake hardware and it ranges from 10 to 100 msec. In mathematical from, the dynamic brake response can be represented as:

$$\dot{T}(t + \Delta t) = \frac{T_d(t) - T(t)}{\tau}$$

where
T = brake torque
T_d = desired brake torque
Δt = pure time delay
τ = time constant

In order to have an understanding of these values, figure 3.2 shows the idealized brake response when a human driver is in control of the vehicle. The pure time delay is due to the perception of some external stimuli, the

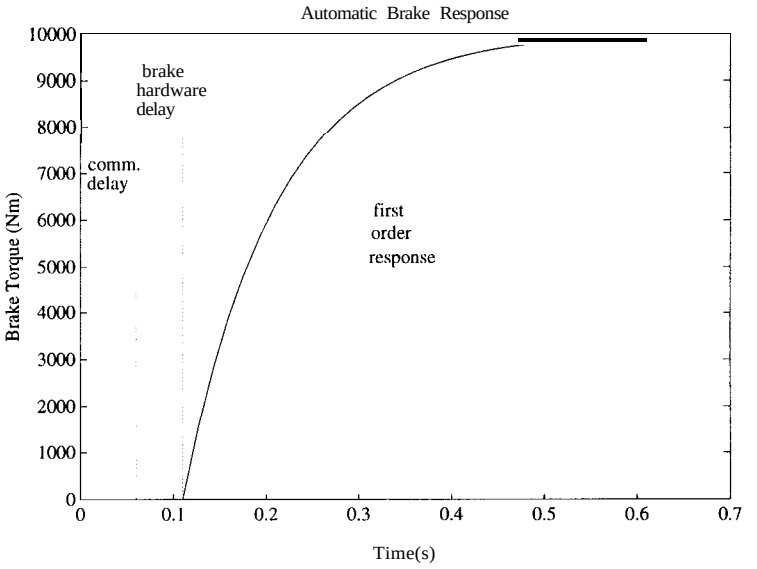

Figure 3.1: Typical Brake Dynamic Response

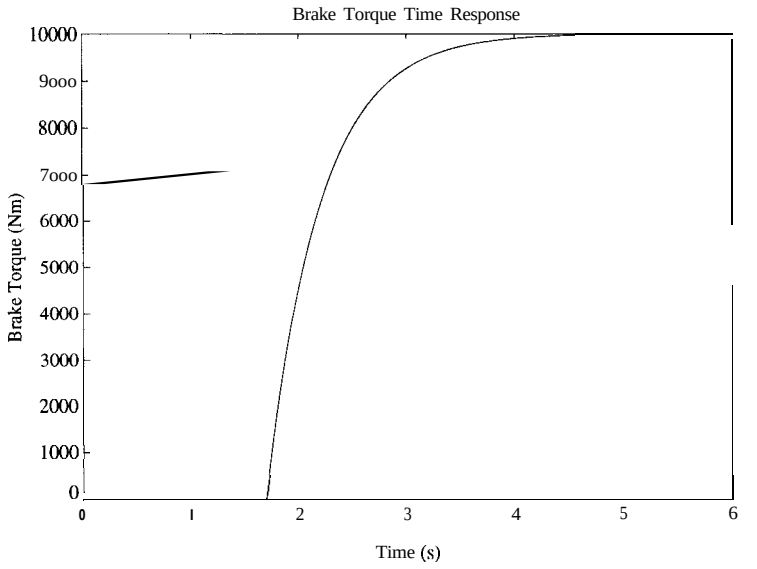

Figure 3.2: Brake Dynamic Response With Human Driver

reaction time to such stimuli, the actual foot transfer and the overcoming of any deadzones in the brake system. In general, the pure delay for a human driver varies from 1.2 to 1.7 seconds (Bidwell, 1961). The first order response time constant is limited by the rate with which a human driver can depress the brake pedal and the bandwidth of any aids present in the brake system. Theses values range from 400 to 500 msec.

It is, therefore, interesting to analyze the behavior of a platoon in which the vehicles are operated under human control in order to appreciate the benefits of an IVHS controlled platoon. In order to achieve 2000 passenger-cars per hour per lane (pcphl) at 110 Km/h $(70\mathrm{MPH})$, an average spacing of 50m must be maintained between vehicles. As figure 3.6 shows, this is a safe spacing since the final relative speed between vehicles during an emergency braking maneuver at this spacing is $0\mathrm{Km/h}$ (i.e. no impact between vehicles occurs). It was assumed that the two vehicles are able to decelerate at the same rate of 6.7 m/s^2. The situation becomes more critical though when the two vehicles are not able to decelerate at the same rate. Figure 3.3 shows how the collision speed varies with the initial spacing when the lead vehicle is able to decelerate at 6.7 m/s^2 while the following vehicle is able to decelerate only at 5.9 m/s^2. However, maintaining an average 50m initial spacing between vehicles, figure 3.4 shows that the final spacing is also kept under $5\mathrm{m}$, the length of an average car. However, without an adequate control scheme, instabilities in the platoon will occur and most human drivers will not be able to maintain a spacing of exactly $50\mathrm{m}$, in order to be safe during an emergency. As a matter of fact, maintaining between 2 and 8 car lengths spacing proves to be the most dangerous situation since the relative speed between cars during a collision is upwards of 40 Km/h (25MPH) as figure 3.6 shows. The inability of a human driver to maintain the required spacing under heavy braking is illustrated in the t-x diagram shown in figure 3.5 The reduction in spacing over this short time interval is easy to notice, pointing the instability of a platoon composed of human driven vehicles.

As figure 3.6 shows, there are two spacing values where the relative speed at impact is minimized. A low relative speed during an accident occurs at very small spacing between vehicles $(0\text{-}5\mathrm{m})$ or very large $(>50\mathrm{m})$. This idea drives the IVHS platoon concept. Two different spacing values can be observed in the platoon schematic in figure 3.7. The intra-platoon distance is kept small enough so that the relative speed between vehicles during an accident is kept below 4 Km/h (2.5 MPH). The 4 Km/h value was chosen since

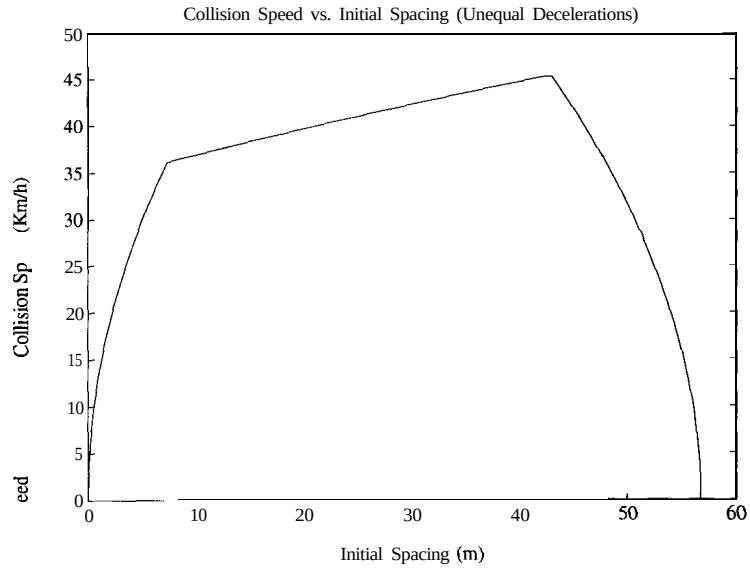

Figure 3.3: Collision Speed for Various Initial Spacings and Unequal Decelerations

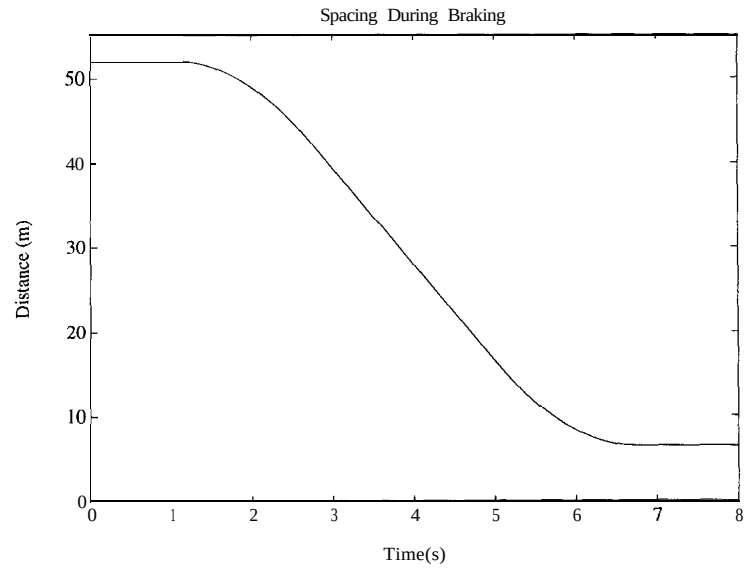

Figure 3.4: Spacing During Braking with Human Driver

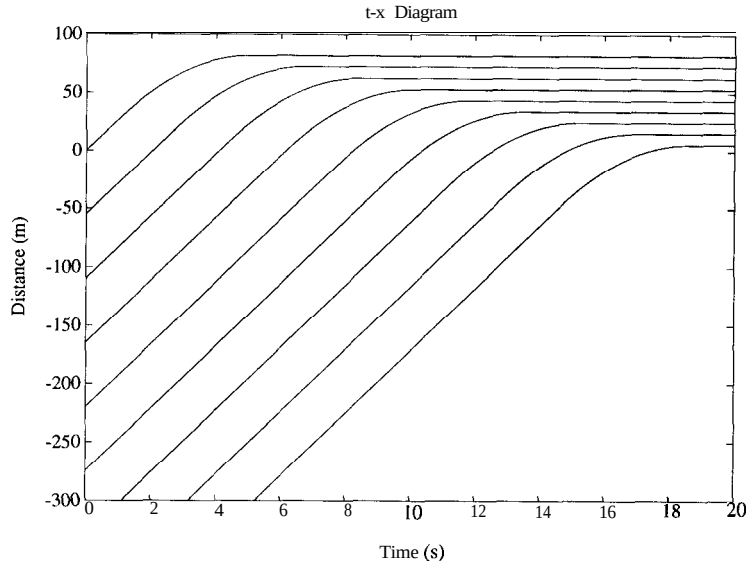

Figure 3.5: Platoon of Human Driven Vehicles Under Braking

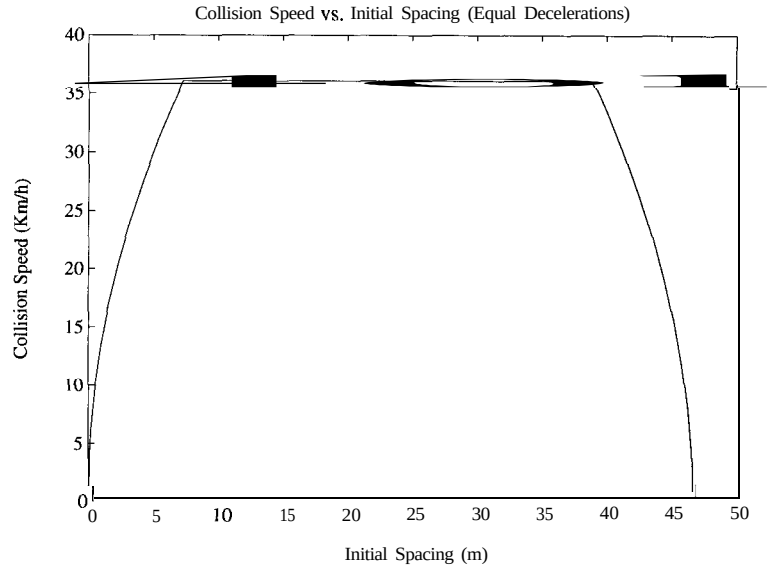

Figure 3.6: Collision Speed for Various Initial Spacings and Equal Decelerations

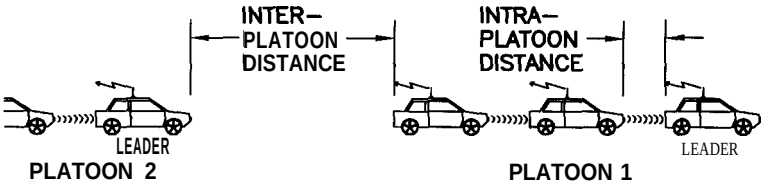

Figure 3.7: IVHS Platoon

the current federal regulations require that a bumper sustain a 4 Km/h impact without damage. The inter-platoon distance is regulated by the "brick wall" safety concept. The idea behind this concept is that the second platoon has to come to a complete stop before touching the last vehicle in the platoon even if that vehicle comes to a complete stop instantaneously.

3.4 IVHS Simulation Results

In order to investigate the full effect of the brake dynamics, the simulation was run for an emergency case. It is obvious that a platoon must perform safely under extreme conditions such as emergency braking. However, the constraints on the platoon are much more stringent under such conditions than under normal operation. The simulation was run using several brake dynamics and platoon sizes. From such simulations, several sets of information were obtained. One of the most important information was the capacity if the IVHS lane. This type of information will determine whether the increase in capacity warrants the cost of developing a brake system with more stringent dynamic constraints.

From a safety interest, the inter-platoon and the intra-platoon distances were determined so that no impact occurs between the vehicles of a platoon or the leader and the last vehicle of two consecutive platoons, even though a 4 Km/h impact is acceptable. The main reason for not allowing collisions to occur is that the dynamics of a multi-vehicle collision are complicated and beyond the purpose of this paper. Furthermore, by not allowing collisions to occur, the simulation will yield more conservative results and thus producing a "worst case" scenario.

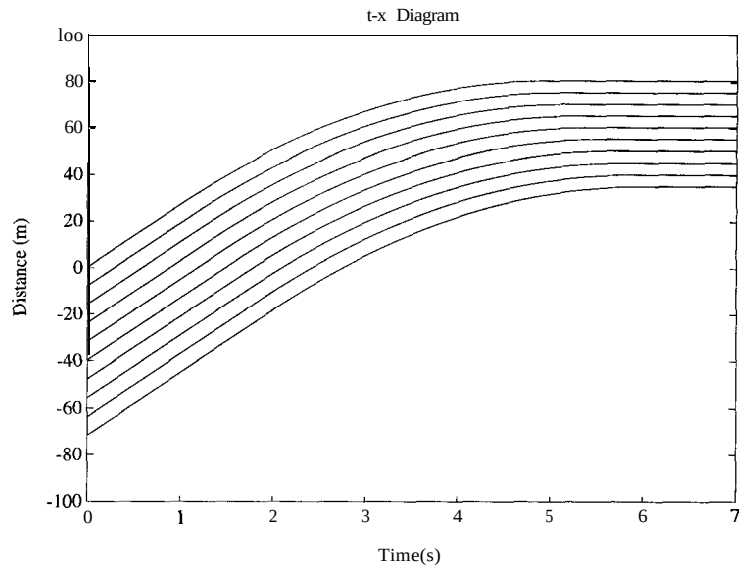

Figure 3.8: IVHS Platoon Under Emergency Braking

3.4.1 Typical Results

A simulation run was performed using "typical" values of brake dynamics and platoon size. These values were chosen from the currently acceptable values in this research area. They are as follows:

Pure time delay: 50 $msec$
Time constant: 50 $msec$
Platoon size: 10 veh
Initial speed: 110 Km/h
Deceleration: 6.7 m/s^2

The t-x diagram of such a platoon under emergency braking is shown in figure 3.8. As it can be seen, the vehicles maintain a more constant spacing than the human driven platoon was able to maintain. The safety issue is also better addressed by the IVHS platoon. Figure 3.9 shows two such platoons and the fact that the second platoon was able to come to a completer stop under the "brick wall" safety concept. Even more important is the effect on the relative speed at impact. As in the human driven vehicles, two regions of low impact speed can be found. However, for the IVHS case, even the

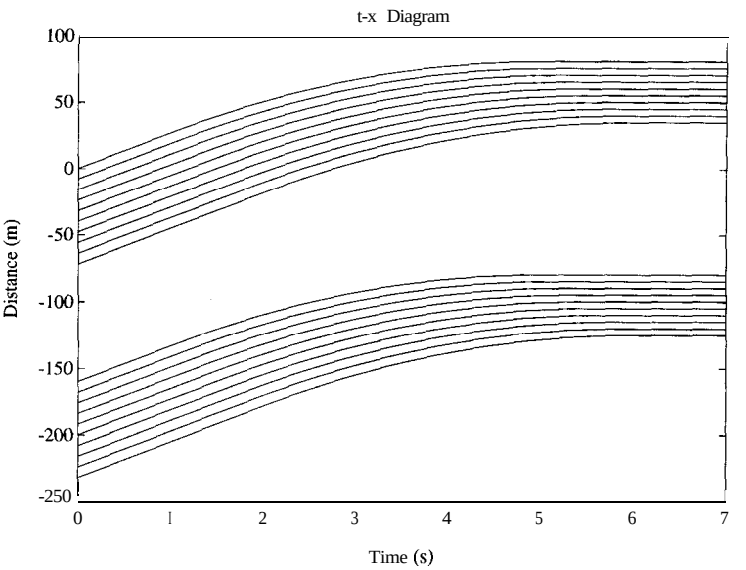

Figure 3.9: Inter-Platoon t-x Diagram

worst impact speed is below 1.5 Km/h. Figure 3.10 shows these facts. The most relevant investigation involves the effect of the brake dynamics on the lane capacity. This type of information is necessary in developing required specifications for the next generation of automatic brake systems. The cost of developing a system with very stringent requirements must be weighted against the improvement in capacity. Early research has shown that from a control issue, a very short pure time delay is desired but the cost to develop such a system is too high using the current technology.

The simulation was, therefore, run with pure time delay and time constant values ranging from 10 to 100 msec for the brake system hardware, or from "ideal" to "currently available." Additionally, a 60 msec pure time delay was added to account for communication delay. The initial speed was 70 MPH. The results are summarized in table 3.1 along with intra-platoon distances.

Several conclusions can be drawn from the above table. First, the time constant has a minimal effect on the capacity. The pure time delay, however, has an important effect on the capacity. Furthermore, the capacity increases almost linearly with the decrease in the pure time delay, as figure 3.11 shows. It is also interesting to notice that even with a brake system pure delay of 10

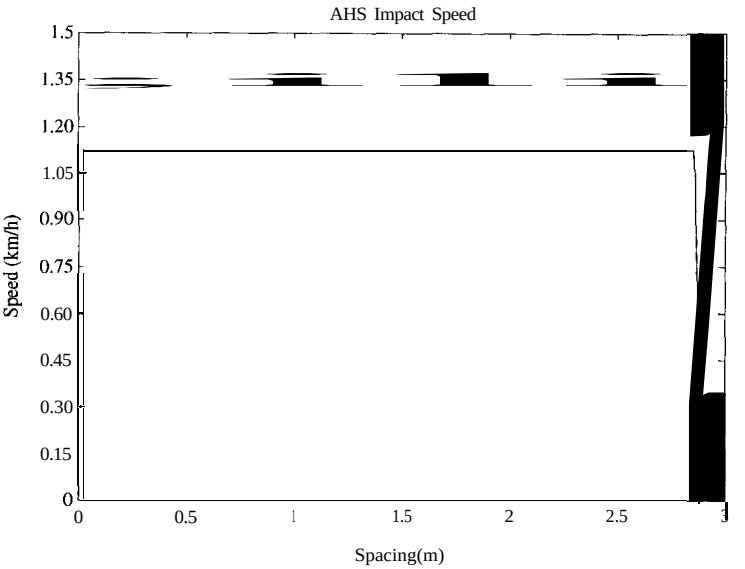

Figure 3.10: Collision Speed for Various Initial Spacings (IVHS platoon)

$\tau \rightarrow$		10 $msec$		50 $msec$		100$msec$
Δ t ($msec$)	Capacity ($pcphpl$)	Intra- (m)	Capacity ($pcphpl$)	Intra- (m)	Capacity ($pcphpl$)	Intra- (m)
100	4707	4.3	4706	4.3	4700	4.3
50	5060	3.0	5059	3.0	5053	3.0
25	5305	2.2	5304	2.2	5297	2.2
10	5403	1.9	5402	1.9	5394	1.9

Table 3.1: Summary of Results

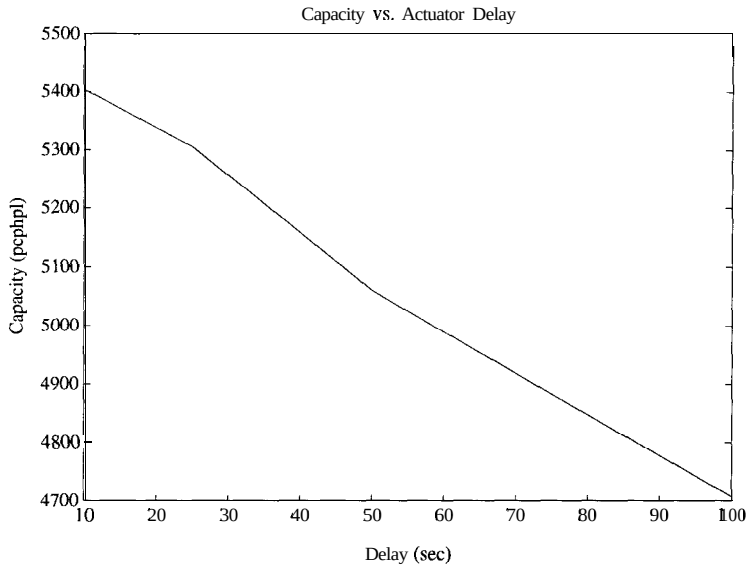

Figure 3.11: Pure Delay Effect on Capacity

Total *Delay*	*Time Constant*	**Capacity**	*Inter-platoon distance*
40 *msec*	25 *msec*	**5716** *pcphpl*	79.7 *m*

Table 3.2: Effect of Total delay, Time Constant on the Capacity

msec, the minimum intra-platoon distance is 1.9m instead of the hypothesized distance of 1.0 m. This is due to the pure time delay of 60 msec caused by the communication protocol and hardware. If the 1.0 m intra-platoon distance is the critical parameter in design, the values in table 3.2 must be achieved.

It is interesting to notice that with a total pure time delay of 40 msec, the achievable capacity is 5716 pcphpl, about three (3) times the present capacity. Since decreasing the communication delay is one way to increase capacity, methods must be found to achieve this goal. The present communication system uses a token protocol, where each vehicle takes its turn in transmitting while the rest are receiving. Therefore, one way to reduce the communication delay is to use smaller platoons. This issue will be investigated in the next section.

	Platoon Size		
	5 veh	10 veh	20 veh
Capacity	**3307** $pcphpl$	**5059** $pcphpl$	**6343** $pcphpl$
Intra. Dist.	2.2 m	3.0 m	4.6 m

Table 3.3: Effect of Platoon Length

3.5 Platooning Strategies

One problem with using smaller platoons is that there will be larger inter-platoon spacings which will reduce the total capacity. The problem with larger platoons is that the communication delay increases linearly with the size of the platoon but there are less inter-platoon spacings. The effect of the platoon length was investigated in this section.

Platoon lengths from 5 to 20 vehicles were used in simulation. A larger platoon was considered unachievable due to the possibility of spacing error propagation along the length of the platoon. The brake system pure time delay was kept at 50 msec in order to have an even comparison basis. The results are summarized in table 3.3.

It is clear from the above table that the maximum capacity can be achieved with a large platoon size. The platoon size will be, however, limited by control, communication and logistical issues. The capacity can be further increased if the communication delay is improved by technological advances.

3.6 Conclusion

An attempt was made to investigate the effect of brake system dynamic characteristics and platooning strategy on the capacity of an IVHS lane. These results should help create realistic goals regarding the specifications of the brake system hardware, communication hardware, lane capacity and safety.

It was shown that a small decrease in the hardware pure time delay can have an important effect on the capacity. Also, a larger capacity can be achieved by using as large platoons as possible. The combination of these

two factors should be able to raise the capacity of an IVHS lane to 3 to 3.5 times the currently achievable capacity.

According to these preliminary results, the following recommendations can be made. Maintain a platoon size of 20 vehicles. Reduce the total pure time delay to 40 msec. This can be achieved by a combination of reduced communication delay and brake system pure time delay. Maintain an intra-platoon distance of 1 m and an inter-platoon distance of 80 m. These distances will guarantee safe operation even during emergency maneuvers. They will also yield an IVHS lane capacity of 6000 pcphpl, about three times the current traffic capacity.

Chapter 4

Brake System Requirements for Platooning

4.1 Introduction

While IC engines possess a natural input in the throttle, automotive brake systems (as shown in figure 4.1) provide no clear actuation point. Because of this, the actuation strategy and hardware determine which components remain in the system and, consequently, define the brake dynamics. As discussed previously, experimental testing of a pedal actuation system (which incorporated the vacuum booster) revealed a deterioration in passenger comfort. Unfortunately, given the complexity of the dynamic model and controller, the exact cause of this deterioration is not immediately clear. The question then arises as to whether or not pedal actuation presents a feasible solution for platooning and, if not, what requirements a suitable actuation scheme should possess. Addressing this question, however, requires some notion of the desired characteristics of a brake system and the interactions between hardware choice and platoon performance.

In this chapter, we offer a controls perspective on this issue of performance. Taking the sliding controller framework, we highlight the critical areas in which the brake system dynamics affect platoon performance. Since the maneuvers, tracking accuracy and comfort required by an automated highway are not firmly defined, we adopt a limiting factor approach. This analysis, therefore, may be viewed as specifying the performance of a brake

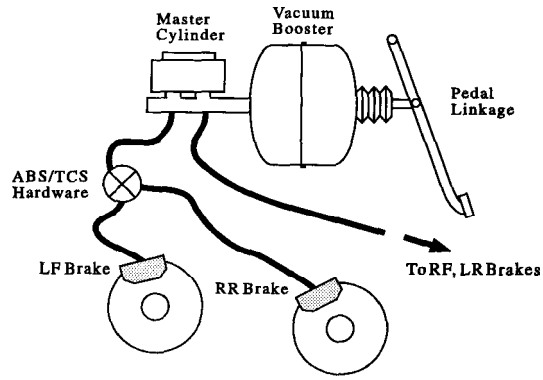

Figure 4.1: Brake System Components

system capable of attaining the tracking and robustness properties demonstrated by the multiple-surface controller in simulation. Coupling the resulting objectives for system design with recent results in brake system modeling and control (Gerdes, Brown and Hedrick, 1995, Gerdes, et.al., 1993, Maciuca, Gerdes, and Hedrick, 1994) we present some specific recommendations on brake system hardware which arise from the analysis.

We begin by presenting the multiple-surface sliding control scheme for platooning, along with a modified criterion for switching between brake and throttle control. Using this framework, we demonstrate the limitations arising from the vacuum booster cut-in and conclude that an actuation scheme for platooning should bypass this component. Appealing to the dynamics of the two sliding surfaces, we illustrate the need for torque feedback to prevent actuation errors from influencing spacing errors. Finally, we demonstrate how pure time delays in the brake system impose gain limitations that severely hinder the tracking and robustness of the controller. A note on the feasibility of a such an actuation scheme concludes the chapter.

4.2 Vehicle Model and Controller

4.2.1 Throttle Control Development

The analytical basis for this simulation study is a three-state vehicle model (McMahon, Hedrick and Shladover, 1990) where the states are the mass of

air in the engine intake manifold, m_a, the engine speed, ω_e, and the brake torque, T_b; the inputs are the throttle angle, α, and the commanded brake pressure, P_{bc}. The state equation for m_a is given by:

$$\dot{m}_a = \dot{m}_{ai} - \dot{m}_{ao} \tag{4.1}$$

where

$$\dot{m}_{ai} = \text{MAX TC } (\alpha) \text{ PRI (m,)} \tag{4.2}$$

$$\dot{m}_{ao} = c_1 \eta_{vol} m_a \omega_e \tag{4.3}$$

In these equations, MAX represents the flow rate at full throttle, $\mathrm{TC}(\alpha)$, an empirical throttle characteristic and $\mathrm{PRI}(m_a)$ a pressure influence function for compressible flow. η_{vol} is a volumetric efficiency and c_1 a constant based upon engine displacement.

Assuming that the transmission is locked in gear and ignoring tire slip, the state equation for ω_e is:

$$J_e \dot{\omega}_e = T_{net}(\omega_e, m_a) - R_g T_b - T_{load} \tag{4.4}$$

where J_e is the vehicle inertia reflected to the engine, T_{net} is the net engine torque and, T_{load}, the drag:

$$T_{load} = C_a {R_g}^3 h^3 {\omega_e}^2 + R_g h F_{rr} \tag{4.5}$$

Here R_g is the gear ratio from engine to wheel, h is the tire radius, C_a the aerodynamic drag coefficient and F_{rr} the total rolling resistance.

The platoon controller is based on the multiple surface sliding control method. Assuming constant desired spacing between vehicles, Δ, we define the spacing error for car i in terms of the position of cars i and $i-1$, x_i and x_{i-1}:

$$\epsilon_i = \Delta - (x_{i-1} - x_i) \tag{4.6}$$

Assuming that lead vehicle information and the car length, L_i, are known, acceptable error dynamics form the first surface (Swaroop and Hedrick, 1994):

$$S_{1i} = \dot{\epsilon}_i + q_1 \epsilon_i + q_3(\dot{x}_i - \dot{x}_{lead}) + q_4(x_i - x_{lead} - \sum_{j=0}^{i} L_i) \tag{4.7}$$

We drive the system to this surface by defining

$$\dot{S}_{1i} = -\lambda_1 S_{1i} \tag{4.8}$$

and solving for $\dot{\omega}_{e,des}$ as a synthetic control:

$$\dot{\omega}_{e,des} = \frac{\ddot{x}_{i-1} - q_1\dot{\epsilon}_i + q_3\ddot{x}_{lead} - q_4\left(\dot{x}_i - \dot{x}_{lead}\right) - \lambda_1 S_{1i}}{(1 + \text{43})\, R_g h} \tag{4.9}$$

Substituting back into Equation 4.4, we determine a corresponding $T_{net,des}$ and, through table look-up, $m_{a,des}$. Defining the second sliding surface:

$$S_{2i} = m_a - m_{a,des} \tag{4.10}$$

we set

$$\dot{S}_{2i} = -\lambda_2 S_{2i} \tag{4.11}$$

and solve for the desired throttle characteristic:

$$TC_{i,des}(\alpha) = \left(\dot{m}_{ao} + \dot{m}_{a,des} - \lambda_2 S_{2i}\right) / (\text{MAX PRI}) \tag{4.12}$$

Inverting this characteristic yields the control, α.

4.2.2 Brake Control Development

In this work, we assume that the actuation system chosen controls the brake pressure at the wheels and possesses a first-order response with transport lag, t_d:

$$\dot{P}_b(t + t_d) = \left(P_{bc}(t) - P_b(t + t_d)\right)/\tau_b \tag{4.13}$$

Within this description, τ_b reflects an effective time constant of the actuator and brake system components and t_d approximates the effects of pure time delays, filling properties, valve spool delays, etc. described in Gerdes, Brown and Hedrick (1995), Gerdes, et.al. (1993) and Ioannou and Xu (1994). Admittedly, this is a simplification, though sufficient to examine system requirements; more accurate models can be used for implementation. The brake torque is assumed proportional to the pressure through an (uncertain) gain, K_b:

$$T_b = K_b P_b \tag{4.14}$$

If braking is necessary, we substitute Equation 4.9 into Equation 4.4 to determine $T_{b,des}$. Defining:

$$S_{3i} = T_b - T_{b,des} \tag{4.15}$$

and setting

$$\dot{S}_{3i} = -\lambda_3 S_{3i} \tag{4.16}$$

we solve for the input, $P_{bc,des}$, from Equation 4.13:

$$P_{bc} = \left[\tau_b \left(\dot{T}_{b,des} - \lambda_3 S_{3i}\right) + T_b\right] / K_b \tag{4.17}$$

To reflect the difficulty caused by the vacuum booster, one modification is required. Acting as a force amplifier, the booster possesses an internal feedback which moves to command a finite threshold value of braking once triggered. We model this booster "cut-in" by including an additional state:

$$\dot{P}_{vb} = \left(P_{bc,des} - P_{vb}\right) / \tau_{vb} \tag{4.18}$$

with the threshold incorporated as:

$$P_{bc} = \begin{cases} 0 & P_{vb} \leq P_{trig} \\ P_{thresh} & P_{trig} < P_{vb} < P_{thresh} \\ P_{vb} & P_{vb} \geq P_{thresh} \end{cases} \tag{4.19}$$

For detailed treatment of this component and its other associated control problems, see the previous section or Gerdes, Brown and Hedrick (1995), Gerdes, et.al.(1993), Maciuca, Gerdes, and Hedrick (1994).

4.2.3 Controller Integration

Because of its roots in engine control, the original controller switched between throttle and brakes depending upon the throttle surface, S_2. In this formulation, switching was based upon the value of α:

$$\begin{array}{ll} \alpha \geq 0 \implies & \text{Throttle} \\ \alpha < 0 \implies & \text{Brake} \end{array} \tag{4.20}$$

Since the switching condition depends upon the gain of the throttle sliding surface, λ_2, problems can arise when switching from brakes to throttle. As

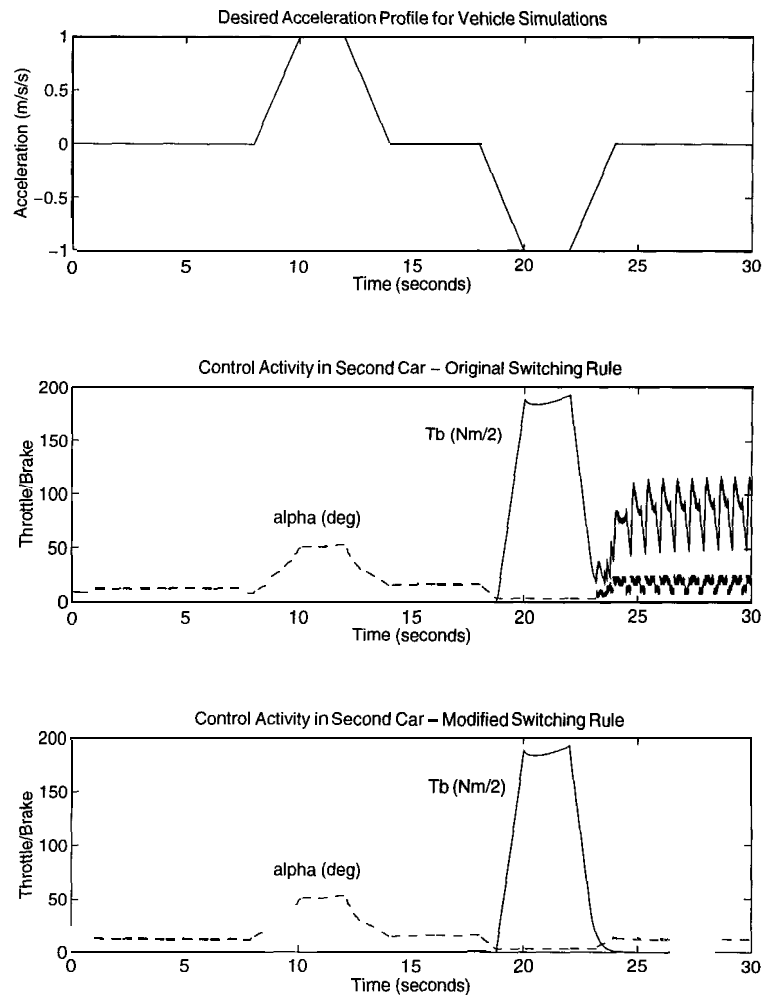

Figure 4.2: Comparison of Switching Rules

demonstrated in figure 4.2, situations exist where the throttle cuts in before the brakes have released sufficiently, resulting in competing control inputs. In previous work McMahon, Hedrick and Shladover (1990), this problem was eliminated by ignoring the brake torque when using Equation 4.4 to determine $T_{net,des}$. Since braking and robustness to braking torque represent key issues of this particular study, we require a more rigorous solution.

We therefore propose a switching strategy where the vehicle enters either throttle or brake control depending upon the level of deceleration commanded. Since rolling resistance and drag provide a certain level of deceleration in the absence of braking, we divide T_{net} into two parts: $T_{e,min}(\omega_e)$ representing the drive torque with no throttle input and T_{ec} denoting the remainder of T_{net}. Then:

$$J_e\dot{\omega}_{e,des} = T_{ec} + T_{e,min} - R_g T_b - T_{load} \tag{4.21}$$

Taking T_b and T_{ec} as our synthetic controls, define

$$T_c = T_{ec} + R_g T_b \tag{4.22}$$

Substituting into Equation 4.21, we get

$$T_{c,des} = J_e\dot{\omega}_{e,des} + T_{load} - T_{e,min} \tag{4.23}$$

A positive value of $T_{c,des}$ therefore requires throttle control and a negative value results in braking. Since T_{load} and $T_{e,min}$ are functions of engine speed, switching becomes a function of ω_e and $\dot{\omega}_{e,des}$ alone. Removing the dependence on λ_3 results in well-defined periods of throttle control and braking (figure 4.2).

4.3 Simulation Results

4.3.1 Methodology

Numerical simulations involving platoons of 10 and 20 vehicles following the maneuver depicted in figure 4.2 were performed using the simulation code described in McMahon, Hedrick and Shladover (1990). The vehicle parameters correspond to the Lincoln Town Cars used as experimental vehicles by the California PATH Program and may be found in McMahon, et.al. (1992).

As noted in the Introduction, a limiting factor approach was taken. The results and implications that follow, therefore, are based upon the premise that platoon performance should not be hindered by that of the brake system. The vehicle parameters correspond to the Lincoln Town Cars used as experimental vehicles by the California PATH Program and may be found in McMahon, et.al. (1992). The specific brake and control constants used for this study, except where noted were: λ_1=1, λ_2=40, λ_3=25, q_1=1, q_2=1, q_4=0.5, τ_b=0.10s, τ_{vb}=0.010s, K_b=1.11 Nm/kPa, P_{thresh}=300 Nm, P_{trig}=0.5 Nm.

4.3.2 Vacuum Booster

As figure 4.2 shows, the braking required by the standard simulation maneuver is gradual and of low amplitude. This contrasts sharply with human brake commands and, consequently, the vacuum booster cut-in. Intuitively, there are two methods for reconciling this: modulate the input in an attempt to achieve lower values of brake torque or actuate the brakes only after this threshold level of deceleration is commanded. Figure 4.3 demonstrates the difficulties caused by modulation. The rapid changes in the brake torque cause passenger comfort to suffer from increased jerk while tracking of the desired torque and spacing also deteriorates. Admittedly, this is more illustration than proof, since the booster remains uncompensated in the control law. However, more sophisticated control efforts have produced similar results in theory and experiment (Maciuca, Gerdes and Hedrick, 1994). The amplitude and frequency of modulation changes with actuator and control choice, but the basic problem persists.

A possible solution, then, is to emulate a human driver and switch to braking only after the threshold corresponding to booster cut-in is commanded. Assuming that the large jerk upon application is smoothed (similar to the acceleration limit in Ioannou and Xu, 1994), ride quality may be achieved. Spacing, as illustrated in figure 4.4, however, suffers. Such effects are even more noticeable when levels of deceleration below the cut-in threshold are commanded and when lead vehicle position is not available (q_4=0).

These spacing errors arise because the sliding surface dynamics in Equation 4.7 assume that $T_{c,des}$ is tracked accurately. Since the dynamics of this upper surface must provide ride quality (and control activity translates to acceleration and jerk), they are too slow to compensate for actuation errors.

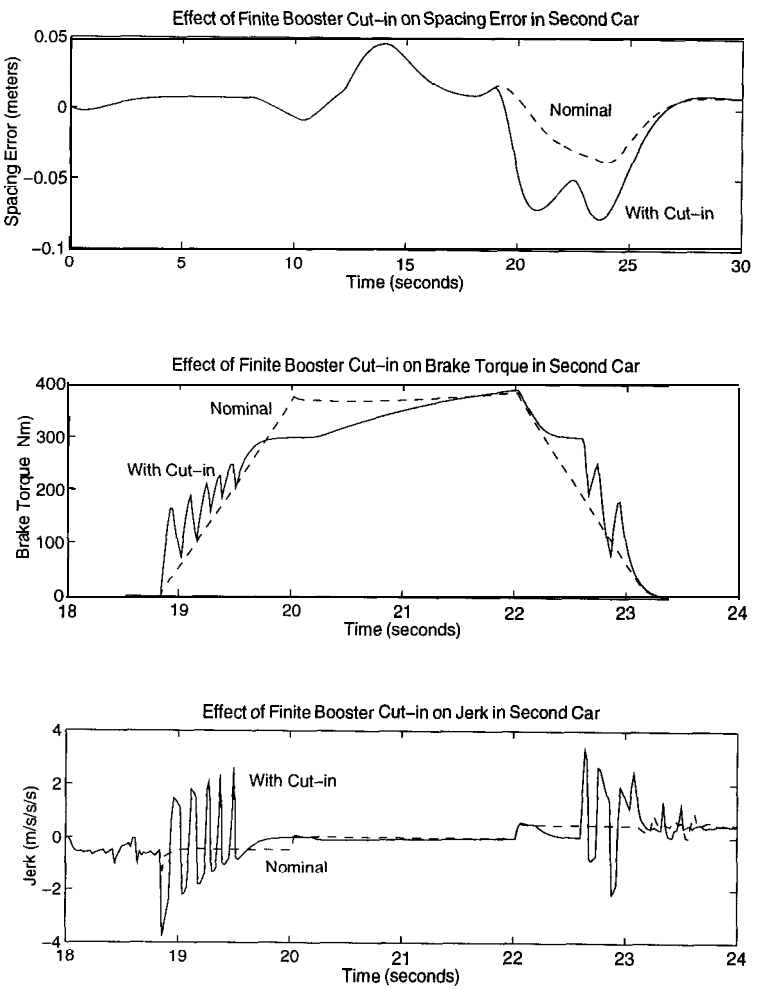

Figure 4.3: Effects of Booster Cut-in Force

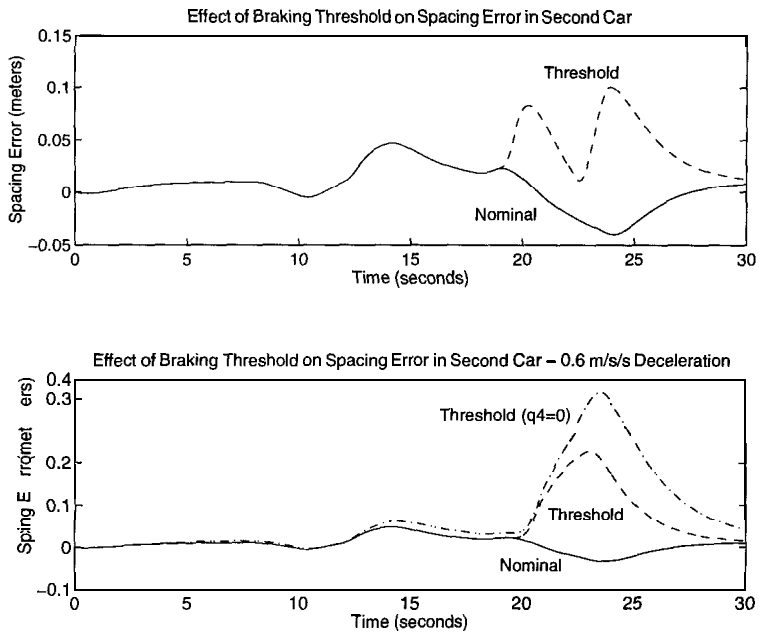

Figure 4.4: Effects of Braking With Threshold

As a result, braking errors propagate to spacing errors. This need for tight tracking of brake torque is the key to defining performance requirements.

4.3.3 Torque Feedback

Because of the problems with the cut-in, bypassing the booster clearly represents a more appealing strategy than modulating or thresholding. In practice, this bypass may be achieved either by inserting an actuator between the booster and master cylinder or by modulating the brake pressure directly (perhaps through a Traction Control System). Since either approach entails substitution of actuator dynamics for brake dynamics, some notion of the desired characteristics of such a system is required for design. We begin with the question of feedback.

Since the gain K_b can vary up to 40% due to temperature effects alone (Radlinski ,1991), controlling brake pressure is not equivalent to controlling the torque. Furthermore, the upper surface provides little correction for actuation errors, so potential mismatch in this gain must be compensated

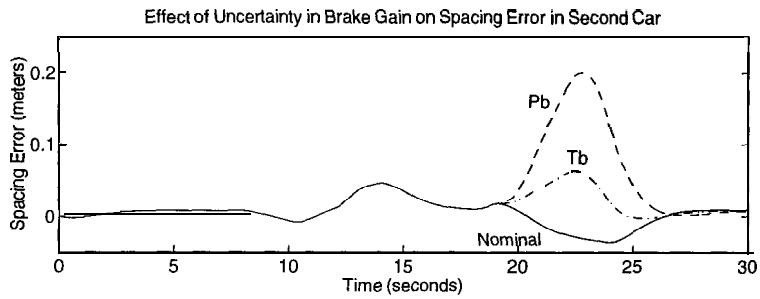

Figure 4.5: Performance With Brake Gain Mismatch

by the brake controller. Figure 4.5 compares nominal controller performance with performance when the controller underestimates K_b by 30%, assuming feedback of either T_b or P_b. With torque feedback, the gain is countered by the robustness term in the brake surface, with tracking comparable to the nominal case; with pressure feedback, large spacing errors occur. As with the threshold, setting q_4=0 produces even larger disturbances.

While the need for feedback is clear, the method is not as obvious. Although brake torque has been extracted from accelerometer measurements for analysis purposes Gerdes, Brown and Hedrick (1993) and Gerdes, et.al (1993), the presence of suspension modes and other vibrations in the data presents a serious obstacle for measuring low torques. Direct measurement (Hurtig, et.al., 1994, Perronne, Renner and Gissinger, 1994) appears to be a more promising solution, and represents a current research area.

4.3.4 Actuator Dynamics

Having established the booster limitations and the need for feedback, we turn to the desired dynamic response of a brake system. In the context of the brake model assumed in Equation 4.13, the time constant τ_b represents the least stringent requirement. Ideally, this value is cancelled by the control law in Equation 4.17. Practically, saturation becomes an issue, though the smooth variation in the desired brake torque results in reasonable control inputs for τ_b in the range of 0.10 to 0.20 (the stock brake hydraulics possess a time constant on the order of 0.08-0.10 seconds).

The time delay, however, represents a more serious problem. Because of the relatively large gain on the surface S_3, delays result in oscillatory braking

commands, hindering both tracking and comfort. Figure 4.6 contrasts the performance of the system without delay to that with an 80 millisecond delay. Since the effects of this delay increase down the platoon (due to dependence on previous vehicle information), this case shows a loss of string stability by the 8th car. Furthermore, the comfort level (measured by the jerk) deteriorates rapidly down the platoon. Such problems can be eliminated by either reducing the sliding gain, λ_3, or boosting the time constant, τ_b. Boosting the time constant, however, requires actuating downstream of the master cylinder with an extremely fast actuator. While possible, this presents a serious design task. Reducing the sliding gain is much easier, but produces a decrease in performance. As illustrated in figure 4.7, spacing errors increase slightly when this gain is reduced, but robustness to the brake gain error of Section 4.3.3 decreases noticeably. A number of simulations similar to those above were conducted to quantify acceptable levels of delay. From these results, we conclude that a brake system with a time constant of 0.10 seconds and delay time of 20 milliseconds requires no reduction in λ_3 from the ideal case and exhibits no noticeable decrease in comfort or tracking for a 20 car platoon. Physically, this implies that actuation at the master cylinder is acceptable, provided the system is capable of overcoming seal friction and brake filling (Gerdes, Brown and Hedrick, 1995) without much delay.

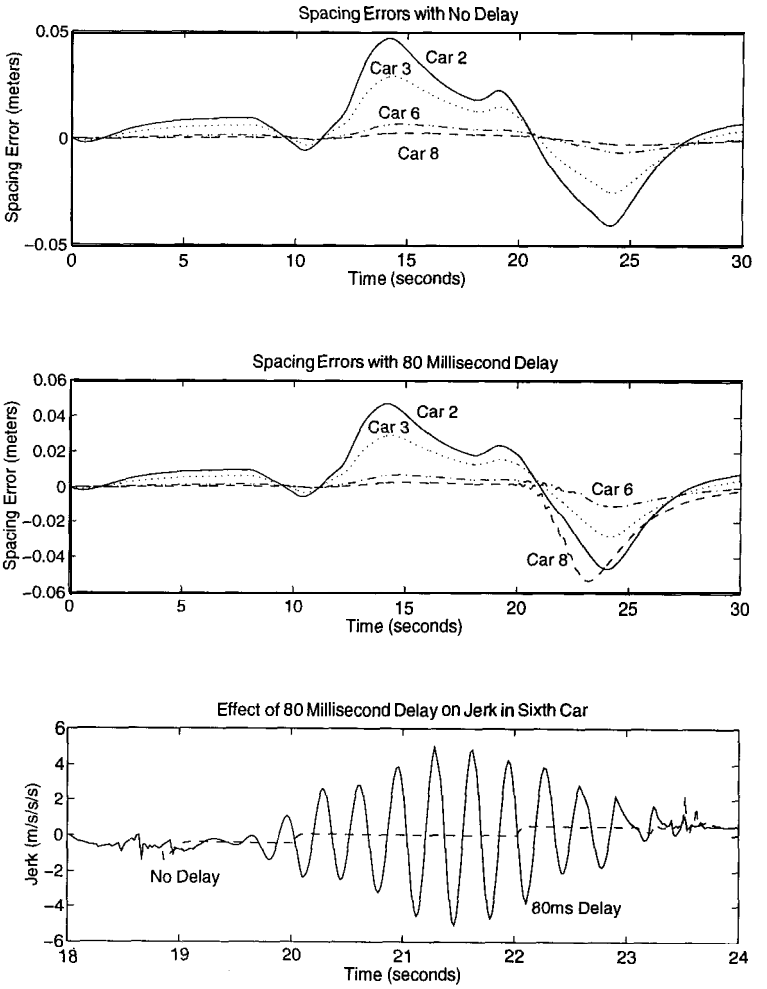

Figure 4.6: Effects of 80 Millisecond Delay

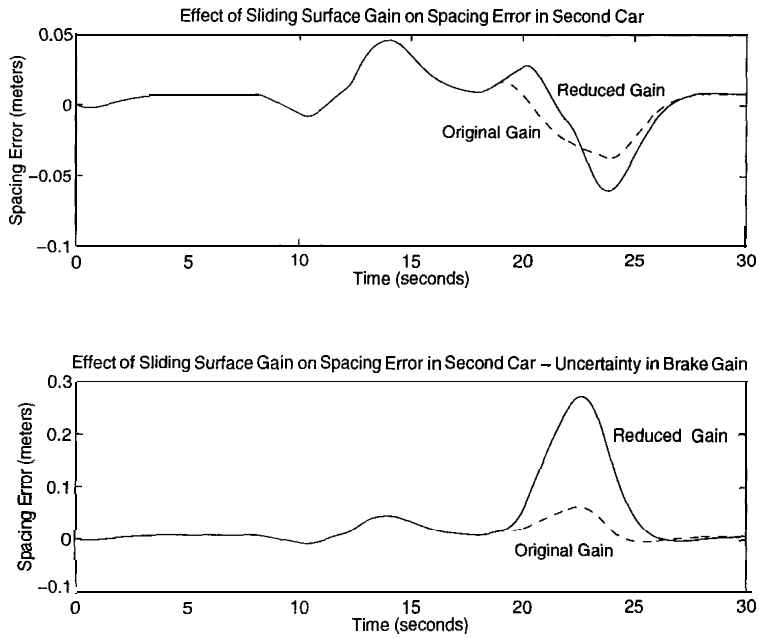

Figure 4.7: Effect, of Sliding Gain on Spacing Errors

4.4 Conclusions

This chapter has demonstrated, through simulation, the need for accurate brake torque control to ensure tight tracking and comfort in a platoon of vehicles. As a result of these simulations, we conclude that an actuation scheme capable of providing acceptable performance must bypass the booster, include some mechanism for torque feedback and eliminate time delays in the response. This requirement on the time delay is quite consistent with demands of emergency braking and highway capacity, described elsewhere in this report. While such requirements are strict, they are nevertheless feasible, and may be achieved either through actuating the master cylinder or modulating the brake pressure directly, perhaps through modulation of TCS hardware.

Chapter 5

Platooning Strategies

5.1 Introduction

Platoon control strategies directly affect traffic flow capacities. Analysis of different platooning control strategies serves two purposes: 1) Based on the information available, the most effective platooning strategy can be chosen. 2) In case of sensor failure, it provides a back-up control strategy. The effectiveness of a platoon control strategy can be gauged by the maximum traffic flow capacity, the attenuation of spacing errors, that it can guarantee and the amount of information that is needed to implement the strategy in real-time.

In this chapter, we consider the following platooning strategies : Some of the platoon control strategies have been discussed in the earlier report. We will briefly review them in this report.

1. Constant Spacing control strategies : In these strategies, the desired intervehicular spacing is independent of the velocity of the controlled vehicle. The tracking requirement is stringent, since every controlled vehicle has to match its position, velocity and acceleration with the vehicle ahead. As a consequence, these strategies require more information to guarantee performance. The achievable traffic capacity is very high in a constant spacing control strategy. We consider the following constant spacing strategies:

   Control with information of reference vehicle information only.

Autonomous and semi-Autonomous control.

Semi-Autonomous control with vehicle index information.

Control with information of preceding and reference vehicles.

Control with information of "r" immediately preceding vehicles.

Mini-platoon control.

Mini-platoon control with lead vehicle information.

2. Variable Spacing control strategies : The desired intervehicular spacing varies with the velocity of the controlled vehicle in these platooning strategies. The tracking requirement is not as stringent as the previous case. Some of the variable spacing control strategies can, therefore, be implemented with onboard sensors. However, the achievable traffic capacity is limited. We consider the following variable spacing strategies in this chapter:

   Autonomous Intelligent Cruise Control (AICC).

   Control with information of "r" immediately preceding vehicles.

3. Hybrid strategies : Constant spacing and variable spacing strategies can be combined to develop strategies that are compatible with the given information and to guarantee robustness. These strategies, however, are not analyzed in this chapter.

We also determine their performance limits in terms of string stability. The method of analysis involves the use of linear input-output norm relationships to convert the problem of the stability of a string of moving vehicles into the stability of linear difference equation with constant coefficients. We then derive sufficient conditions to ensure string stability. We demonstrate the limitations/effectiveness of these schemes by simulation results.

5.2 String Stability

The following figure illustrates the definitions of spacing errors in the platoon:

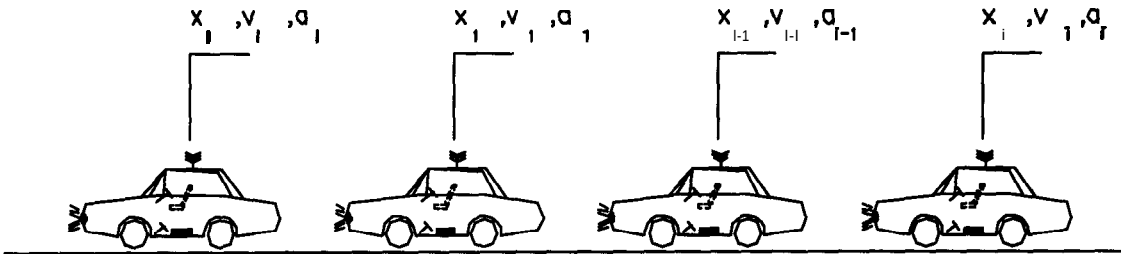

Figure 5.1: Spacing errors in a platoon

The spacing error in the i-th vehicle, ϵ_i is given by $\epsilon_i = x_i - x_{i-1} + L_i$, where L_i is the desired intervehicular spacing. The following are the platooning specifications:

1. **Individual vehicle stability:** The ability of any vehicle in the platoon to track any bounded acceleration and velocity profile of its predecessor with a bounded spacing and velocity error.

2. **String Stability:** It is required to ensure that the spacing errors do not amplify upstream from vehicle to vehicle in a platoon.

3. **Zero Steady state spacing error:** Irrespective of the lead vehicle maneuvers, it is required that every controlled vehicle maintain the desired spacing in the steady state. This is desirable to maintain a reliable traffic capacity and for safety.

Before defining string stability precisely, we need the following notations: We use $||f_i(\cdot)||_\infty$ or simply $||f_i||_\infty$ to mean $sup_{t\geq 0}|f_i(t)|$, and $||f_i(0)||_\infty$ or simply $||f(0)||_\infty$ to mean $sup_i|f_i(0)|$. Similarly $||f_i(\cdot)||_1$ or $||f_i||_1$ means $\int_0^\infty |f_i(\tau)|d\tau$, and $||f_i(0)||_1$ denotes $\sum_1^\infty |f_i(0)|$.

Definition 1: A platoon is string stable if, given $\gamma > 0$, $\exists \delta > 0$ such that whenever

$$\max \ [||\epsilon_i(0)||_\infty, ||\dot{\epsilon}_i(0)||_\infty, ||\sum_1^i \epsilon_j(0)||_\infty, ||\sum_1^i \dot{\epsilon}_j(0)||_\infty] < \delta \Rightarrow \sup_i \ ||\epsilon_i||_\infty < \gamma$$

Definition 2: A platoon is string stable in the weak sense if, given $\gamma > 0$, $\exists \delta > 0$ such that whenever

$$\max \quad [||\epsilon_i(0)||_1, ||\dot{\epsilon}_i(0)||_1] < \delta \Rightarrow \sup \quad ||\epsilon_i||_\infty < \gamma$$

Definition 3: A platoon has uniformly bounded spacing errors if given $\delta > 0$, $\exists \gamma > 0$ such that

$$\max \quad [||\epsilon_i(0)||_\infty, ||\dot{\epsilon}_i(0)||_\infty, ||\sum_1^i \epsilon_j(0)||_\infty, ||\sum_i^i \dot{\epsilon}_j(0)||_\infty] < \delta \Rightarrow \sup_i \quad ||\epsilon_i||_\infty < \gamma$$

Intuitively, string stability of the platoon implies that the spacing errors of vehicles in the platoon can be made arbitrarily small at all time, if the initial spacing errors are sufficiently small. There is an underlying difference equation which relates the maximum spacing error of the i-th vehicle with the maximum spacing errors of the vehicles preceding it. If this difference equation has all its roots inside the unit circle, then the platoon is string stable. If the difference equation has a simple root on the unit circle, then the platoon is weak sense string stable. It is clear that, every platoon of finite number of stable vehicles is string stable. Although, in practice, no platoon has infinite vehicles in it, it is necessary that platooning specifications be satisfied independent of the size of the platoon to prevent actuator saturation.

A vehicle model for control based on Cho and Hedrick, 1989 and McMahon, Hedrick and Shladover, 1990 in the previous chapter is given by:

$$\ddot{x}_i = \frac{u_i - c_i \dot{x}_i^2 - f_i}{M_i} \tag{5.1}$$

where u_i is the effective control torque (net engine/brake torque), c_i is the effective aerodynamic drag coefficient, f_i is the effective tire drag, and M_i is the effective mass of the i-th controlled vehicle. The control effort u_i is chosen to be

$$u_i = c_i \dot{x}_i^2 + f_i + M_i u_{isl} \tag{5.2}$$

so that

$$\ddot{x}_i = u_{isl} \tag{5.3}$$

where the synthetic input u_{isl} is based on the information that is available for feedback and is chosen to satisfy the performance objectives. The spacing error dynamics of vehicles in a platoon depends on the choice of u_{isl}.

Designing decentralized controllers to guarantee individual vehicle stability is a trivial design problem. However, designing decentralized controllers that ensure string stability of the platoon requires additional information such as lead vehicle velocity, acceleration information. To understand the design, consider the following interconnection of infinite identical subsystems.

Figure 5.2: Infinite Interconnection of identical systems

If ρ is the maximum gain of the system S, then

$$||\epsilon_i||_\infty \leq \rho||\epsilon_{i-1}||_\infty \leq \rho^{i-1}||\epsilon_1||_\infty$$

Clearly, to guarantee the boundedness of the output of every individual subsystem, ρ is required to be less than or equal to unity. One could associate a (worst-case) difference equation $||\epsilon_i||_\infty = \rho||\epsilon_{i-1}||_\infty$ with the above interconnected system and conclude from the characteristic equation $z = \rho$ that the above interconnected system is stable if $\rho \leq 1$. Weak string stability refers to the case when $\rho = 1$ or when some of the roots of the string stability polynomial are on the unit circle.

In the platooning scenario, ϵ_i corresponds to the spacing error dynamics of the i-th following vehicle in the platoon. The system S corresponds to the transfer function that relates the spacing error of the i-th vehicle to that of the i-l st vehicle, with the controller currently used in experimentation. S, in general, will be more complex than just a simple transfer function. For example, in control strategies where the information of two immediately preceding vehicles is available, as you will see in the following sections that, the spacing error of the i-th following vehicle is the sum of filtered versions of the spacing errors fo the i-l st and i-2 nd following vehicles. In this case, S takes in two inputs, ϵ_{i-1} and ϵ_{i-2} and the output is ϵ_i. In this case, for

string stability, the sum of the maximum gains from ϵ_{i-1} to ϵ_i (given by ρ_1) and ϵ_{i-2} to ϵ_i (given by ρ_2) is required to be less than or equal to unity. Mathematically,

$$||\epsilon_i||_\infty \leq \rho_1||\epsilon_{i-1}||_\infty + \rho_2||\epsilon_{i-2}||_\infty$$

It can be seen that the corresponding difference equation $z^2 - \rho_1 z - \rho_2 = 0$ has all its roots inside the closed unit disk, if $\rho_1 + \rho_2 \leq 1$. It is intuitive, now, that there exists a string stability polynomial associated with every platoon control algorithm and a natural metric for comparison of performance for platoon control algorithm is the spectral radius (i.e. the largest absolute value of the roots of the string stability polynomial), and is given by p.

In the ensuing discussion, we will leave the details of how ρ is calculated. Instead, we will simply describe the platoon control algorithm and present the string stability polynornial and its spectral radius, ρ. We will also discuss how ρ varies with unknown modeling errors such as parasitic actuator dynamics, sensor lags.

5.3 Constant spacing control strategies

5.3.1 Control with information of reference vehicle information only

It is insightful to look into the advantages of having reference vehicle information.

Control Law :

Consider the following control law

$$u_{isl} = \ddot{x}_l - c_v(\dot{x}_i - \dot{x}_l) - c_p(x_i - x_l + \sum L_j)$$

Henceforth, x_l refers to the position of the lead vehicle in the platoon.

Spacing Error Dynamics :

The spacing error dynamics for all strategies is obtained using the following equation :

$$\ddot{\epsilon}_i = \ddot{x}_i - \ddot{x}_{i-1} = u_{isl} - u_{(i-1)sl}$$

From the above two equations, we obtain

$$\ddot{\epsilon}_i + c_v\dot{\epsilon}_i + c_p\epsilon_i = 0$$

The stability polynomial associated with this strategy is $z = 0$. This is the "best" achievable platoon performance. It is unsafe since it does not take the information of the preceding vehicle into consideration. In the context of lateral vehicles, the road serves as a reference vehicle for all the vehicles and hence, it is the best possible lateral control algorithm for lateral string stability of the platoon.

5.3.2 Autonomous control

In this strategy, control law is based only on the on-board sensor measurements.

Control Law :

$$u_{isl} = -k_v\dot{\epsilon}_i - k_p\epsilon_i$$

Spacing Error Dynamics :

$$\hat{\epsilon}_i(s) = \hat{H}(s)\hat{\epsilon}_{i-1}(s)$$

where

$$\hat{H}(s) = \frac{k_v s + k_p}{s^2 + k_v s + k_p}$$

$$\Rightarrow |\hat{H}(jw)| = \frac{k_p^2 + k_v^2 w^2}{(k_p - w^2)^2 + k_v^2 w^2}$$

For all $k_v > 0$, $k_p > 0$, $|\hat{H}(jw)| \geq 1$ for sufficiently small frequencies. A sinusoidal lead vehicle acceleration profile at that frequency results in errors amplifying along the platoon. Consequently, $\rho > 1$ and the stability polynomial associated with this strategy, $z = \rho$, is unstable.

5.3.3 Semi-Autonomous control

In this control strategy, preceding vehicle's acceleration information is assumed to be available or estimated accurately.

Control Law :

$$u_{isl} = k_a\ddot{x}_{i-1} - k_v\dot{\epsilon}_i - k_p\epsilon_i$$

Spacing Error Dynamics :

$$\hat{\epsilon}_i(s) = \hat{H}(s)\hat{\epsilon}_{i-1}(s)$$

where

$$\hat{H}(s) = \frac{k_a s^2 + k_v s + k_p}{s^2 + k_v s + k_p}$$

If $k_a > 1, |\hat{H}(jw)| > 1$ for w sufficiently high. Hence, any lead vehicle acceleration at such a high frequency results in errors getting amplified along the platoon. If $k_a < 1$, then for all $k_v > 0$, $k_p > 0$, $|H(jw)| \geq 1$ for sufficiently small frequencies. Therefore, for string stability, $k_a = 1$ and $\hat{H}(s) \equiv 1$. The string stability polynomial, in this case, is $z = 1$. Potentially, weak string stability can be guaranteed.

Robustness to Signal Processing/ Actuator Lags : As a result of signal processing/actuator lags, the control effort, u_{isl}, is the output of a filter

$$\tau\dot{u}_{isl} + u_{isl} = k_a\ddot{x}_{i-1} - k_v\dot{\epsilon}_i - k_p\epsilon_i$$

The perturbed transfer function $\hat{H}_p(s) = \frac{s^2+k_v s+k_p}{\tau s^3+s^2+k_v s+k_p}$ and $|\hat{H}_p(jw)| > 1$ for all $\tau > 0$ and for sufficiently small frequencies. Consequently, $\rho > 1$ and the stability polynomial associated with this strategy, $z = \rho$, is unstable and therefore, this scheme cannot be used for platooning.

5.3.4 Control with information of lead and preceding vehicles

With lead vehicle acceleration, velocity and position information, Hedrick, et.al., 1991, define S_i as

$$S_i = \dot{\epsilon}_i + q_1\epsilon_i + q_3(v_i - v_l) + q_4(x_i - x_l + \sum_{j=1} L_j)$$

S_i incorporates the information of the lead and preceding vehicles. It is chosen in such a way that the spacing error dynamics on the surface $S_i = S_{i-1} = 0$ is string stable.

Spacing Error Dynamics :

$$\hat{\epsilon}_i(s) = \frac{s + q_1}{(1 + q_3)s + (q_1 + q_4)}\hat{\epsilon}_{i-1}(s) + \frac{(S_i - S_{i-1}) + ((1 + q_3)\epsilon_i(0) - \epsilon_{i-1}(0))}{(1 + q_3)s + (q_1 + q_4)}$$

with

$$\dot{S}_i + \lambda S_i = 0$$

Control Law :

$$u_{isl} = \frac{1}{1 + q_3}[\ddot{x}_{i-1} + q_3\ddot{x}_l - (q_1 + \lambda)\dot{\epsilon}_i - q_1\lambda\epsilon_i - (q_4 + \lambda q_3)(v_i - v_l) - \lambda q_4(x_i - x_l + \sum_{j=1}^{i} L_j)]$$

With this control law, $\rho = \frac{q_1}{q_1+q_4}$ and the string stability polynomial is $z = \rho$, which is stable.

Robustness to Actuator/Signal processing lags

With actuator/signal processing lags, the actual input (throttle/brake) to the system is a first order filtered output, u_f, of u_i.

$$\ddot{x}_i = \frac{u_f - c_i\dot{x}_i^2 - f_i}{M_i}$$

where

$$\tau\dot{u}_f + u_f = c_i\dot{x}_i^2 + f_i + M_i u_{isl}$$

$$\Longrightarrow \tau\frac{d}{dt}\ddot{x}_i + \ddot{x}_i(1 + \frac{2c_i\dot{x}_i}{M_i}) = u_{isl}$$

It can be shown that for small actuator lags, the string stability polynomial is $z = \rho$ where $\rho = \frac{q_1}{q_1+q_4}$.

5.3.5 Semi-Autonomous control with vehicle ID knowledge

It is desirable to guarantee string stability or at least uniform boundedness of spacing errors with as little external information as possible. In such a case, autonomous/ semi-autonomous implementation is possible. In this section, we will investigate such a scheme.

Modifying the control law from the earlier subsection,

$$u_{isl} = \frac{1}{1+q_3}[\ddot{x}_{i-1} - (q_1+\lambda)\dot{\epsilon}_i - q_1\lambda\epsilon_i - (q_4+\lambda q_3)(v_i - v_l) - \lambda q_4(x_i - x_l + \sum_{j=1}^{i} L_j)]$$

Notice that the lead vehicle acceleration information is not utilized in this scheme. If the lead vehicle velocity and position information can, somehow, be reconstructed knowing vehicle index, then a semi-autonomous implementation is possible.

Spacing Error Dynamics :

$$\hat{\epsilon}_i(s) = \hat{H}(s)\hat{\epsilon}_{i-1}(s)$$

$$\hat{H}(s) = \frac{1}{1+q_3}\frac{(s+q_1)}{(s+\frac{q_1+q_4}{1+q_3})}$$

$$\hat{\epsilon}_{i-j} = \hat{H}^{-j}(s)\hat{\epsilon}_i$$

The last equation is used to estimate the spacing error in the j-th vehicle ahead of every controlled vehicle. The string stability polynomial for this scheme is $z = \rho$ with $\rho = \frac{q_1}{q_1+q_4}$.

Control Law :

The control law is implemented as follows:

$$u_{isl} = \frac{1}{1+q_3}[\ddot{x}_{i-1} - (q_1+\lambda)\dot{\epsilon}_i - q_1\lambda\epsilon_i - [1 + \hat{H}^{-1} + \ldots + \hat{H}^{-(i-1)}]\{(q_4+\lambda q_3)\dot{\epsilon}_i + \lambda q_4\epsilon_i\}]$$

Knowing $\epsilon_i, \dot{\epsilon}_i, \ddot{x}_{i-1}$ and i, the vehicle index, we can guarantee that $\rho = \frac{q_1}{q_1+q_4}$. Knowledge of $\ddot{x}_{i-1}$ is essential, otherwise, H(s), is strictly proper and $\hat{H}^{-1}$ is not realizable. This scheme is attractive, since it requires the minimum information to guarantee uniform boundedness of spacing errors

for a constant spacing strategy. Autonomous implementation is dependent on how smooth the signals $\ddot{x}_i$ and $\dot{\epsilon}_i$ are, to allow for estimating $\ddot{x}_{i-1}$ via numerical differentiation. Drawbacks include requiring very accurate signals of $\epsilon_i, \dot{\epsilon}_i$ and requiring $q_4 << q_1$. The number of vehicles in the platoon is constrained, since our performance objective is to let $||\hat{H}(jw)|| \leq 1$. While estimating the lead vehicle information, inversion of this transfer function is necessary, which leads to amplification of the noise.

Another way to utilize the information of vehicle ID is to vary the gains in the controller depending on the vehicle index. However, in order to guarantee uniform boundedness for this case, the gains have to increase at least linearly. This results in increased control effort at the tail of the platoon, leading to saturation in the throttle angle input in the corresponding vehicles. Real-time implementation details are shown in Swaroop, 1994.

5.3.6 Control With Information of "r" Vehicles Ahead

If a platoon consists of a large number of vehicles, the communication delays of information from the lead vehicle to the end of the platoon could degrade the platoon performance significantly. In order to circumvent such delays, a platoon strategy in which every controlled vehicle requires only the information of vehicles in its vicinity, is desirable. However, the string stability aspect of such a scheme has to be analyzed.

Control Law :

Consider the following control strategy where every controlled vehicle has the information of its "r" preceding vehicles:

$$u_{isl} = \sum_{j=1}^{r} k_{aj}\ddot{x}_{i-j} - k_{vj}(v_i - v_{i-j}) - k_{pj}(x_i - x_{i-j} + \sum_{k=\max[0,i-j+1]}^{i} L_k)$$

with $x_{i-j} \equiv x_l \qquad \forall \ i \leq j.$

Spacing Error Dynamics :

$$\hat{\epsilon}_i(s) = \sum_{j=1}^{r} \hat{H}_j(s)\hat{\epsilon}_{i-j}(s)$$

$$\hat{H}_j(s) = \frac{k_{aj}s^2 + k_{vj}s + k_{pj}}{s^2 + \sum_{j=1}^{r}(k_{vj}s + k_{pj})}$$

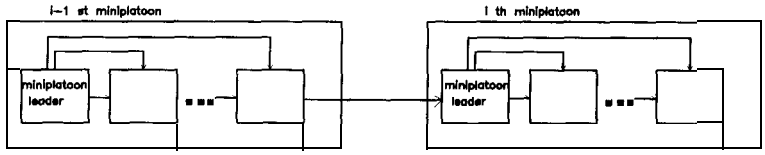

Figure 5.3: Mini-platoon information structure

The string stability polynomial for this scheme can, at best, be made $z^r = \sum_1^r \rho_j z^{r-j}$ with $\sum_1^r \rho_j = 1$. As a result, there is a pole on the unit circle at $z = 1$, and we can guarantee string stability in the "weak" sense only. The platoon performance, in terms of string stability, is limited.

Robustness to Actuator/ Signal Processing Lag :

In order to achieve the best possible platoon performance, weak sense string stability, $\hat{H}_j(s)$ has to be a constant. In the presence of actuator lag, the string stability polynomial is $z = \rho$ where $\rho > 1$. The magnitude of ρ depends on the value of the actuator lag.

5.3.7 Mini-platoon control strategy

String stability is guaranteed in the constant spacing control strategies proposed in Hedrick, et.al., 1991, because every controlled vehicle receives information from a reference (lead) vehicle. The mini-platoon control strategy uses the idea that feeding back information from a reference vehicle improves the robustness properties of the string, while reducing the effects of communication delays associated with transmitting the lead vehicle information. In this control strategy, every platoon is divided into mini-platoons and the last vehicle of a mini-platoon becomes the reference vehicle for the following mini-platoon. Figure 5.3 show how the information is transmitted between vehicles in the platoon. The controller given in Hedrick, et.al., 1991 is modified as follows:

$$S_i = \dot{\epsilon}_i + q_1\epsilon_i + q_3(v_i - v_{ref}) + q_4(x_i - x_{iref} + \sum_{j=iref+1}^{i} L_j)$$

where the subscript ref refers to the index of the reference vehicle for the controlled vehicle (i.e., index of the leader of the mini-platoon to which the

controlled vehicle belongs). For the sake of analysis, we assume that every mini-platoon consists of "r" vehicles.

Control Law :

The control input u_{isl} is chosen to make $\dot{S}_i + \lambda S_i = 0$. The corresponding control input is given below:

For $nr + 1 \leq$ i < (n $+1)r, \forall\ n = 0, 1, 2, ..,$ where n denotes the n-th mini-platoon,

$$u_{isl} = \frac{1}{1+q_3}[\ddot{x}_{i-1} + q_3\ddot{x}_{nr} - (q_1 + \lambda)\dot{\epsilon}_i - q_1\lambda\epsilon_i$$

$$-(q_4 + \lambda q_3)(v_i - v_{nr}) - \lambda q_4(x_i - x_{nr} + \sum_{j=nr+1}^{i} L_j)] \tag{5.4}$$

For $i = nr,\ \forall\ \ n = 1, 2, .$

$$u_{isl} = \frac{1}{1+q_3}[\ddot{x}_{i-1} + q_3\ddot{x}_{(n-1)r} - (q_1 + \lambda)\dot{\epsilon}_i - q_1\lambda\epsilon_i$$

$$-(q_4 + \lambda q_3)(v_i - v_{(n-1)r}) - \lambda q_4(x_i - x_{(n-1)r} + \sum_{j=(n-1)r+1}^{i} L_j)] \tag{5.5}$$

Spacing Error Dynamics :

For $nr + 2 \leq i \leq (n+1)r,$

$\hat{\epsilon}_i(s) = \hat{H}(s)\hat{\epsilon}_{i-1}(s)$

and

$\hat{\epsilon}_{nr+1}\ (s) = \hat{\epsilon}_{(n-1)r+1}\ (s)$

where $\hat{H}(s) = \frac{s+q_1}{(1+q_3)s+(q_1+q_4)}$. From the last equation, the spacing error dynamics of the first following vehicle in the miniplatoon determine the stability of the platoon. The worst case difference equation associated with their error dynamics is $||\epsilon_{nr+1}||_\infty = ||\epsilon_{(n-1)r+1}||_\infty$. Since the roots of the string stability polynomial, $P_r(z) = z^r - 1 = 0$, are simple and lie on the unit circle, this

platooning strategy is string stable in the "weak" sense. Due to signal processing lags, the perturbed polynomial is given by $z^r - \alpha = 0$ where $\alpha > 1$. The roots of the perturbed polynomial are all outside the unit circle and their magnitude is $\alpha^{\frac{1}{r}}$. Hence, the spacing errors of the first followers increase with mini-platoon index. The magnitude of the perturbed roots gives the average attenuation/amplification upstream from vehicle to vehicle. The spacing errors attenuate geometrically within the mini-platoon. Since the number of vehicles in the platoon is finite, in practice, the maximum number of vehicles in a mini-platoon is determined by the hardware/communication limitations.

The advantage of this scheme is that we need to focus our attention only on the leaders of the mini-platoon. One could treat the dynamics of a platoon by the dynamics of its leader in a higher level of control for automated highway systems. If every controlled vehicle in the platoon has the information of its "r" preceding vehicles, we have seen that constant spacing strategy yields limited robustness. Instead, we should organize the platoon into miniplatoons of "r" vehicles. At least, vehicles in the mini-platoon exhibit geometric attenuation and good robustness property to actuator/sensor lags.

5.3.8 Mini-platoon control with lead vehicle information

The motivation for this scheme is to improve the robustness property of the leaders of the mini-platoon by making lead vehicle information available to the leaders of the mini-platoon. Consider a scheme in which the leader of every mini-platoon gets information from its preceding vehicle and the leader of the platoon and all the vehicles in the mini-platoon get information from their predecessors and the leader of the mini-platoon. For the sake of analysis, we assume that every mini-platoon has "r" vehicles in it. For real-time implementation, it is envisaged that the lead vehicle information is updated on a slower time scale compared to the other information that is required for feedback control law.

Control Law:

Consider the following control law:

$$u_{jsl} = \frac{1}{1+q_3}[\ddot{x}_{jsl} + q_3\ddot{x}_{ir+1} - (q_1+\lambda)\dot{\epsilon}_j - q_1\lambda\epsilon_j - (q_4+\lambda q_3)(\dot{x}_j - \dot{x}_{ir+1})$$

$$-\lambda q_4(x_j - x_{ir+1} + \sum_{ir+2}^{j} L_q)] \ \forall \ ir+1 < j \leq ir + r, i = 0, 1, 2, ..$$

and

$$u_{ir+1} = \frac{1}{1+q_3}[\ddot{x}_r + q_3\ddot{x}_1 - (q_1+\lambda)\dot{\epsilon}_{ir+1} - q_1\lambda\epsilon_{ir+1} - (q_4+\lambda q_3)(\dot{x}_{ir+1} - \dot{x}_1)$$

$$-\lambda q_4(x_{ir+1} - x_1 + \sum_{2}^{ir+1} L_j)] \quad \forall \text{ i} = 1, 2, 3, \ldots \tag{5.6}$$

Spacing Error Dynamics :

With this control law, we can show that

$$\hat{\epsilon}_j(s) = \hat{H}(s)\hat{\epsilon}_{j-1}(s) \ \forall \ ir + 1 < j \leq (\text{i} + 1)r$$

where

$$\hat{H}(s) = \frac{(s+q_1)(s+\lambda)}{1+q_3\ s^2 + (\frac{q_1+q_4}{1+q_3} + \lambda)s + \frac{\lambda(q_1+q_4)}{1+q_3}}$$

Therefore, the maximum spacing errors decrease geometrically within a mini-platoon. The spacing error dynamics of the leaders of mini-platoon is given by the following equations:

$$\epsilon_{ir+1} = \hat{H}^r(s)\hat{\epsilon}_{(i-1)r+1}$$

Therefore, the maximum spacing errors of the leaders of the mini-platoon attenuate with the same geometric ratio. The string stability polynomial for this control algorithm is $z^r = \rho^r$ where $\rho = \frac{q_1}{q_1+q_4}$.

It is hoped that the maximum spacing errors of the leaders of the mini-platoon do not amplify with a slower time scale update of the lead vehicle information. A detailed two scale analysis of this strategy is necessary to implement this strategy.

5.4 Variable Spacing Control Strategies

5.4.1 Autonomous Intelligent Cruise Control (AICC)

It is worthwhile considering the effect of feeding back controlled vehicle's velocity on the platooning specifications. Consider the following control law:

$$u_{isl} = k_a \ddot{x}_{i-1} - k_v \dot{\epsilon}_i - k_p \epsilon_i - k_1 \dot{x}_i$$

The spacing error dynamics is given by:

$$\ddot{\epsilon}_1 + (k_v + k_1)\dot{\epsilon}_1 + k_p \epsilon_1 = (k_a - 1)\ddot{x}_l - k_1 \dot{x}_l$$

$$\ddot{\epsilon}_i + (k_v + k_1)\dot{\epsilon}_i + k_p \epsilon_i = k_a \ddot{\epsilon}_{i-1} + k_v \dot{\epsilon}_{i-1} + k_p \epsilon_{i-1}$$

From the above equations, it is clear that non-zero steady state errors result from a step change in lead vehicle's velocity. The magnitude of the error is given by $-\frac{k_1}{k_p}\Delta v$, where Δv is the step change in velocity. The negative sign indicates that the vehicles fall back whenever Δv is positive. The spacing between vehicles is higher at higher speeds. It is also clear that k_1 is required to be zero for zero steady state spacing error for any step change in lead vehicle velocity. However, in order to ensure string stability, $k_1 \neq 0$. Hence, for the autonomous case, zero steady state spacing error and string stability requirements are at odds with each other. It is intuitive that the magnitude of steady state spacing errors that can be tolerated relates directly to the robustness of this scheme to actuator/signal processing lags. If the zero steady state spacing error specification is relaxed, we can define a generalized spacing error of the i-th vehicle, δ_i, as follows:

$$\delta_i = x_i - x_{i-1} + L_i + h_w \dot{x}_i$$

where h_w is the desired constant headway time [1] to be maintained. This is the basis for AICC law proposed by Chien, Ioannou and Hauser, 1992.

Control Law :

Consider the following law, which requires on-board information only (Chien, Ioannou and Hauser, 1992) :

$$u_{isl} = -\frac{\dot{x}_i - \dot{x}_{i-1} + \lambda \epsilon_i}{h_w} \tag{5.7}$$

[1] Headway time is defined as the time it takes the vehicle i to cover a distance $x_i - x_{i-1} + L_i$

Generalized Spacing Error Dynamics :

The generalized spacing error dynamics is given by:

$$h_w\ddot{\delta}_i + (1 + \lambda h_w)\dot{\delta}_i + \lambda\delta_i = \dot{\delta}_{i-1} + \lambda\delta_{i-1}$$

and

$$h_w\ddot{\delta}_1 + (1 + \lambda h_w)\dot{\delta}_1 + \lambda\delta_1 = 0$$

From the above equations,

$$\hat{H}(s) = \frac{\hat{\delta}_i}{\hat{\delta}_{i-1}}(\mathrm{s}) = \frac{1}{h_w s + 1}$$

Clearly, $\rho = 1$ for all $h_w > 0$. This is a very attractive feature of this strategy considering that no lead vehicle information is fed back. There are two drawbacks of this scheme:

1. The control effort is inversely proportional to the desired headway time. For maintaining a small desired headway time, the brake and engine torques may saturate. This fact is also documented in Chiu, Stupp and Brown, 1977.

2. A small desired headway time implies larger traffic capacity. Hence, there is a limit on the maximum traffic capacity that is achievable.

Robustness to Actuator/Signal processing lags:

As seen earlier, actuator/signal processing lags can be modelled as

$$\tau\frac{d}{dt}\ddot{x}_i + \dddot{x}_i = u_{isl}$$

From equation 5.7 and the above equation, we get,

$$\tau h_w\frac{d}{dt}\ddot{\delta}_i + h_w\ddot{\delta}_i + (1 + \lambda h_w)\dot{\delta}_i + \lambda\delta_i = \dot{\delta}_{i-1} + \lambda\delta_{i-1}$$

$$\Longrightarrow \frac{\hat{\delta}_i}{\hat{\delta}_{i-1}} := \hat{H}_p(s) = \frac{s + \lambda}{\tau h_w s^3 + h_w s^2 + (1 + \lambda h_w)s + \lambda}$$

Claim:

1. For sufficiently small $\tau, ||\mathcal{L}^{-1}(\hat{H}_p(s))||_1 = 1$.

2. $||\mathcal{L}^{-1}(H_p(s))||_1 = 1 \Rightarrow \tau \leq \frac{h_w}{2}$.

Proof:

1. See Swaroop, 1994.
2.A necessary condition for $||L^{-1}(H_p(s))||_1 = 1$ is that $|\hat{H}_p(jw)| \leq 1 \; \forall \, w$. Therefore,

$$w^2 + \lambda^2 \leq (\lambda - h_w w^2)^2 + (1 + \lambda h_w - \tau h_w w^2)^2 w^2$$

$$\Longrightarrow \mathbf{0} \leq \tau^2 h_w^2 w^4 + (h_w^2 - 2\tau h_w(1 + \lambda h_w))w^2 + \lambda^2 h_w^2 \; \forall \; w$$

From theory of quadratic equations, the above inequality holds if and only if one of the following inequalities hold:

1. $h_w^2 - 2\tau h_w(1 + \lambda h_w) \geq 0$

   or

2. $(h_w^2 - 2\tau h_w(1 + \lambda h_w))^2 - 4\lambda^2 h_w^2 \tau^2 h_w^2 \leq 0$

Both the conditions are satisfied only if $\tau \leq \frac{h_w}{2}$.

This result establishes that the robustness in string stability at a small time headway is limited.

5.4.2 Constant headway time control strategy with information of "r" vehicles ahead

Feeding back controlled vehicle's velocity results in non-zero steady state errors for most lead vehicle maneuvers. However, it improves the robustness in string stability to actuator lags and signal processing lags. The degree of robustness in string stability depends on the magnitude of non-zero steady state errors that can be tolerated. This scheme has also been proposed independently by Green and Ren, 1994.

Control Law :

Consider the following control law:

$$u_{isl} = \sum_{j=1}^{r}[k_{aj}\ddot{x}_{i-j} - k_{vj}(v_i - v_{i-j}) - k_{pj}(x_i - x_{i-j} + \sum_{k=\max[0,i-j+1]}^{i} L_k)] - k_v\dot{x}_i$$

with $x_{i-j} \equiv x_l \quad \forall\, i \leq j$. This results in a state state spacing error in i-th following vehicle given by $\epsilon_{iss} = \frac{k_v}{\sum_{j=1}^{r} jk_{pj}}\Delta v$ where Δv is any step change in the lead vehicle's velocity. In this strategy, the desired intervehicular spacing varies as $L_i + h_w v_i$, where $h_w = \frac{k_v}{\sum_{j=1}^{r} jk_{pj}}$.

Generalized Spacing Error Dynamics

$$\ddot{\delta}_i + (\sum_{j=1}^{r} k_{vj} + k_v)\dot{\delta}_i + \sum_{j=1}^{r} k_{pj}\delta_i = \sum_{j=1}^{r}[k_{aj}\ddot{\delta}_{i-j} + k_{vj}\dot{\delta}_{i-j} + k_{pj}\delta_{i-j}]$$

Therefore,

$$\sum_{j=1}^{r} \hat{H}_j(s) = \frac{\sum_{j=1}^{r}(k_{aj}s^2 + k_{vj}s + k_{pj})}{s^2 + \sum_{j=1}^{r}[(k_{vj} + k_v/r)s + k_{pj}]}$$

The string stability polynomial for this scheme is , at best, $z^r = \sum_1^r \rho_j z^{r-j}$ with $\sum_1^r \rho_j = 1$. Only weak string stability can be guaranteed as a result. To guarantee string stability and to maintain a small headway time, the closing rate gains have to be chosen sufficiently high. There is an upper bound on these gains, which is determined by the input bandwidth/saturation constraints, and hence, there is a lower limit on h_w. The limiting case of the headway control strategy, h_w = 0, is the constant spacing control strategy, which clearly lacks robustness to parasitic dynamics in the actuator and signal processing lags as seen in section 3.6. Therefore, an arbitrarily small headway time cannot be maintained. The steady state spacing errors are dependent on the lead vehicle maneuver and may not decay exponentially to zero. In addition to the above limitations, this strategy requires the information of all the "r" vehicles ahead of it, which may put a serious burden on the communication system.

Consider a hybrid mini-platoon strategy in which the leaders of the mini-platoon follow AICC while the vehicles in the mini-platoon follow constant spacing strategy (with the information of the leader of mini-platoon). The Headway control strategy with information of "r" preceding vehicles is inferior to this strategy in two ways:

- Robustness to lags : Follower vehicles in the mini-platoon are robust to actuator/signal processing lags. Robustness of the leaders of the mini-platoon is governed by the time headway they have to maintain.

- Traffic Capacity : The average time headway for hybrid mini-platoon strategy is h_w/r where h_w is the time headway the leaders of the mini-platoon maintain and r is the number of vehicles in the mini-platoon.

In other words, for the same traffic throughput, the leaders of the mini-platoon can maintain "r" times the time headway each vehicle maintains in the other strategy. Since robustness is inversely proportional to time headway, hybrid mini-platoon strategy guarantees better robustness properties.

5.5 Simulation Results

In this section, we will briefly summarize the salient features of all the strategies and show their corresponding simulation results. For all the simulation plots, a 10 vehicle platoon is considered. In all the simulation plots, the number n on the plot represents the n-th following vehicle in the platoon. All the vehicles start with a velocity of $24.5m/s$ and they are positioned in such a way that the initial spacing error is zero. The plant model of the vehicle has a throttle angle saturation rate of $1000°/s$ and a brake saturation limit of 8000N $-$ m.

Figure 5.4 demonstrates the behavior of spacing errors under semi-autonomous constant spacing control. In this strategy, every controlled vehicle requires the acceleration information of its preceding vehicle in addition to on-board sensor information like the spacing and velocity error from the radar. As seen earlier in this chapter, every platooning strategy has an associated string stability polynomial and the spectral radius of the polynomial is a measure of the effectiveness (in terms of string stability) for the strategy. For string stability, the spectral radius of the polynomial should be less than unity. A platoon is string stable in the weak sense if the spectral radius is equal to unity. For this strategy, the string stability polynomial is $z = 1$ and this strategy is string stable in the weak sense. The gains used for this simulation are: k_a = 1; k_v = 2; k_p = 1. As expected, due to mismatched uncertainties in the plant (discretization etc.,), the spacing errors and consequently, the control effort grow with vehicle index. Figure 5.5 shows the effect of signal

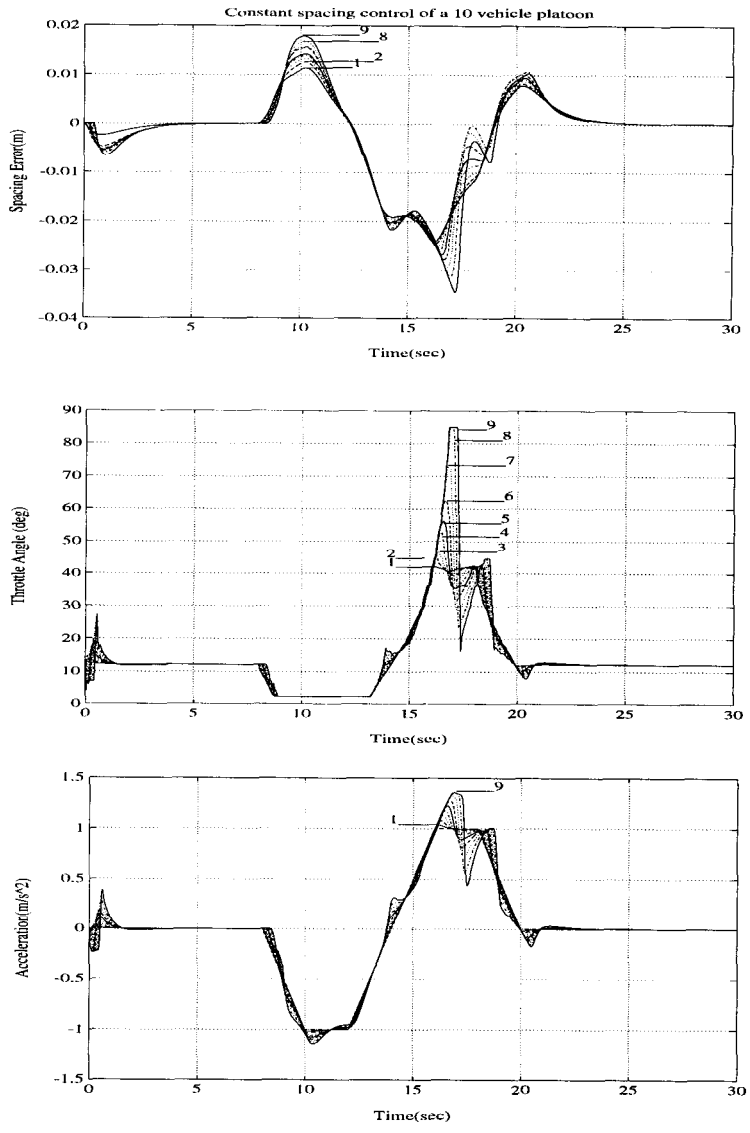

Figure 5.4: Constant spacing semi-autonomous control of a 10 vehicle platoon.

processing lags on the spacing errors. The throttle angle of all the vehicles behind the fourth following vehicle is saturated. In all the above simulations, accelerations of the preceding vehicle is assumed to be available or estimated accurately. With any signal processing or actuator lags, the string stability polynomial is $z = \rho$ where $\rho > 1$ and this scheme is not robust. Clearly, semi-autonomous constant spacing strategy cannot be used for platooning.

Figure 5.6 shows the effect of availability of lead vehicle velocity and acceleration information to every controlled vehicle, on the platoon performance. The spacing errors decrease with vehicle index in this case. The gains selected are as follows: $q_1 = 1.0$, $q_3 = 0.5$, $\lambda = 1$. Figure 5.7 shows the effect of signal processing /actuator lags. The spacing errors, in the presence of signal processing lag of 50ms, are larger in magnitude. The throttle angle increases initially with vehicle index due to the feedback from the lead vehicle. Since the maximum spacing error decreases with vehicle index, the spacing error relative to the lead vehicle remains the same for all the vehicles at the tail of the platoon. As a result, the throttle angle (control effort) is the same for all the vehicles at the tail of the platoon. Although the associated string stability polynomial for this strategy is $z = 1$, the string stability polynomial is robust to actuator/signal processing lags.

In obtaining the simulation result shown in figure 5.8, we have assumed that every controlled vehicle in the platoon has the information of lead vehicle's relative position information. The following gains are chosen: $q_1 = 0.8$; $q_3 = 0.5$; $q_4 = 0.4$; $\lambda = 1$. Clearly, the spacing errors decrease with a geometric ratio given by $\frac{q_1}{q_1+q_4}$. The associated string stability polynomial for this strategy is $z = \frac{q_1}{q_1+q_4}$. The string stability polynomial is robust to signal processing/ actuator lags. In the presence of small signal processing/actuator lags, although the magnitude of spacing errors is high, the attenuation ratio remains constant. Figure 5.9 shows this behavior.

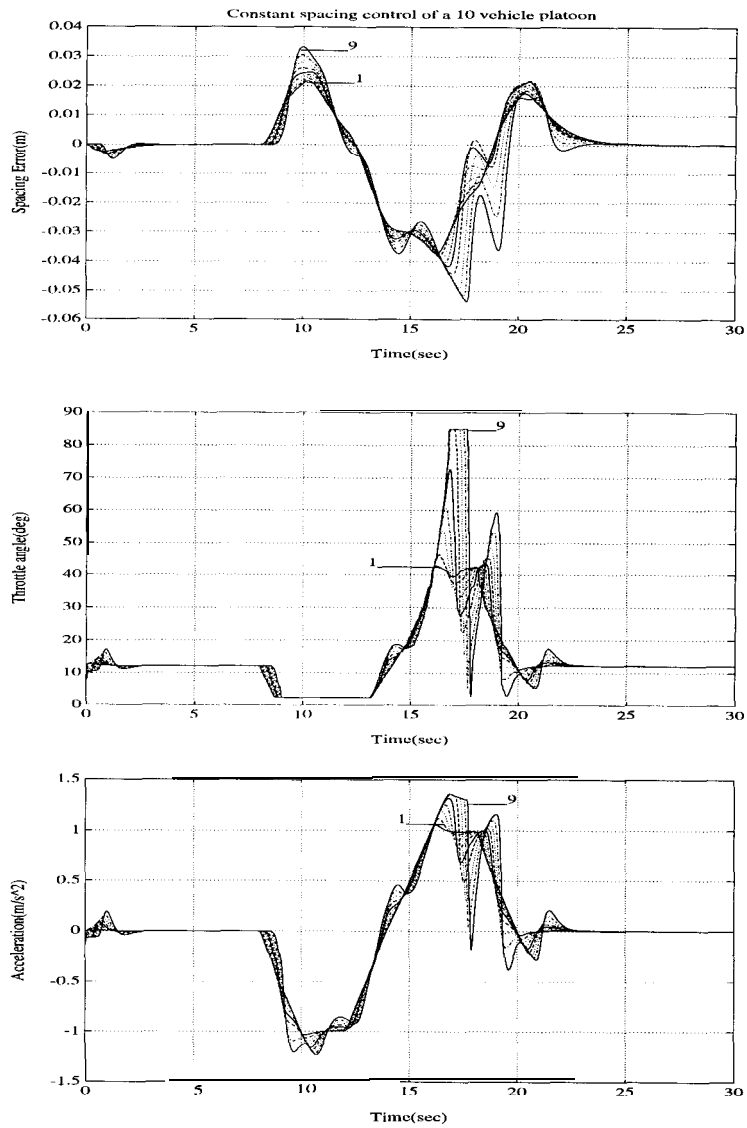

Figure 5.5: Semi-autonomous control with signal processing lag of 50ms.

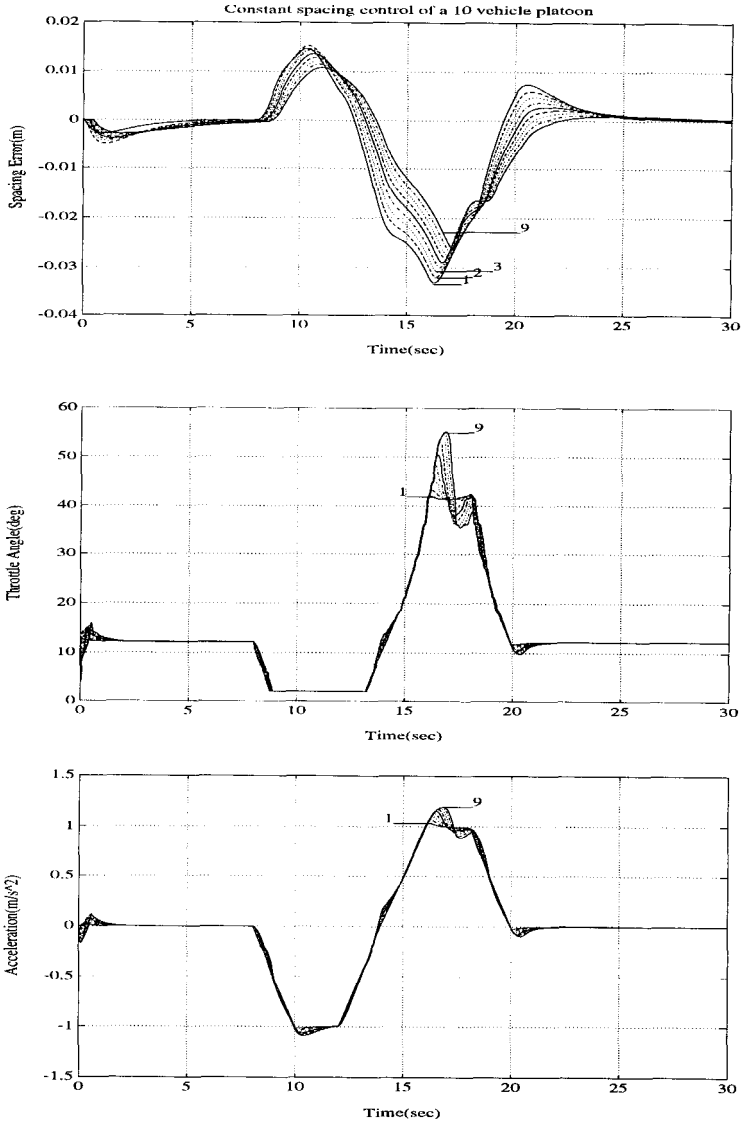

Figure 5.6: Constant spacing control of a 10 vehicle platoon with lead vehicle velocity and acceleration information.

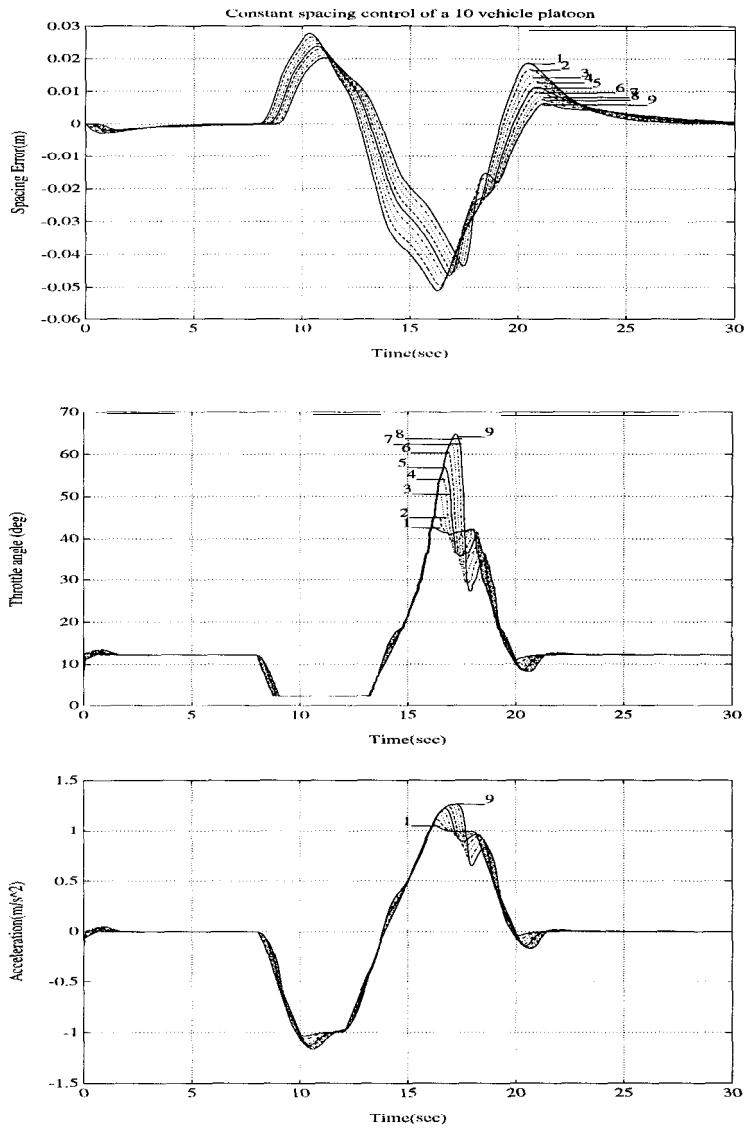

Figure 5.7: Constant spacing control of a 10 vehicle platoon with lead vehicle velocity and acceleration information and with a signal processing lag of 50 ms.

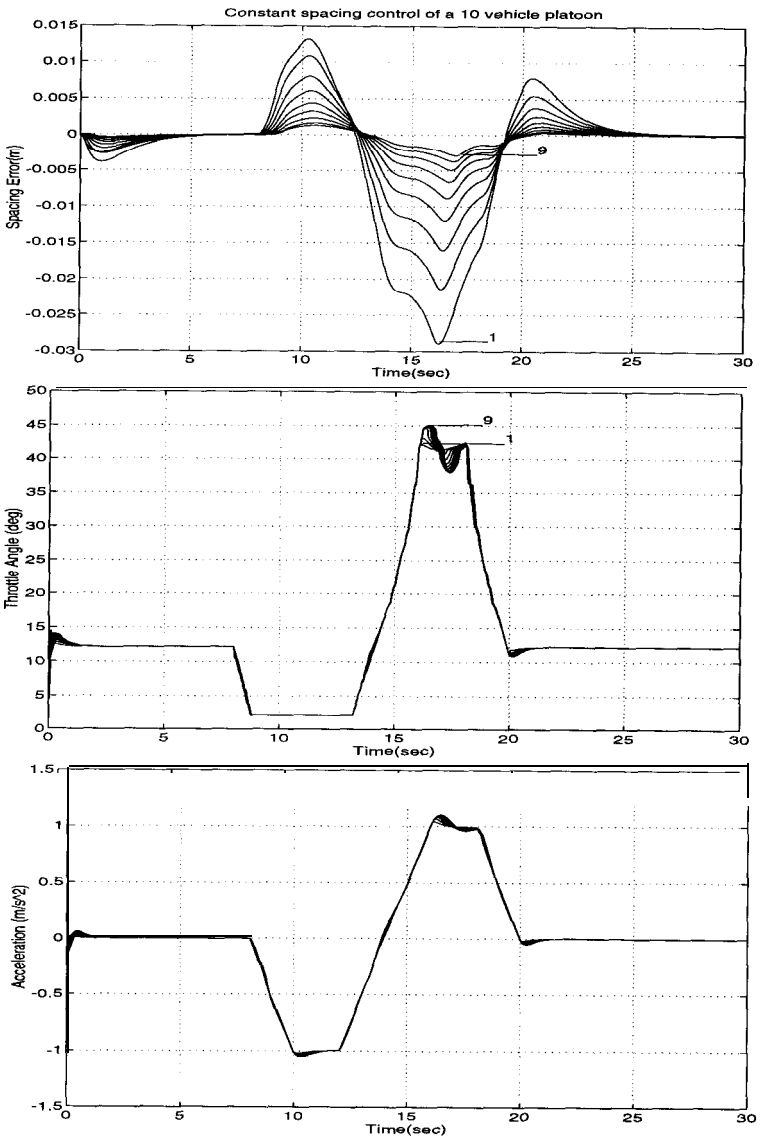

Figure 5.8: Constant spacing control of a 10 vehicle platoon with lead vehicle acceleration, velocity and position information.

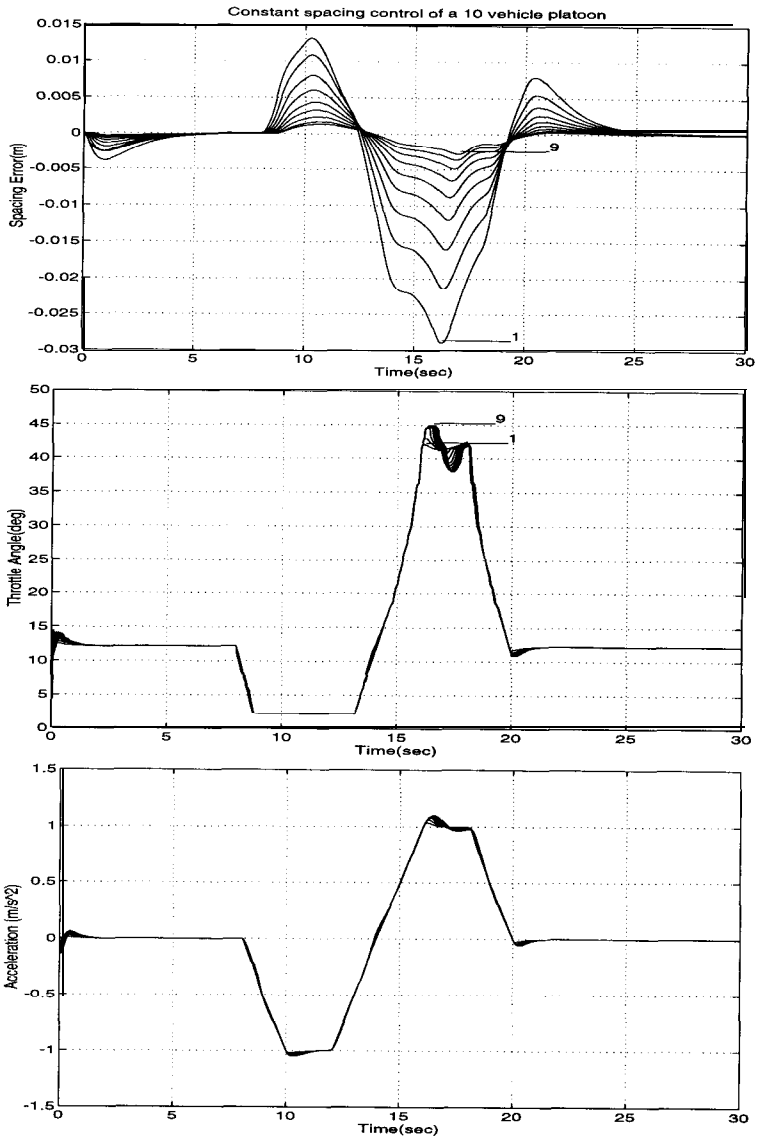

Figure 5.9: Constant spacing control of a 10 vehicle platoon with lead vehicle acceleration, velocity and position information and with a signal processing lag of 50ms.

In order to obtain the relative position information of the lead vehicle relative to the controlled vehicle, we plan to do the following:

1. Integrate numerically the velocity of the controlled vehicle relative ot the lead vehicle. We assume that the lead vehicle information is continually broadcast.

2. Every vehicle is required to broadcast its position relative to the lead vehicle to all its following vehicles. Hence, the position of the j-th vehicle relative to the lead vehicle can be obtained by adding the position of the j-th vehicle relative to the j-1st vehicle (which is available from sensors like radar) and the position of the j-1st vehicle relative to the lead vehicle. Estimate using 1 is updated by this estimate to get a better estimate of the controlled vehicle's position relative to the lead vehicle.

Although there are delays/lags associated with obtaining such estimates, all the simulations do not incorporate such features other than signal processing/actuator lag. It is recommended, for the constant spacing strategy, that lead (reference) vehicle information be utilized as much as possible for platooning.

Knowledge of vehicle ID helps attenuate maximum spacing errors.

It is desirable to utilize as little external information as possible to guarantee the attenuation of maximum spacing errors. External information in the form of knowledge of vehicle ID and the preceding vehicle information helps attenuate maximum spacing errors if the vehicle controller model is accurate. The idea behind this strategy is to reconstruct lead vehicle's relative velocity and position information from the spacing and velocity error information of the controlled vehicle and feed it back into the control law. Very roughly speaking, knowing the controlled vehicle's ID in the platoon, we build an observer for the error dynamics of every vehicle preceding the controlled vehicle in the platoon. Figure 5.10 shows the behavior of spacing errors in the platoon with information of knowledge of vehicle ID and preceding vehicle's acceleration. In figure 5.10, the spacing errors are an order of magnitude larger than the spacing errors in the earlier strategy using lead vehicle information. This is due to two reasons. First, lead vehicle acceleration information is not available/utilized. Second, we assume that every

vehicle is I/O linearized so that there is an exact transfer function relationship between the errors of consecutive vehicles. Although, this rarely is the case, lead vehicle information is reconstructed using the spacing and velocity error measurements and the spacing error attenuation is guaranteed. The other disadvantages of this strategy are : the controller computations for the vehicles at the tail of the platoon gets complex with vehicle ID and the amount of spacing error attenuation that can be guaranteed is limited.

Figure 5.11 shows the behavior of the platoon with every controlled vehicle in the platoon having the information of 5 vehicles ahead. The motivation for this strategy is to investigate how the platoon performance is affected if every controlled vehicle has the information of "r" vehicles in its vicinity. The string stability polynomial corresponding to this strategy is $z = 1$. In the presence of any signal processing lags, the string stability polynomial gets perturbed to $z = \rho$ where $\rho > 1$. The first five vehicles in the platoon behave exactly the same way as in the previous case. In this platooning strategy, the maximum spacing errors of the following vehicles are guaranteed to be less than or equal to the maximum spacing error of the first follower in the platoon. Since the maximum spacing error at the tail of the platoon is approximately equal to the spacing error in the first vehicle, the throttle/control effort increases with vehicle index. This causes saturation of the throttle at the tail of the platoon. Furthermore, with signal processing lags, this scheme cannot ensure weak string stability. This scheme is not recommended for platooning.

Figure 5.12 depicts the behavior of the spacing errors in the platoon under miniplatoon control strategy. The rationale behind this strategy is that feeding back reference vehicle information improves the string stability and robustness properties. In this strategy, every platoon is divided into mini-platoons of "r" vehicles each. Within the mini-platoon, every controlled vehicle is assumed to have access to the mini-platoon leader's information. The leaders of the mini-platoon have only the information of the vehicle ahead. As one would expect, the spacing errors in the miniplatoon decrease geometrically with vehicle index in the mini-platoon and the leaders of the miniplatoon experience larger errors due to the lack of lead vehicle information. The spacing errors of the leaders of the miniplatoon increase with miniplatoon index, in the same way the spacing errors increase when only the preceding vehicle's information is available, as shown in Hedrick, et.al., 1991. Miniplatoon can be modeled as a single vehicle when a constant intraplatoon

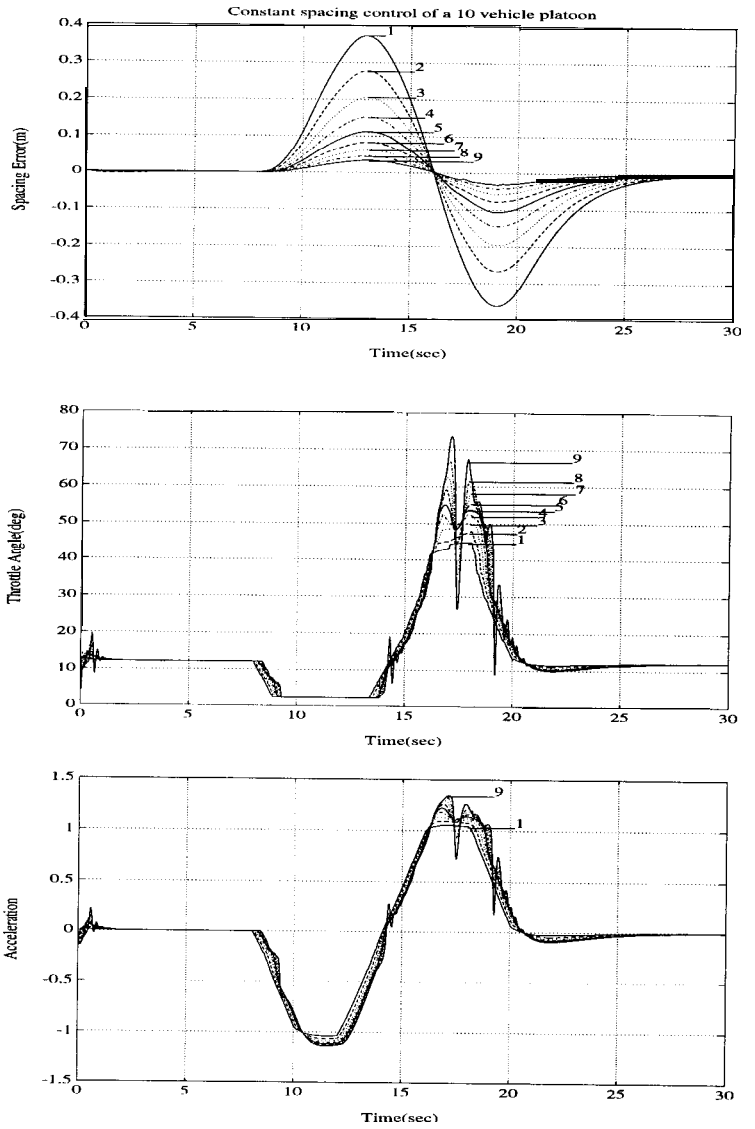

Figure 5.10: Constant spacing control of a 10 vehicle platoon with knowledge of vehicle ID in the platoon and preceding vehicle acceleration

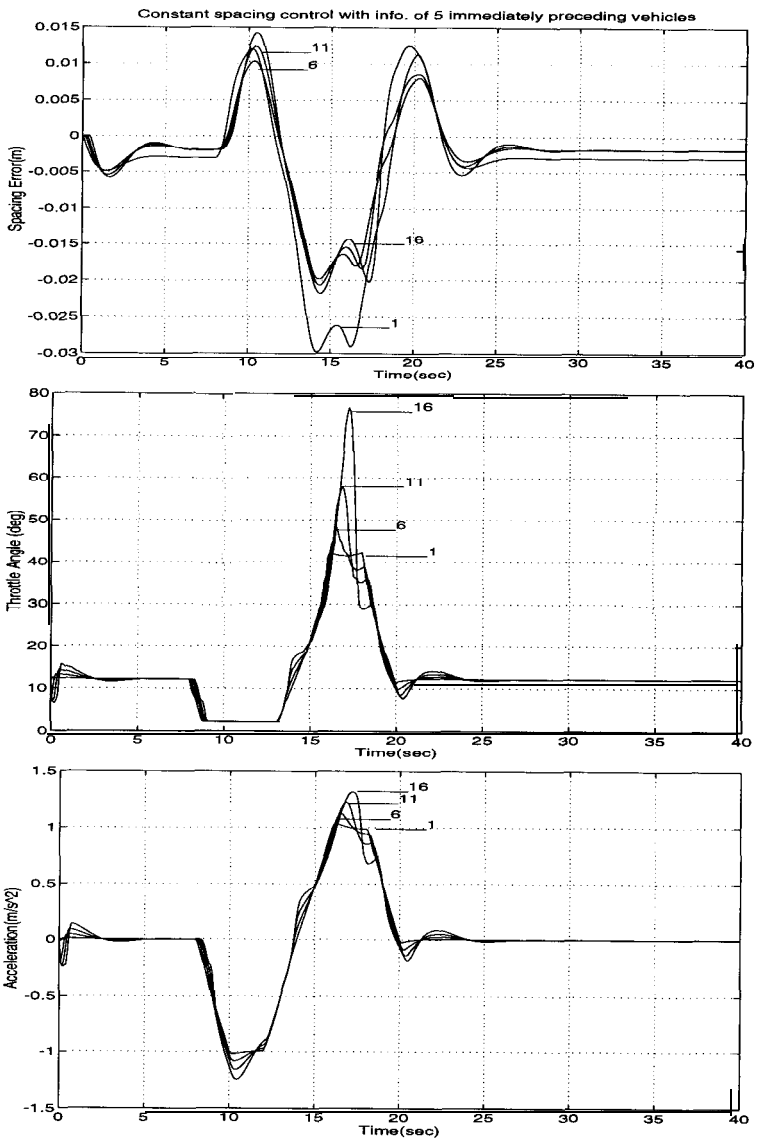

Figure 5.11: Constant spacing control with information of 5 vehicles ahead

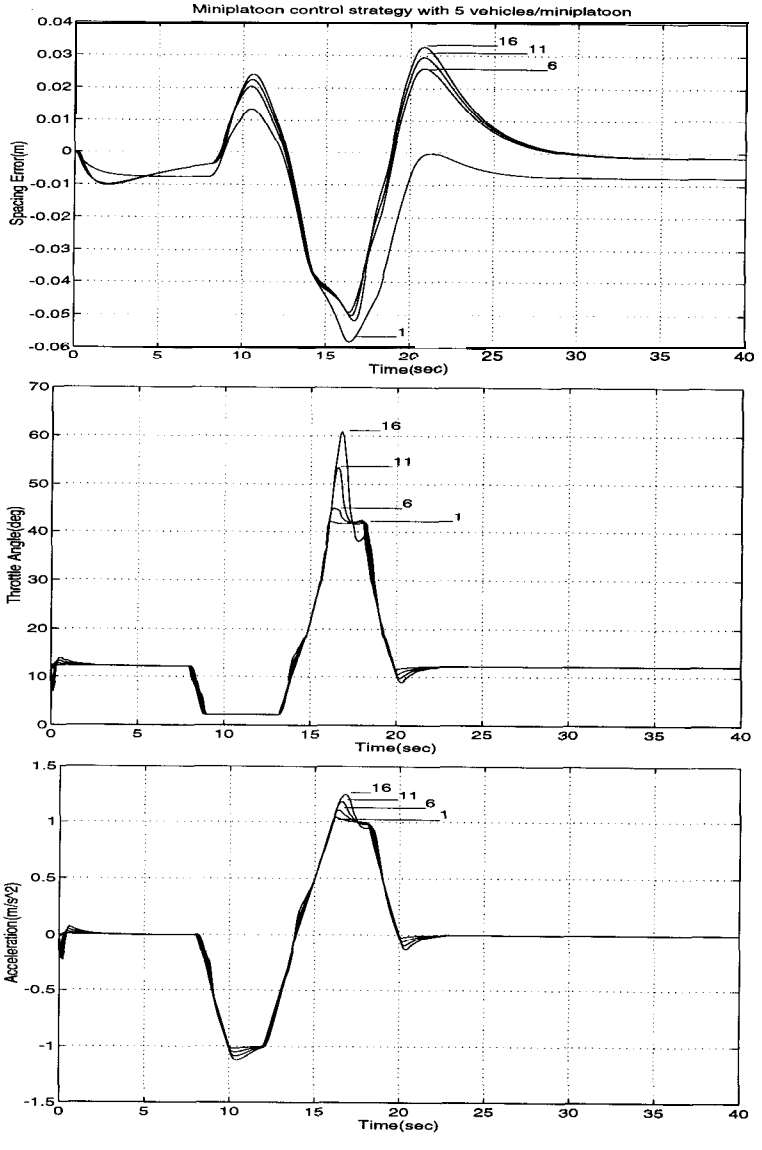

Figure 5.12: Miniplatoon control strategy

spacing is maintained. The control input increases with miniplatoon index, limiting the number of miniplatoons allowable per platoon. If every controlled vehicle has the information of its "r" preceding vehicles, mini-platoon strategy should be employed, so that improved robustness is obtained.

If we feed the information of the lead vehicle in the platoon to the leaders of the miniplatoons, it is shown in section 5.3.8 that the performance of the platoon is similar to the case when every controlled vehicle in the platoon utilizes the lead vehicle information. A two time scale update is suggested for implementing the miniplatoon control algorithm, in which all the vehicles in the miniplatoon get the information from their respective leaders on a faster time scale and the leaders of the miniplatoon get the information of the leader broadcast on a slower time scale. However, further analysis is required to study the string stability of this scheme.

In order to improve the robustness in string stability, feeding back the velocity of controlled vehicle at the expense of non-zero steady state spacing errors and consequently, traffic capacity is necessary. In AICC strategy, velocity of the controlled vehicle is fed back in addition to the on-board information from radar. The advantage of this strategy is that external information is not required. The disadvantage of this strategy is that the control effort is inversely proportional to the desired time headway and the robustness to actuator lag decreases with decreasing time headway. Figure 5.13 illustrates the behavior of the generalized spacing errors and throttle angles of vehicles in the platoon. The maximum generalized spacing error and throttle angle decreases with vehicle index. This strategy does not require maintaining a constant spacing between vehicles. Consequently, the controlled vehicle is not required to track the preceding vehicles' acceleration profiles exactly, which leads to a reduction in control effort. From simulations, a headway time of at least 0.2 sec is necessary to maintain smooth throttle angles and accelerations.

It is no coincidence that all the (proposed) control strategies which do not avail of the lead (reference) vehicle information can, at best, guarantee only weak sense string stability. Since they do not use the lead (reference) vehicle information, their associated string stability polynomials have at least a simple root at $z = 1$. Furthermore, they are not robust to signal processing lags/actuator lags. The advantage of using reference vehicle information is shown in section 5.3.1 . Therefore, it is imperative to have a single reference vehicle information for platooning.

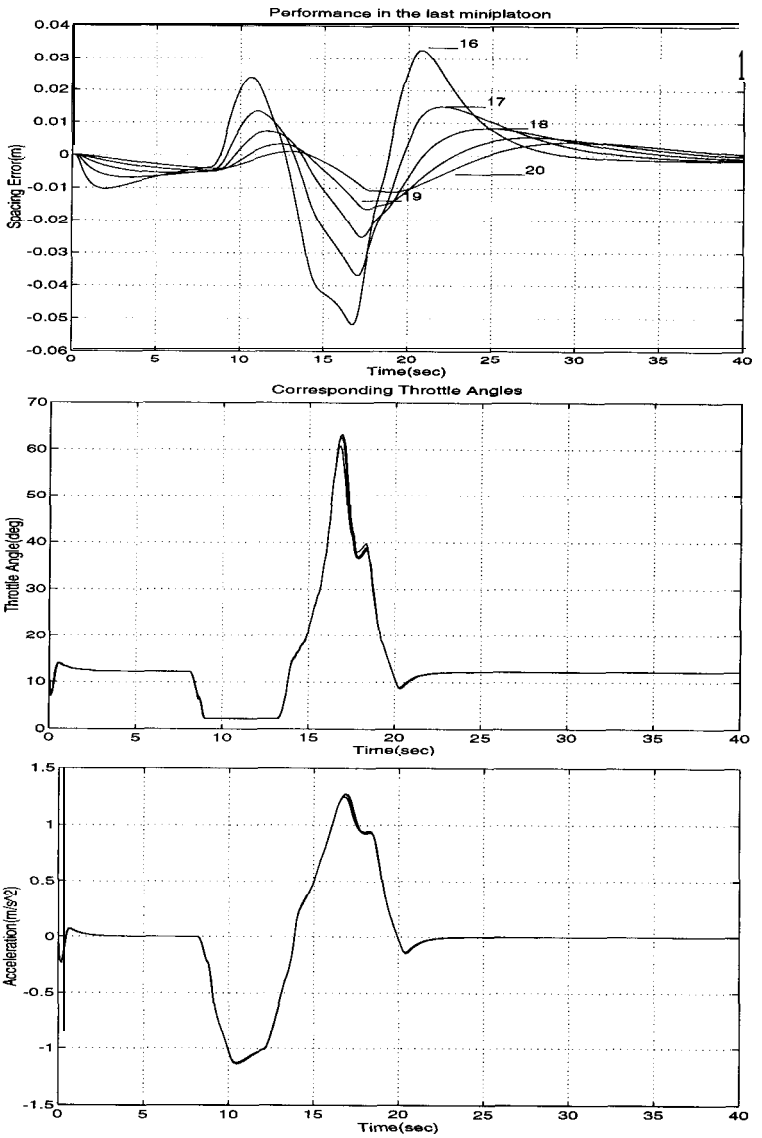

Figure 5.13: Behavior of the vehicles in the last Miniplatoon

If the lead vehicle information is not available to all the vehicles in the platoon, the mini-platoon strategy has some benefits over the other platooning strategy discussed in section 5.3.6 and 5.4.2. Firstly, it can guarantee geometric attenuation of the spacing errors within the platoon. Secondly, for a medium size platoon of 20-30 vehicles, which can be split into 3 or 4 mini-platoons, we need to focus only on the first follower in each mini-platoon. The first follower in every mini-platoon can be made to maintain a relatively large spacing compared to the nominal intervehicular spacing. Another alternative is to treat every mini-platoon as a vehicle and make the reference vehicles follow an AICC law. As a result, the traffic capacity achievable is much higher than the other strategy discussed in section 5.3.6 and 5.4.2.

The results of this chapter are summarized in Table 5.1 .

5.6 Steady State traffic Capacity Calculations and Evaluation of platooning strategies

Consider a platoon of N vehicles maintaining a distance L_p from its preceding one. Let L_v be the inter-vehicle spacing in the platoon and L_c be the vehicle length. The ideal (steady state) traffic capacity, Shladover, 1979, Varaiya, 1993, is given by :

$$\phi_{id} = \frac{3600v}{L_v + L_c + \frac{L_p}{N}} veh/lane/hr$$

where v is the velocity of the platoon. For the case of spacing control strategies, $L_v = L_0$, a constant. For the case of headway control strategies, $L_v = L_0 + h_w v$ where h_w is the desired headway time. In order to account for merge and lane changing, the steady state traffic capacity is derated by 20%. L_p is estimated assuming that no collisions are allowed when the platoons are moving at $v_c m/s$ and when the lead vehicle platoon decelerates at $d_1 m/s^2$ and the following platoon decelerates at $d_2 m/s^2, \Delta t\, sec$ after the lead vehicle platoon has started decelerating.

$$L_p = v_c \Delta t + \frac{v_c^2}{2}[\frac{1}{d_1} - \frac{1}{d_2}]$$

Spacing Strategy	ρ	*Robustness*	*Implementation Requirements*	*Capacity*
Constant Spacing				High
With reference vehicle info. only	0	Unsafe. Does not consider preceding vehicle info.	Reference vehicle info. broadcast requires radio	
Autonomous Control	>1	Not robust		
Semi-Autonomous Control	$= 1$	Not robust	preceding vehicle info. required	
Control with knowledge of vehicle ID	< 1	$\rho \approx 1$	Require preceding vehicle info. and accurate vehicle model	
Control with lead and preceding vehicle info.	≤ 1	Robust	Require preceding and lead vehicle info.	
Control with info. of "r" vehicles ahead	≥ 1	Not Robust	Info. of "r" vehicles should be broadcast	
Miniplatoon Control	$= 1$	Not robust entirely	Info. of preceding and lead vehicles in the miniplatoon required	
Variable Spacing				Low to Medium
AICC	$= 1$	Proportional to time headwav		
Headway Control with info. of "r" vehicles	$= 1$	Proportional to time headway	Info. of "r" vehicles should be broadcast	

Table 5.1: Summary of Platooning Strategies

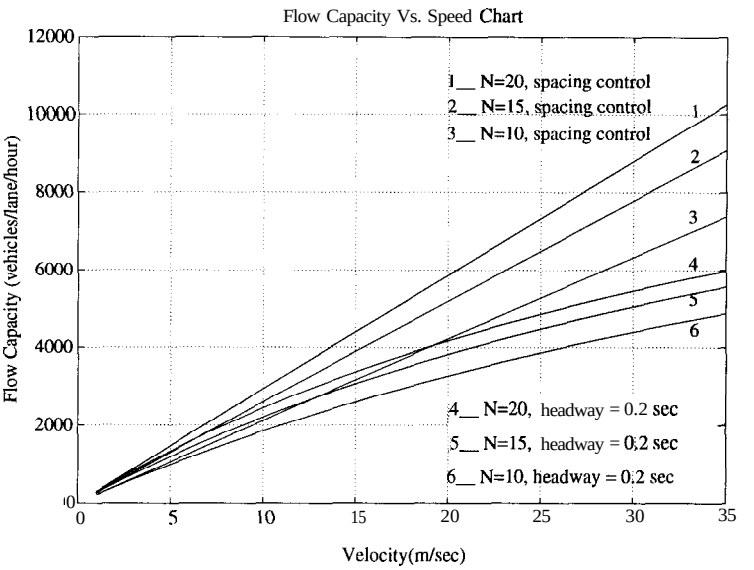

Figure 5.14: Capacities

Typical values of these parameters: $v_c = 30m/s$; $At = 0.3sec$; $d_1 = 4m/s^2$; $d_2 = 10m/s^2$; L_0 = lm; $L_p = 76.5m$. For spacing control strategy:

$$\phi_{act} = \frac{2880v}{6 + \frac{76.5}{N}}$$

For headway control strategy,

$$\phi_{act} = \frac{2880v}{6 + h_w v + \frac{76.5}{N}}$$

From the above formula, it is clear that a lower headway time yields higher lane capacity. The lane capacities for both the schemes, given by the two equations above, are shown in figure 5.14, where N in the plot refers to the corresponding platoon size. From the previous section, a headway of 0.2 sec is chosen for comparison. It can be seen that the spacing control has atleast 30% more traffic capacity than the headway control.

Chapter 6

Sensor/Actuator Fault Detection

6.1 Introduction

The following topics related to fault detection in longitudinal control of vehicles in the AHS framework are discussed in this chapter :

- The effects of sensor and actuator faults on system performance. Analysis of these effects is done by approximate feedback linearized transfer function relationships between the fault error term and the resulting error in tracking.
- Redundancy relations among longitudinal sensors are identified and exploited for fault detection purposes. A feedback linearizing filter is designed to detect actuator faults and results of experimental verification of the filter are also presented.
- Application of a Variable Threshold Algorithm to ensure a fixed false alarm rate and minimum detection delay in detection of signal changes. This algorithm is applied to residuals obtained from redundancy relations between speed sensors and the radar closing rate.
- Application of detection filters to the longitudinal platooning problem.
- Conclusions and future research options.

6.2 Sensor / Actuator Fault Effects

This section discusses potential fault modes among sensors and actuators in longitudinal control of vehicle follower systems, on which AHS is based. Analysis of the effects of these modes on the desired response of the platoon is presented.

The methodology followed to analyze faults in the system was to study the effect of bias in sensor measurements on the vehicle tracking performance. Typically, threshold determination for making fault decisions is based on desired false alarm rates. This study enables us to determine the bias threshold that can be tolerated from a desired output standpoint. Therefore, this study obviates the danger of choosing a threshold too high to satisfy a low false alarm rate without taking into consideration the effect of small sensor biases on the overall system performance. Analysis was done using approximate feedback linearized transfer functions from sensor measurement error terms to spacing error. Based on Bode plots and time domain characteristics of the transfer functions, one can get a good idea of effect of faults in sensors and actuators. 4-Vehicle platooning simulations are presented, depicting various failure scenarios and resulting spacing error characteristics of the vehicle follower system.

6.3 Transfer Function Fault Relationships

Swaroop, et.al. showed that approximate feedback transfer function from lead vehicle acceleration to spacing error $(\hat{g}(s))$ in the first vehicle can be computed as

$$\hat{g}(s) = \frac{\hat{\epsilon_1}(s)}{a_l\hat{(s)}} = \frac{k_a + k_l - 1}{s^2 + (k_v + c_v)s + (k_p + c_p)} \tag{6.1}$$

$\hat{g}(s)$ describes the performance of the first vehicle following the lead vehicle as it describes how the spacing error changes with change in speed of the lead vehicle from its previous steady state value.

The transfer function from spacing error in a vehicle to that of the subsequent vehicle is given by

$$i,(s) = \frac{\epsilon_j(s)}{\epsilon_{j-1}(s)} = \frac{k_a s^2 + k_v s + k_p}{s^2 + (k_v + c_v)s + (k_p + c_p)} \tag{6.2}$$

Gain Parameter	*Magnitude*
k_p	*0.9*
k_v	1.6
c_v	*0.3*
c_p	0.0
k_l	*0.333*
k_a	*0.667*

Table 6.1: Control Gain Parameters

$\hat{h}(s)$ describes the spacing error propagation down the platoon. The design problem is to minimize the norms $||g||_1$ and $||h||_1$ over the admissible set of gains to attain the best possible performance. $||g||_1$ is given by

$$||g||_1 = \int_0^\infty |g(t)|dt$$

g(t) is the Laplace inverse of $\hat{g}(s)$.
The gain parameters $k_p, c_p, k_v, c_v, k_a, k_l$ are determined to satisfy the two norms as shown in Swaroop, et.al., table 6.1 shows the gains used in the simulations.
Under perfect operation of the control the nonlinearities are compensated for and the input-output response can be described by the transfer functions as mentioned in the previous section. In case a sensor develops a fault i.e. develops a bias or a drift, the control effort would be erroneous. It is possible to derive transfer functions from the terms which contribute to the error and the resulting tracking error. From the response of these transfer functions one can get a good idea of threshold values to select for each particular sensor fault. The difference in approach in this case is that a sensor fault threshold is chosen depending on the effect that particular fault has on the overall system performance objective and not just based on the noise characteristics of the individual sensor, which may result in a different threshold selection.

6.3.1 Four Vehicle Simulations

Simulation of failure scenarios in four vehicle platoons was done using the longitudinal vehicle model described in McMahon, et.al., 1992. The aim

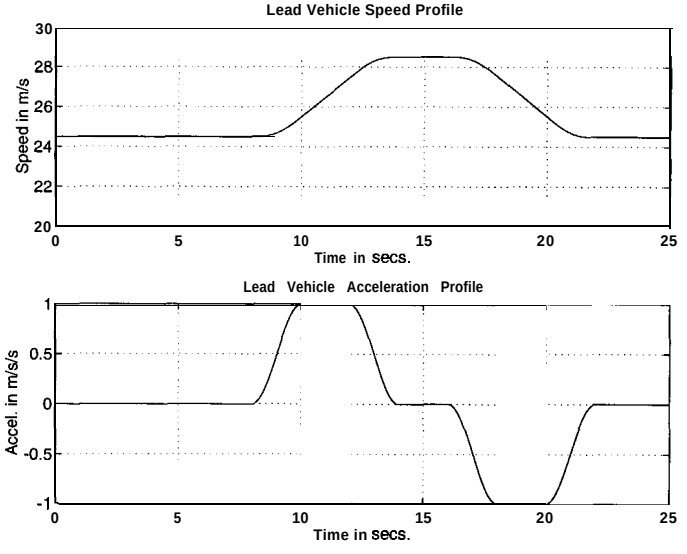

Figure 6.1: Lead Vehicle Maneuver

was to study sensitivity of the tracking performance to sensor measurement accuracy.

The desired constant inter-vehicle spacing is 2m. The standard lead vehicle speed and acceleration profile used is shown in figure 6.1. Speeds upto $30m/s$ and acceleration magnitudes of the order of $1m/s^2$ were simulated. Figure 6.2 shows the nominal tracking performance of the vehicle platoon without any faults. The sensor noise characteristics are assumed zero mean Gaussian and white. Table 6.2 shows their respective variances. It should be noted that the spacing errors of all the vehicles are under $0.15\mathrm{m}$ and decrease down the platoon.

In the following sections, transfer function relationships between the error term in sensor measurement and resulting spacing error are derived for different sensors.

6.3.2 Radar Range Measurement Fault

Radar range measurement fault was simulated by feeding back erroneous spacing error(ϵ_j) data to the controller.

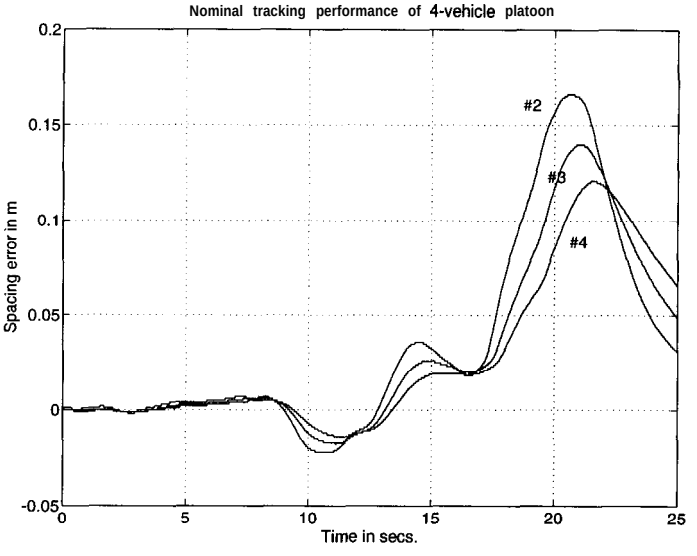

Figure 6.2: Nominal tracking performance

Sensor	*Typical* range of operation	*Standard deviation of noise*
radar range(m)	o-4	0.05
radar closing rate(m/s)	o-1	0.05
accelerometer(m/s^2)	o-2	0.06
Wheel speed(rad/s)	30-90	0.04
engine speed(rad/s)	100-300	5.7

Table 6.2: Sensor Noise Characteristics

The linear relationship between the error term in feedback due to a range measurement fault and the resulting spacing error makes it simple to analyze the effect of a radar range bias. The effect of a bias in range measurement can be studied by analyzing the following transfer function

$$\frac{k_p + c_p}{s^2 + (k_v + c_v)s + k_p + cp} \tag{6.3}$$

This transfer function relates the bias in range measurement to the resulting spacing error and is obtained by substituting $\epsilon_1 + \partial\epsilon$ for ϵ_1 in the spacing error feedback term for the input, where $\partial\epsilon(s)$ is the range bias. This signifies a faulty control input given to the plant because of faulty sensor measurement feedback. In fact the complete relation for the spacing error in terms of lead vehicle acceleration and the fault term is given by

$$\epsilon_1(s) = \hat{g}(s)a_l(s) + \frac{k_p + c_p}{s^2 + (k_v + c_v)s + k_p + c_p}(\partial\epsilon(s)) \tag{6.4}$$

where $\hat{g}(s)$ is from Eq. 6.1.

It can be seen that the relationship between the spacing error and the bias term is not speed dependent. Figure 6.3 simulates a range bias of 0.5m in the radar of Vehicle $\#3$ (third vehicle in platoon). The steady state spacing error is also 0.5m in Vehicle $\#3$ and the other vehicles are unaffected. The steady state error can be found by Final Value Theorem. Therefore, a bias of 0.3m can be chosen as a safe bias amount from this analysis as 0.3m is 15% of the nominal inter-vehicle spacing. The fault threshold to be eventually selected depends on the fault detection scheme and noise characteristics of the range sensor but the threshold should not be chosen more than 0.3m.

A radar fault in the j^{th} vehicle only affects the j^{th} vehicle and the extent of propagation down the platoon depends on the kind of the fault. In other words, if the fault is sudden and of large magnitude and no reconfigurative action is taken then the j^{th} vehicle will respond in a drastic fashion which translates to tracking an extreme maneuver for the following vehicles which in turn would result in deterioration of tracking performance of the following vehicles too.

6.3.3 Closing Rate Measurement Fault

The following transfer function relationship between the error term due to radar closing rate measurement fault and the resulting spacing error shows

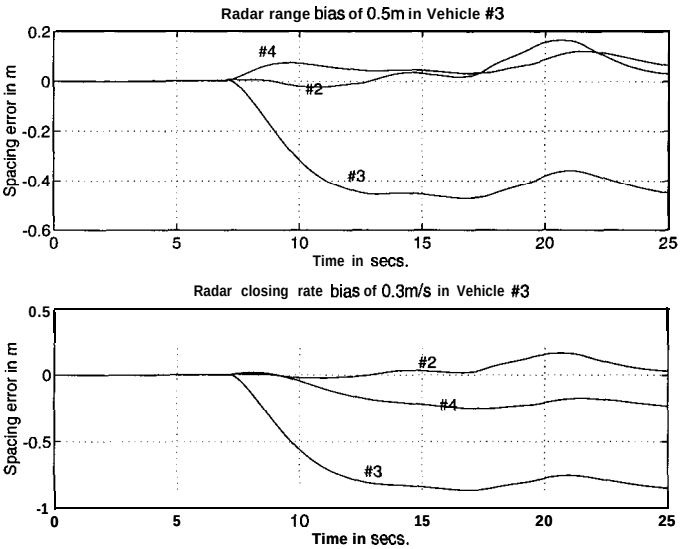

Figure 6.3: Effect of radar fault on spacing errors

the criticality of this kind of fault. As shown in figure 6.3, a bias of $0.3\mathrm{m/s}$ in the closing rate measurement results in spacing errors of the order of $0.8\mathrm{m}$ within 5 seconds of the fault occurence.

$$\epsilon_1(s) = \hat{g}(s)a_l(s) + \frac{k_v + c_v}{s^2 + (k, + c_v)s + k_p + c_p}(\partial\dot{e}) \tag{6.5}$$

where $\partial\dot{e}$ represents the bias in the closing rate measurement.
The relationship is not speed dependent or profile dependent, as in the case of range measurement fault. The errors have linear dependence on the bias term. A bias of O.lm/s can be considered safe in this case as it would result in a steady state spacing error of $0.26\mathrm{m}$ which is 13% of the nominal spacing. Figure 6.3 shows that the Vehicle #4 is also affected by the closing rate error in Vehicle #3. This is because in this simulation the velocity error between the j^{th} vehicle and the lead vehicle is calculated by adding the respective closing rates of each of the vehicles between the j^{th} and the lead vehicle. But in practice, this value can be obtained by the communication of the lead vehicle speed directly. Therefore, a closing rate error in the j^{th} vehicle does not directly affect any other vehicle in the platoon.

6.3.4 Engine Speed Sensor Fault

The commanded throttle angle is calculated from steady state maps as a nonlinear function of the engine speed and T_{net} in implementation assuming that the manifold dynamics can ne neglected since the manifold dynamics are considerably faster than the vehicle longitudinal and engine dynamics. The spacing error is not heavily dependent on accuracy of the engine speed measurement. Figure 6.4 shows that a 25% error in the engine speed measurement results in spacing errors of the order of 0.4m for the standard profile of freeway speeds and acceleration of $1m/s^2$. Spacing errors of the following vehicles in the platoon show that engine speed faults are not propagated down the platoon. There is a direct dependence of the spacing error on the speed of the profile, errors being higher at higher speeds. A bias of $30rad/s$ (12% of 250) can be chosen as degree of tolerance for the engine speed sensor.

6.3.5 Wheel Speed Sensor Fault

Wheel speed sensor fault is also not critical compared to radar faults. Figure 6.4 shows that a 75% error in the wheel speed measurement in Vehicle $\#3$ is less than 0.3m. The wheel speed sensor measurement is used to compensate for the nonlinear wind drag term $c_a v^2$ and so the transfer function between the error term and the spacing error is given by

$$\epsilon_1(s) = \hat{g}(s)a_l(s) + \frac{c_a h^4}{J_e s^2 + (k, + c_v)s + k_p + c_p}(2\omega_{wl}\partial\omega_{wl} + \partial\omega_{wl}^2) \qquad (6.6)$$

where ω_{wl} is the wheel speed. Wheel speed faults are not propagated down the platoon. There is a direct dependence of the spacing error on the speed of the profile, errors being higher at higher speeds. For the same amount of bias the relationship between speed of profile and the spacing error is linear. A bias of magnitude $20rad/s$ can be tolerated by the system with spacing errors less than 0.2m at all operable vehicle speeds, therefore it can be chosen as the threshold value.

6.3.6 Accelerometer Fault

The following relation shows the effect of accelerometer bias on the spacing error in Vehicle #2.

$$\epsilon_1(s) = \hat{g}(s)a_l(s) + \frac{k_a + k_l}{s^2 + (k, + c_v)s + k_p + c_p}(\partial a_l) \tag{6.7}$$

where ∂a_l represents the bias in the lead vehicle accelerometer measurement. Accelerometer measurement of the lead vehicle is transmitted to other vehicles to avoid spacing error propagation down the platoon. But the effect of the accelerometer fault in the lead vehicle is felt most in Vehicle #2 because acceleration of the lead vehicle is required by Vehicle #2 as feedforward information in addition. If the lead vehicle acceleration is off by 30 percent the resulting spacing errors are of the order of 0.5m from figure 6.5.

Accelerometer fault in any other vehicle in the platoon is not as critical and affects only the vehicle immediately behind it. Figure 6.5 shows the effect of an accelerometer fault in Vehicle #2. 30 percent error in this case gives rise to a spacing errors of 0.3m in the Vehicle #3.

6.3.7 Throttle Actuator Fault

A throttle actuator fault can be depicted as torque production being a fraction of the T_{net} commanded. Figure 6.6 shows the effect of 30 percent less actuation results in errors of about lm.

From a transfer function point of view a throttle actuator fault is equivalent to simultaneous 30% error in engine speed, spacing error, closing rate, lead and the previous vehicle's acceleration measurements. This is because these measurements are the main contributors to the T_{net} term. Since at the time the fault occurs it can be assumed that the spacing error and the closing rate are small, therefore, in the initial stages of the fault occurence a throttle actuator fault can be likened to a fault in the lead and previous vehicle's accelerometer and in the engine speed sensor. This assertion can be verified from figures 6.4 and 6.5 and comparison with figure 6.6. An error in torque production of more 5% can be considered unsafe since it can give rise to transient spacing errors of 0.25m.

Based on simulations and the transfer function analysis recommended sensor bias tolerance limits are specified in table 6.3. These values were chosen based on lead vehicle maneuvers.

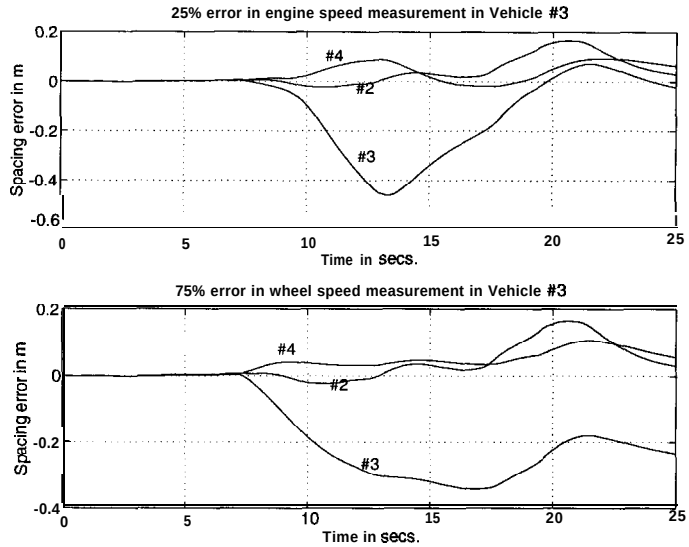

Figure 6.4: Effect of speed sensor faults on spacing errors

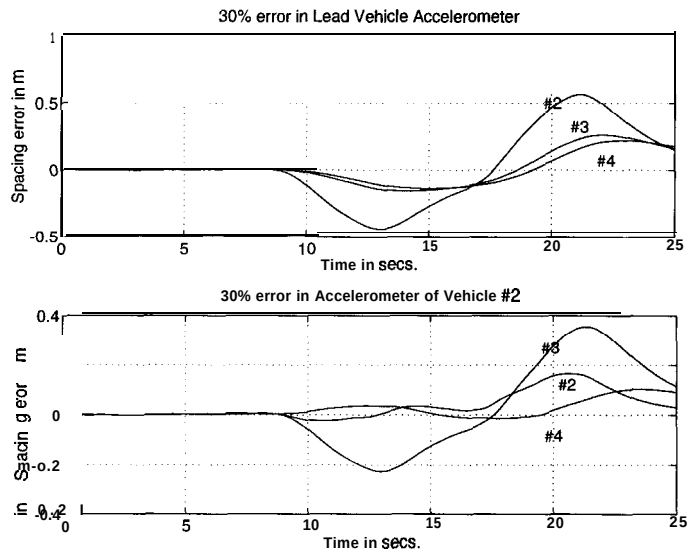

Figure 6.5: Effect of accelerometer fault on spacing errors

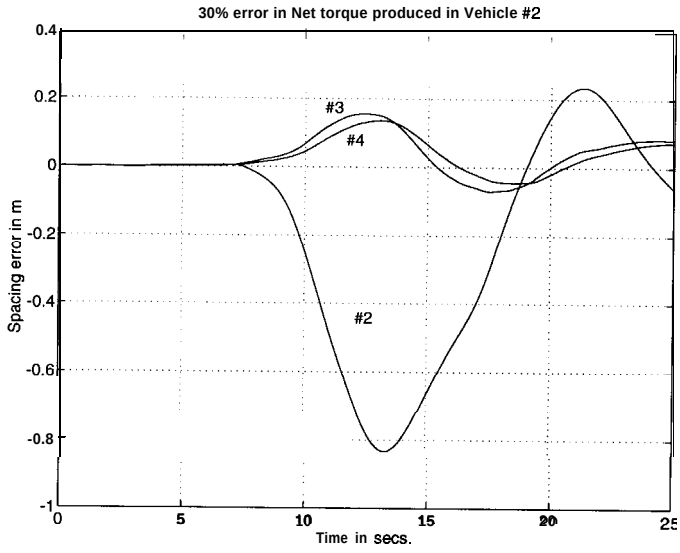

Figure 6.6: Effect of throttle actuator fault on spacing errors

Sensor Measurement	*Tolerance magnitude*
Radar range(m)	0.2
Radar closing rate(m/s)	0.1
Accelerometer(m/s^2)	0.15
Wheel speed(rad/s)	20
Engine speed(rad/s)	30

Table 6.3: Sensor Tolerance Recommendations

6.4 Redundancy Management in the Vehicle Follower Problem

To achieve fault tolerance in the vehicle follower system it is necessary to detect all possible modes of sensor and actuator faults promptly and whenever possible reconfigure the fault by reconstructing the information lost using system redundancy. This would enable decentralization of the control tasks involved because faults can be dealt with within the affected vehicle rather than discontinuing the platooning maneuver because of a sensor fault.

System redundancy is the availability of multiple measurements of a particular variable from similar or dissimilar sensors. It is in general not viable to have physical redundancy in systems because multiple sensors demand additional space, and are expensive. In addition, similar sensors may be expected to have similar failure patterns, and therefore may not be useful for fault detection.

The redundancy referred to here is temporal redundancy, where dissimilar sensors measuring different variables which are temporally related are used to create redundant measurements.

In this chapter, redundancy management methods are discussed pertaining to sensors used for longitudinal control. Redundancy is used for fault detection and failed sensor reconstruction.

The general methodology suggested is to exploit the redundancy in sensor measurements, create doubly redundant sensor output information and use simple voting schemes for fault detection and identification. Double *redundancy* refers to systems in which three reliable estimates of a measurement are possible either by having redundant sensors or by using groups of interrelated measurements. The logic for fault detection in such systems is to monitor the inconsistency in these measurements i.e. if measurements from two sensors differ considerably from the third, the third sensor would be diagnosed as faulty.

The fault decision is based on three residuals that are constructed from the estimates. The residuals are difference between each pair of estimates. Under fault-free conditions, each of the residuals are small and under the condition that one of the sensors is faulty, the residuals that involve the faulty sensor will be large and the residual independent of the faulty sensor will still be small. In this way, faults in any of the three sensors can be detected.

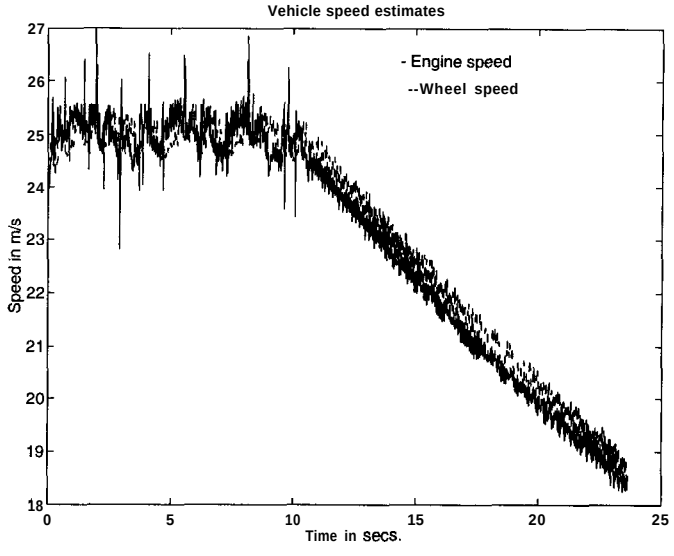

Figure 6.7: Estimates of vehicle speed using wheel and engine speed sensors

6.5 Speed Sensor Redundancy

Automatically controlled vehicles are fitted with various speed sensors measuring engine speed, wheel speed and transmission speed. Redundant measurements for the wheel speed can be obtained in the following ways :

- At higher speeds i.e. above 30mph, the torque converter in the transmission system is for all practical purposes locked. Hence, the engine speed can be directly related to the wheel speed by the gear ratio, thus the wheel speed can be estimated using the engine speed. figure 6.7 shows the proximity of this estimate to the actual wheel speed measurement under normal driving conditions. The data in figure 6.7 is from platooning experiments done on the 115 freeway in San Diego with the PATH program.

- Radar closing rate measurement measures the relative speed of the following vehicle with respect to the preceding vehicle. The preceding vehicle's speed is communicated back by the radio link, therefore, the

longitudinal speed of the following vehicle can be estimated by adding the closing rate to the preceding vehicle's speed. The wheel speed is given by vehicle longitudinal speed divided by the wheel radius. The underlying assumption here is that the wheel slip in the following vehicle is the same as that of the preceding vehicle. This assumption is reasonable since the inter-vehicle spacing is small and the vehicles are performing the same maneuver. Another issue to be considered is the frequency of information update of the preceding vehicle speed by the communication link. The link model considered has an update rate of 60ms and is sufficient for the maneuvers in consideration.

- The actual wheel speed measurement is the third estimate.

Table 6.4 shows the truth table for the voting scheme used to decide which of the three estimates is faulty, if any.
The underlying assumption in the fault identification procedure here is that the speed of the preceding vehicle communicated back is accurate. This assumption is not debilitating because a preliminary check can be done by the previous vehicle before communicating its speed back. In other words, wheel speed may be communicated back only if the wheel speed sensor is not faulty, otherwise, it's reconfigured value is sent back. In addition, the engine speed sensor figures in another doubly redundant group namely, the engine sensors, as mentioned later. This is particularly useful since the lead vehicle would not have access to the previous vehicle's speed because of its status as the first vehicle in the platoon.
Another problem with this scheme is the possibility of a communication fault. A communication fault refers to whether the packet of information that is transmitted from the preceding vehicle is received by the receiver in the following vehicle. But this kind of fault can be detected independent of other sensors. If no packet is received, the information from the last packet is frozen till the next packet arrives. If no packet is received for more than 3 consecutive cycles, a communication fault is declared.

6.6 Engine Sensors

Engine sensors refers to the group of sensors comprising of the mass flow rate sensor, manifold pressure sensor and the engine speed sensor. Redundant

Faulty Component	*Residuals of errors of wheel speed estimates*		
	R_1	R_2	R_3
Radar Closing Rate	Low	High	High
Engine Speed Sensor	High	Low	High
Wheel Speed Sensor	High	High	Low

Table 6.4: Truth Table for Speed Sensor Fault Detection

measurements of the mass of air in the intake manifold can be obtained as listed here

1. Intake manifold pressure(p_m) can be directly related to the mass of air(m_a) by a static relation. $m_a = \frac{p_m}{k_1}$ where k_1 is a constant depending on the temperature of the manifold which does not vary much during nominal maneuvers.

2. Mass of air in the intake manifold can be estimated using a nonlinear observer based on the engine speed measurement as shown at the end of this chapter.

3. Mass of air can be estimated using the mass of air flow rate sensor.

Therefore, using these three equivalent estimates of the mass of air in the manifold a similar voting scheme as in the previous section can be employed for fault detection in the engine speed, manifold pressure and mass of air flow rate sensors.

6.7 Calculation of Residuals

Typically all residuals are contaminated by sensor noise and fault decisions depend on characterization of the residuals. Therefore, the effect of sensor noise on the residuals needs to be investigated. In this section, we consider the redundancy residuals involving the speed sensors as described in the previous section.

6.7.1 Assumptions

The following assumptions are made on the sensor noise

1. All the sensors are assumed to have Gaussian white noise of zero expectation and known variance. Hence,

$$E(n_i(t_1)n_i(t_2)) = 0, \qquad \forall t_1 \neq t_2 \tag{6.8}$$

   where $E(\cdot)$ refers to the expectation function and n_i is the noise component of i^{th} sensor.

2. Noise from different sensors are independent.

$$E(n_i(t_1)n_j(t_2)) = 0, \qquad \forall i \neq j, \forall t_1 \text{and} t_2 \tag{6.9}$$

6.7.2 Wheel Speed/Engine Speed Residual

Let the wheel speed measurement be characterized by

$$v_{meas} = v_{wl} + n_{wl}$$

where n_{wl} is the wheel speed sensor noise, v_{wl} is actual wheel speed and v_{meas} is the measured wheel speed. n_{wl} is described by

$$n_{wl} : \mathrm{E}(n_{wl}) = 0, \qquad \mathrm{Var}(n_{wl}) = \sigma_{wl}^2 \tag{6.10}$$

$\mathrm{Var}(\cdot)$ is variance.
Engine speed noise is characterized by :

$$n_{\omega_e} : \mathrm{E}(n_{\omega_e}) = 0, \qquad \mathrm{Var}(n_{\omega_e}) = \sigma_{we}^2 \tag{6.11}$$

where n_{we} is the noise component in the engine speed measurement, ω_e is the actual engine speed.
Engine speed/Wheel Speed Residual, R_1, is given by

$$R_1 = (v_{wl} + n_{wl}) - R(\omega_e + n_{\omega_e}) \tag{6.12}$$

R is the gear ratio.

Variance of the residual R_1 can be given by

$$R_1 : \mathrm{E}(R_1) = 0, \qquad \mathrm{Var}(R_1) = \sigma_{wl}^2 + (R)^2\sigma_{we}^2 \tag{6.13}$$

since under fault free conditions, $v_{wl} = Rw,$. The variance relation is as a result of the following fact about Gaussian signals, x and y with σ_x^2 and σ_y^2 as their respective variances. Let $z = ax(.) + by(-)$ where a $\in \mathcal{R}, b \in \mathcal{R}$. Then σ_z^2 is given by

$$\sigma_z^2 = a^2\sigma_x^2 + b^2\sigma_y^2 \tag{6.14}$$

Therefore, characterization of residual noise can be done in terms of that of the sensors.

6.7.3 Closing Rate/Wheel Speed Residual

Let the radar closing rate measurement be denoted by $\dot{\epsilon}$ and let its noise component have variance σ_r^2. Let v_{wl}^{prev} denote the wheel speed of preceding vehicle and assume that its variance is also σ_{wl}^2.
The Residual R_2 is given by

$$R_2 = \dot{\epsilon} + v_{wl}^{prev} - v_{wl}; \tag{6.15}$$

Using Eq. 6.14 the characteristics of R_2 can be determined as

$$R_2 : E(R_2) = 0, \qquad Var(R_2) = \sigma_c^2 + 2\sigma_{wl}^2 \tag{6.16}$$

6.7.4 Engine Speed/Radar Residual

The third residual, R_3, is between the wheel speed estimate, using the engine speed and the estimate using radar closing rate and the previous vehicle's wheel speed.

$$R_3 = \dot{\epsilon} - v_{wl}^{prev} + Rw,; \tag{6.17}$$

Again, using Eq. 6.14 we obtain

$$R_3 : E(R_3) = 0, \qquad Var(R_3) = \sigma_c^2 + \sigma_{wl}^2 + (R)^2\sigma_{we}^2 \tag{6.18}$$

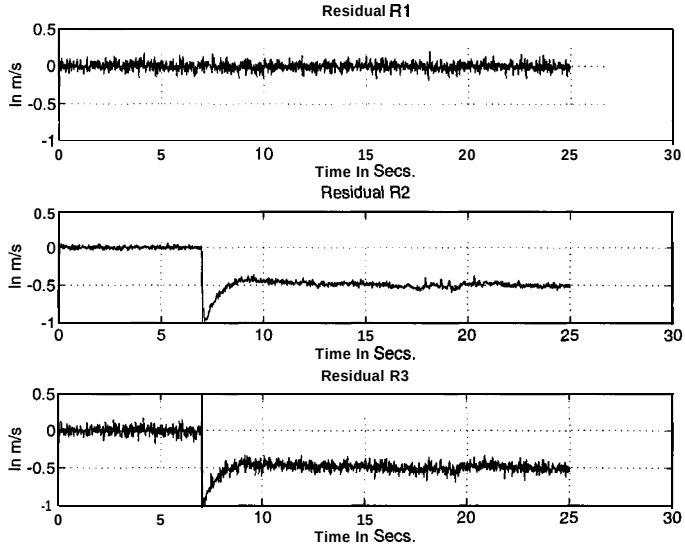

Figure 6.8: Sensor residuals : Radar closing rate fault

A fault involving one of the sensors in a particular residual is declared based on how the magnitude of the residual compares with a predetermined threshold value. This threshold value is chosen based on a desired false alarm rate of the detector, length of the time-window over which the residuals are monitored and probability of missed detections. Later on in this chapter, a variable threshold algorithm is discussed which minimizes detection delay and ensures that the fault detector satisfies a desired false alarm rate. Detection results using the algorithm on these residuals are also presented.

Qualitative simulation results show efficacy of this detection scheme. Figure 6.8 shows how a fault in radar closing rate can be detected. At time t=7s, a bias of $0.5\mathrm{m/s}$ was introduced in the closing rate measurement and the the residuals R_2 and R_3 show biases whereas R_1 does not.

6.8 Throttle Actuator/Throttle Angle Sensor Fault

To isolate different faults it is necessary to devise a method to differentiate between an actuator and a sensor fault. Actuator and sensor faults may have similar effects on system performance. In this section, we show how a feedback linearizing filter is designed to identify actuator faults. A feedback linearizing filter assumes that all states can be measured. In the hierarchy of fault detection decisions, it is first assumed that all sensors are working satisfactorily and then feedback linearization would be accurate, hence actuator fault detection is effected.

The simplified longitudinal model used in Swaroop, et.al. can be represented by the following dynamic equation

$$\dot{x} = f(x) + b(x)u + \gamma(t)b(x)u; \tag{6.19}$$

$x \in \mathcal{R}, u \in \mathcal{R}$. The state x refers to the engine speed, ω_e, and u is the throttle angle α. γ represents the bias factor of the input i.e. $\gamma(t)$=-1 would indicate complete failure of the throttle actuator.

Consider a one-state filter of the form

$$\dot{\hat{x}} = f(x) + b(x)u + l(x - \hat{x}); \tag{6.20}$$

where $\hat{x}$ is the engine speed estimate. l is chosen to stabilize the state-filter error dynamics. An appropriately chosen positive value of l will suffice in the absence of faults, depending on modeling error and noise considerations.

The observer error dynamics in presence of an actuator fault is given by

$$\dot{e} = -Z(e) + \gamma(t)b(x)u; \tag{6.21}$$

where e is $x - \hat{x}$. Since in absence of faults the filter is stable, e(t) will be close to zero at the onset of the actuator fault. Assuming that the fault happens at time t_0, then the error e(t) grows in magnitude in the following fashion

$$e(t) = \int_{t_0}^{t} e^{l(t-\tau)} b(x(\tau))u(\tau)d\tau \tag{6.22}$$

Therefore, when this residual, e exceeds a threshold value a throttle actuator fault can be declared. Identification of the throttle actuator as the faulty component still remains to be established because an engine speed sensor fault would cause e to grow in magnitude too. The detection logic used to distinguish a sensor fault from that of the throttle actuator is as follows :

- Case 1 : If a sensor is malfunctioning then the corresponding residual from the sensor will become large as well as the residual from the above feedback linearized actuator residual since the measurement fed back is erroneous in feedback linearization. In other words, if the engine speed sensor is faulty, it can be identified by redundancy methods described earlier.

- Case 2 : If actuator is malfunctioning, only the actuator residual will grow and the various sensor residuals would be small since an actuator fault will not affect the sensor residuals. The error between the commanded and actual throttle angle measurement would grow too.

- Case 3 : Throttle angle sensor fault : In this case, the error between the throttle angle sensor measurement and the commanded throttle angle would grow and the throttle actuator residual would still be small, since there is no feedback from the throttle angle sensor measurement.

6.8.1 Experimental Verification

A throttle actuator fault was simulated in a single vehicle tracking experiment on the 115 freeway in San Diego as part of PATH longitudinal control experiments. Software simulation of this fault was done by commanding a faulty value of throttle angle as the input. Figure 6.9 shows the result of a slowly growing throttle actuator fault in a ramp fashion. Figure 6.9 shows that the throttle actuator feedback linearizing filter residual is near zero under fault free conditions and grows rapidly after the fault occurs. The velocity tracking error is just beginning to grow, therefore, the fault is detected before the system performance deteriorates considerably.
An issue that arises is how to reconfigure after an actuator fault occurs. One alternative would be to notify all other vehicles in the platoon of the fault and slow down the platoon. Then the vehicle operator can convert to manual mode and exit the automated lane on the freeway following the appropriate lane change protocol. A redundant throttle actuator is recommended to obviate this situation. Thus the ‘healthy’ actuator can be switched on as a safety measure.

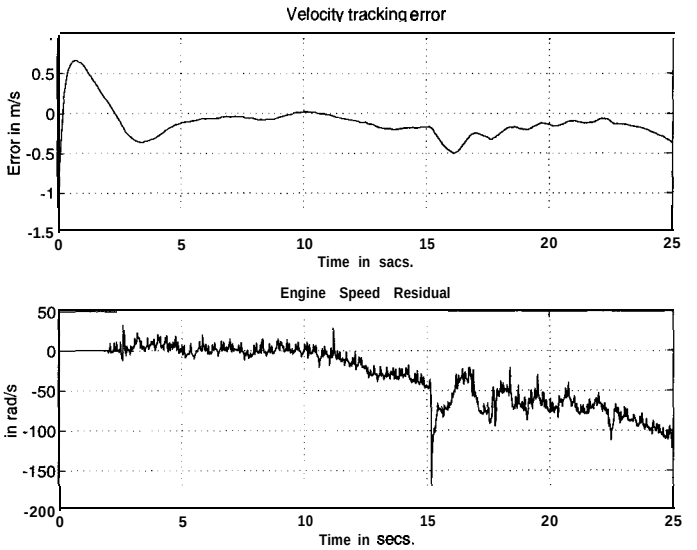

Figure 6.9: Experiment : Throttle actuator fault

6.9 Residual Processing

Residual Processing is an integral part of failure detection algorithms because its function is to compensate for 'non-idealness' of the system. In other words, the residual processor is designed keeping in mind that real systems are plagued with sensor/actuator noise, modeling errors etc.
Desirable features in a fault detection scheme are :

- Low false alarm rate (fault declared when not actually present)
- Low missed alarms (fault not declared when actually present)
- Low detection delay (delay in alarm after actual fault occurrence)

The complexity of design is enhanced by the fact that many of these features are in contradiction. For example, both false alarms and detection delay increase when the sensitivity of the detector is decreased with respect to high frequency. Another design tradeoff results as threshold chosen should be higher to keep the false alarm rate low but that results in lower probability of detection of faults.

A simple *Variable Threshold Algorithm* was developed which computes the threshold as a function of the detection time estimate, see Garg,1995. Threshold determination and detection logic is developed for residuals obtained from analytical redundancy relations from speed sensors as described earlier. The residual noise is assumed Gaussian and white. The algorithm can be applied to detection filter residuals as well, in which case the noise will not be white, but will still be Gaussian for linear systems. The algorithm is designed taking into consideration the following criteria : false alarm rate, missed alarm rate, detection delay, computational complexity and effect on overall control objective. To elaborate on the last point, high threshold selection would mean that high biases could go undetected and result in undesirable performance. In context of the vehicle platooning problem, if the sensors are excessively noisy, the threshold selected to ensure low false alarm rate will have to be high. If the particular sensor develops a bias which is high in magnitude but less than the threshold then its effect on the resulting spacing error would accrue with time and result in performance degradation. This emphasizes the significance of the transfer function study done in the beginning of this chapter. Before deciding on the threshold value to be implemented, it must be ascertained that it is not so high that it would result in poor performance before being detected.
A bias fault is hypothesized to show up as a jump in the mean of the residual signal.
Salient features of the *Variable Threshold Algorithm* are :

- The size(N) of a moving window is chosen, i.e. the number of previous measurement samples to be taken into consideration.
- The algebraic sum of the measurements are calculated over the window for i = 1, N. The i for the maximum of these sums is called i_{max}. i_{max} refers to the estimate of the time of the maximum likelihood of the fault.
- The sum corresponding to i_{max} is compared to a threshold which depends on i_{max} and the desired false alarm rate.
- If the sum is more than the threshold, a fault is declared and fault reconfiguration algorithm is activated otherwise the window is slid.

The detection test is based on likelihood ratio testing. But because of the Gaussian characteristics of the noise it can be transformed to a simple sum-check test as just alluded to.

The probability of detection depends on the magnitude of the bias in addition to the threshold value chosen. Since, the threshold depends on the maximum likelihood estimate of jump time, this algorithm does not give an explicit method to determine the window size ***n*** or the number of previous samples considered in the sliding window. The window size could be chosen based on extreme values of r i.e. for $r = n$ and on the false alarm and detection probability tradeoffs. Computational considerations also dictate the window size. A minimum limit on the value of r could be placed to further decrease false alarms.

In conclusion, because of Gaussian properties of the signal, the likelihood test simplifies to a sum-check test, simultaneously ensuring a desired false alarm rate. This methodology is very simple to implement and the on-line calculations are restricted mainly to finding the maximum value of S_r^n for r varying from 1 to n.

6.10 Speed Sensor Residual Threshold Determination

Linear algebraic operations are used to establish redundant measurements in sensors like engine speed sensors, wheel speed sensors, and radar as discussed earlier. The speed sensor residuals $R_i, \mathrm{i} = 1, 3$ satisfy the conditions assumed for application of the decision algorithm described in the previous section.

Figure 6.10 shows the residual history in the case of a radar closing rate fault in Vehicle $\#3$ and the corresponding fault alarm chart of the algorithm. The fault indicator (value = 1) indicates a fault at time = 7.2 secs. The fault is caused by a closing rate bias of $1\mathrm{m/s}$ at time = 7secs. The thresholds tend to be relatively high i.e. $0.4\text{-}0.8\mathrm{m/s}$, to ensure a false alarm probability of 0.001 in the residual. But since both R_2 and R_3 have to indicate a fault for the radar fault, the false alarm probability with respect to a radar fault is 10^{-6}. The probability of detection is approximately 1.0 corresponding to a fault of bias $1\mathrm{m/s}$. The reason for the high magnitude of the threshold is

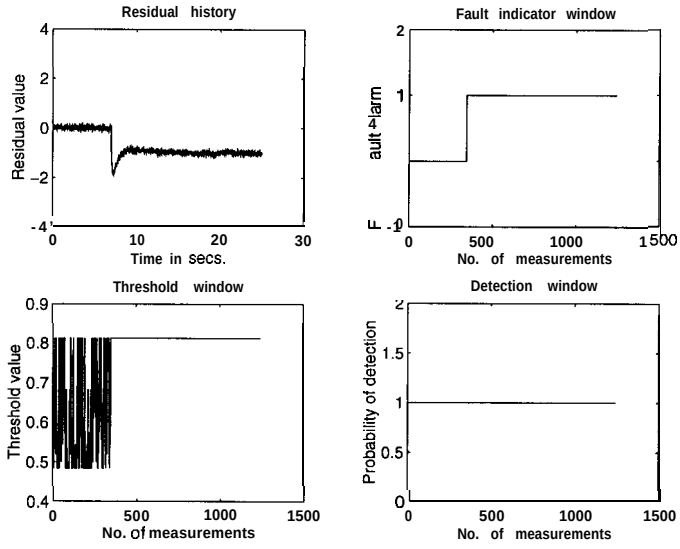

Figure 6.10: Residual processing chart for radar closing rate fault

high variance of the noise. The standard deviation of the residual without fault is 0.07468. Thresholds in the range of 0.3-0.4m can only ensure a false alarm rate of 0.1 for this residual. An alternative therefore, is to filter the residuals and decrease the effective variance of the signal. This would however introduce delay in the signal. If the resulting detection delay introduced is not significant from system performance point of view, filtering would be a good option.

6.10.1 Properties of Residual Processor

Advantage of variable threshold : As mentioned earlier, a varying threshold ensures that the false alarm probability of the detector is constant. Figure 6.11 shows the comparison of the false alarm probability in the case where the threshold is kept constant and in the case when the threshold is calculated to keep the false alarm rate constant. The false alarm rate can get significantly higher for the constant threshold case. The constant value chosen was the minimum value reached by the threshold in the variable threshold case. It is of course preferable to have thresholds as small as possible to detect small biases.

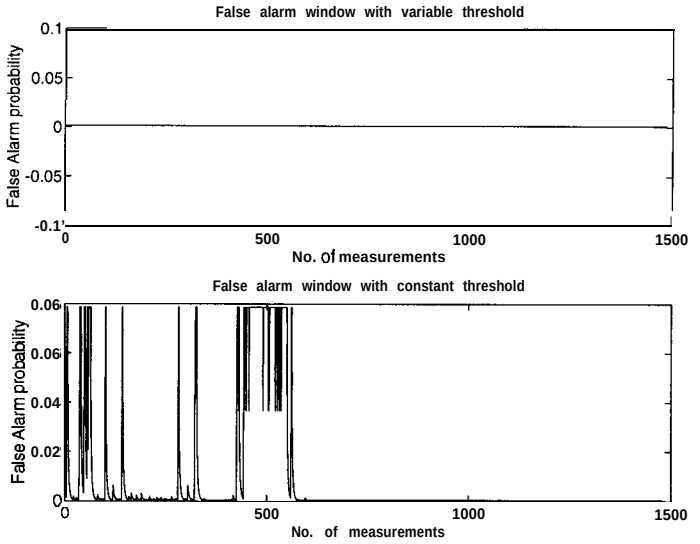

Figure 6.11: False alarm rate comparison of variable and constant threshold algorithms

6.10.2 Extension to Colored Noise Case

The variable threshold determination and detection logic method can be extended to the case when the signal noise is Gaussian but not white. It is assumed that the noise is stationary Gaussian and its power spectral density is known. This can be done by using a whitening filter which transforms the problem to the case dealt with in the previous sections. For details on the whitening filter see for example Mohanty, 1987.

6.11 Observers and Detection Filters for Application to Vehicle Model

In this section, we apply techniques of fault detection namely detection filters developed in Garg and Hedrick, 1995, to the longitudinal platoon model. The model of the longitudinal dynamics is extremely nonlinear and there is no explicit linear part in the dynamics. Theoretical development was necessary both for observer design as well as detection filter design for this class of

systems.

6.11.1 Observer Design

A viable method of observer design for systems of the following form is described in Garg, 1995.

$$\dot{x} = \text{f(x)} + g(x)u; \qquad y = \text{cx}; \tag{6.23}$$

Assumptions

- System in Eq. 6.23 is observable in the operating range.
- $||f(x_1,t) - f(x_2,t)|| \leq \gamma_f ||x_1 - x_2||, \qquad \forall x_1, x_2, t$ i.e. f(x,t) is Lipschitz bounded.
- $||g(x_1,t) - g(x_2,t)|| \leq \gamma_g ||x_1 - x_2||, \qquad \forall x_1, x_2, t$ i.e. g(x,t) is Lipschitz bounded.
- Actuator input is bounded

$$||u(t)|| \leq u_{max}, \qquad \forall t \tag{6.24}$$

Consider the observer

$$\dot{\hat{x}} = \text{f(i)} + g(\hat{x})u + L(y - \hat{y}); \qquad \hat{y} = C\hat{x}; \tag{6.25}$$

The observer gain, L, is determined by an iterative method which depends on the Lipschitz constants of the nonlinearities involved. For details please refer Garg, 1995.
A major tradeoff of this method is that the combined Lipschitz constant of all nonlinearities can be high since the bounds are conservative. Therefore, the Lipschitz constant should be calculated accurately.

6.11.2 Detection Filter Design

Detection filters are basically observers but the gain is calculated in a special way. Under normal (fault-free) operation the detection filter is a stable observer but on the occurence of a fault the output error between the measurements and the estimated measurements grow in a directional manner. The directions are designed different for different faults and therefore a direct detection logic can be developed. The concept of detection filters was developed for linear time-invariant systems. Only recently the concept has found applicability to nonlinear systems too. Garg and Hedrick, 1995 showed how the detection gain can be chosen to ensure stability of the observer as well as guarantee fault specific directionality in the initial stages of detection in a class of nonlinear systems with Lipschitz nonlinearities.

6.11.3 Platooning Application

The longitudinal system model can be expressed in the form of Eq. 6.23. The Lipschitz constant of the nonlinearity is 8.0, which necessitates the need for high gains.

The four states are m_a, ω_e, T_{br} and ϵ_i. Here m_a is mass of air in the intake manifold, ω_e is the engine speed, T_{br} is the brake torque and ϵ_i is the spacing error for the i^{th} vehicle. The three inputs are $TC(\alpha), T_{bc}$ and v_{prev}, where $TC(\alpha)$ is the throttle characteristic and T_{bc} is the commanded brake torque. The input v_{prev} is the feedforward value of the speed of the previous vehicle which is used by the observer to estimate the spacing error (ϵ_i).

The detection filter gain matrix used was

$$D = \begin{bmatrix} 8 & 0.17 & 0 & 0 \\ -0.5 & 9.27 & -0.3 & 0 \\ 0 & 0 & 5 & 0 \\ 0 & 0.477 & 0 & 4 \end{bmatrix}$$

Figure 6.12 shows the m_a, ω_e and ϵ residuals in the case of a throttle actuator fault. At time t = 7s, the throttle actuator performance drops to 75% of its desired amount. The mass of air residual grows instantly whereas the other residuals are not affected. Figure 6.13 shows the case when the accuracy of v_{prev} measurement is 20% off. This particular fault shows up similar in form to an actuator failure in the observer error dynamics because it is not a state

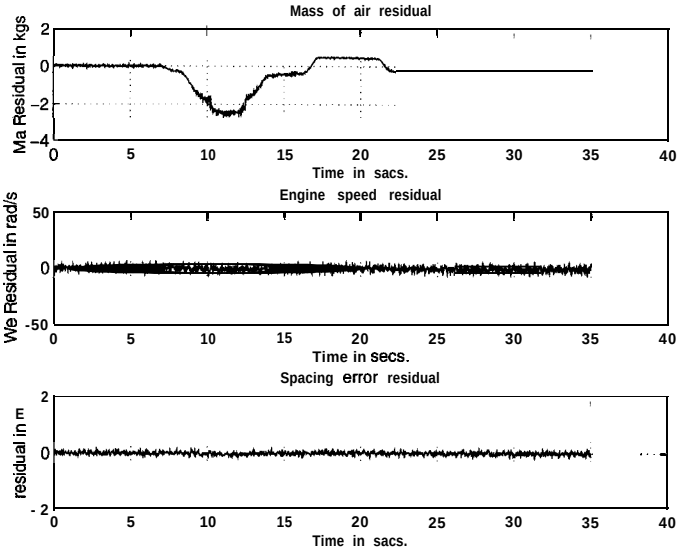

Figure 6.12: Detection filter residuals for throttle actuator fault

of the vehicle's system model. It should be noted in figure 6.13 that only the spacing error residual is affected when the v_{prev} fault occurs. Thus, there is a directional dependence of residuals on the particular kind of fault.

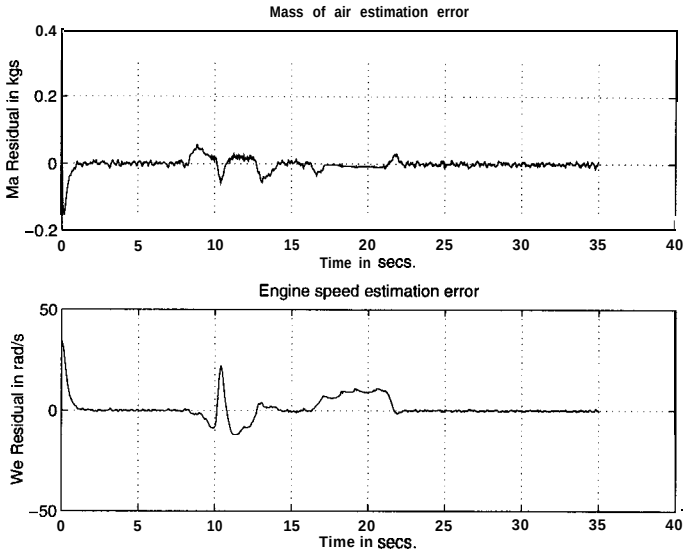

Figure 6.13: Engine speed reconstruction observer

6.11.4 Observer-Based Reconfiguration

Reconfiguration schemes can be either redundancy based or observer-based. An illustration of redundancy based method was shown earlier. Observer-based redundancy is more preferable not only because of cost, weight considerations but also because it is in closed loop form, therefore, has enhanced robustness. The observer structure just described is implemented to estimate the engine speed using only the mass of air flow rate sensor. As expected for a system with high Lipschitz constant, the observer gains tend to be high. But, high gains are not difficult to implement as it is in control problems because there is no risk of actuator saturation. High observer gain does tend to exhibit inferior performance if sensors are noisy. But, the longitudinal sensor noise characteristics as in table 6.2 do not impede the observer response much as shown in figure 6.14. The engine speed estimation error is under $20 \mathrm{rad/s}$. It must be noted that a bias in the engine speed measurement of this amount affects the spacing errors negligibly. Therefore, in case of an engine speed sensor fault, this observer can be used to reconfigure reliably.

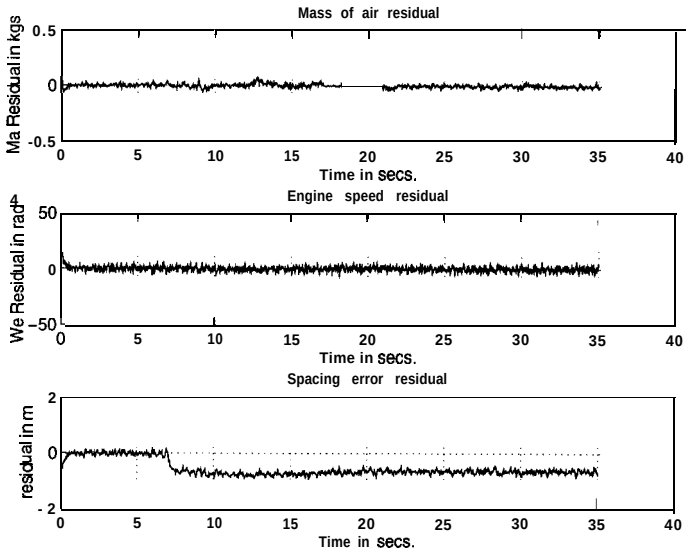

Figure 6.14: Detection filter residuals for previous vehicle speed fault

The two state model used the following observer gain matrix

$$D = \begin{bmatrix} 15 \\ -608 \end{bmatrix}$$

The gains are applied on the mass of air estimation error.

6.12 Conclusion

The emphasis of this work is towards design of a fault tolerant control system architecture for the automated highway systems problem. The contribution of this work is mostly in the area of fault detection.

Issues related to effects of sensor and actuator faults on the performance of the longitudinal vehicle platooning problem were studied. Redundancy based fault detection logic in vehicle control system was developed for sensor fault detection. Actuator fault detection was achieved by a feedback linearizing filter.

Detection filter theory was extended to the class of nonlinear systems in which nonlinearities are Lipschitz bounded. It was shown that directionality properties of the detection filters in linear systems can be ensured even in presence of Lipschitz nonlinearities in the early stages of detection as well as stability of the nonlinear observer can be guaranteed. Detection filters were designed for the longitudinal vehicle model for detecting actuator faults using a modified observer scheme.

A computationally efficient detection logic algorithm was developed. Salient features of this algorithm are on-line threshold determination ensuring a fixed false alarm rate and minimizing detection delay. This algorithm was implemented on residuals obtained from sensor redundancy relations. It can be applied to detection filter residuals also.

Observer design was extended to systems with no linear part. One of the advantages of the scheme used is that it is a fully nonlinear observer, i.e. no linear approximations are done. It can be used even when the Taylor expansion of the nonlinearities does not have a linear part. However the observer gains computed by this method can be high.

Feasibility of redundancy based and observer based state reconstruction techniques in event of sensor faults was demonstrated. Nonlinear observers were employed to estimate states in absence of the entire state information and were used as back up states in the system in case of failure of sensors.

In the vehicle platooning problem, an FDI scheme for the integrated lateral and longitudinal dynamics needs to be developed. Other issues which need to be addressed are communication protocol for degraded modes of platooning. Detection filter design for sensor faults is a straighforward extension of actuator FDI methodology but it needs to be looked into as well. Advances in FDI and observer design for nonlinear systems are contiguous. Observers for

nonlinear systems which account for modeling uncertainties and component noise are still far from established.

Chapter 7

Conclusions

In this report, a nonlinear brake controller was developed. The controller takes advantage of the operating mode of the vacuum booster present in the brake system. The controller is robust to modeling errors and input disturbances. However, it was theoretically shown and experimentally confirmed that there is a significant trade-off between tracking and passenger comfort.

Necessity of lead vehicle information is theoretically demonstrated in this report. The tradeoffs associated with different platoon schemes utilizing different communicated information are characterized in terms of string stability performance parameter and robustness to actuator lags.

The emphasis of the fault management work in this report is towards design of a fault tolerant control system architecture for the automated highway systems problem. The contribution of this work is mostly in the area of fault detection. Specifically, actuator fault detection was achieved by a feedback linearizing filter. Detection filter theory was extended to the class of nonlinear systems in which nonlinearities are Lipschitz bounded. It was shown that directionality properties of the detection filters in linear systems can be ensured even in the presence of Lipschitz nonlinearities in the early stages of detection as well as stability of the nonlinear observer can be guaranteed. Detection filters were designed for the longitudinal vehicle model for detecting actuator faults using a modified observer scheme.

A computationally efficient detection logic algorithm was developed. Salient features of this algorithm are on-line threshold determination ensuring a fixed false alarm rate and minimizing detection delay. This algorithm was implemented on residuals obtained from sensor redundancy relations. It can be

applied to detection filter residuals also.

Observer design was extended to systems with no linear part. One of the advantages of the scheme used is that it is a fully nonlinear observer, i.e. no linear approximations are done. It can be used even when the Taylor expansion of the nonlinearities does not have a linear part. The observer gains used by this method can be high.

Feasibility of redundancy based and observer based state reconstruction techniques in event of sensor faults was demonstrated. Nonlinear observers were employed to estimate states in absence of the entire state information and were used as back up states in the system in case of sensor failures.

Bibliography

[1] Bidwell, J. B., "*The* Car-Road *Complex- Theory of Traffic Flow,"* Elseveir Publishing Co., New York, 1961.

[2] Buschmann, G., Roth, M., Saalbach, K., "Tandem Master Cylinder in Change - Due to Specific Requirements of Anti-Lock and Traction Control Systems," *SAE Paper No. 930504,* 1993.

[3] Caudill, R. J., and Garrard, W. L., "Vehicle Follower Longitudinal Control for Automated Transit Vehicles," *Journal of Dynamic Systems, Measurements and Control,* Vol. 99, No. 4, December 1977, pp. 241-248.

[4] Chien, C.C., Ioannou, P., "Automatic Vehicle Following," In *Porceedings of the 1992 American Control Conference,* 1992.

[5] Chiu, A. Y., Stupp Jr., G. B., Brown Jr., S. J., "Vehicle Follower Control with Variable gains for short Headway automated guideway transit systems," *Journal of Dynamic Systems, Measurements and Control,* September 1977, pp. 183-189.

[6] Cho, D., and Hedrick, J.K., "Automotive Powertrain modelling for Control," *ASME Transactions on Dynamic Systems, Measurements and Controls, 111(4):-, December 1989.*

[7] Chu, Kai Chung "Decentralized Control of high speed vehicle strings," *Transportation Research,* pp. 361-383, June 1974.

[8] Chu, Kai Chung "Optimal Decentralized Regulation for a String of Coupled Systems, *'IEEE Transactions on Automatic* Control," June 1974, pp 243-246.

[9] Desoer, C. A., and Vidyasagar, M., *Feedback System: Input-Output Properties,* Academic Press, 1975.

[10] Fenton, R.E., Bender, J.G., " A study of automatic car following," *IEEE Transactions* on *Vehicular Technology,* Vol. VT-18, 110.3, November 1969.

[11] Fisher, D. K., "Brake System Component Dynamic Performance Measurement and Analysis," *SAE* 700373, pp. 1157-1180, 1970.

[12] Frank, A. A., Liu, S. J., and Liang, S. C., "Longitudinal Control Concepts for Automated Automobiles and Trucks operating on a Cooperative Highway," *SAE891708*, pp. 1308-1315, 1989.

[13] Garg, V., Hedrick, J. K., "Fault Detection and Control of Automated Highway Systems," Proceedings of the Winter Annual Meeting, New Orleans, 1993.

[14] Garg, V., "Fault Detection in Nonlinear Systems : An application to Automated Highway Systems," Ph. D. Dissertation, University of California, Berkeley, 1995.

[15] Garg, V., Hedrick, J. K., "Fault Detection Filters for a Class of Nonlinear Systems, " accepted for presentation at the American Control Conference, 1995.

[16] Garrard, W.L., Caudill, R. J., Kornhauser, A.L., MacKinnon, D., Brown, S.J., 'State-of-the-Art of Longitudinal Control of Automated Guideway Transit Vehicles," *High Speed Ground Transportation Journal,* Vol. 12, no.2, 1978.

[17] Gerdes, J. C., Maciuca, D. B., Devlin, P. E., and Hedrick, J. K., "Brake System Modeling for IVHS Longitudinal Control," *Advances in Robust and Nonlinear* Control, DSC-Vo1.53, pp.119-126, ASME Winter Annual Meeting, 1993.

[18] Gerdes, J.C., Brown, A.S., Hedrick, J.K., "Brake System Modeling for Vehicle Control, submitted to *1995 ASME Winter Annual Meeting.*

[19] Hall, Randolph W., "Longitudinal and Lateral Throughput on an Idealized highway," University of California, Berkeley: Institute of Transportation Studies, UCB-ITS-PRR-93-24, 1993.

[20] Hedrick, J. K., Garg, V., "Issues in Fault Tolerant Control of Automated Highway Systems," MOU-43, PATH Final Report Draft, July 1992.

[21] Hedrick, J. K., McMahon, D. H., Narendran, V. K., Swaroop, D., " Longitudinal Vehicle Controller Design for IVHS Systems," In *Proceedings of the American Control Conference,* Boston, pp. 3107-3112, 1991.

[22] Hedrick, J. K., McMahon, D. H., Swaroop, D., " Vehicle Modeling and Control for Automated Highway Systems," *California Path Report,* UCB-ITS-PRR-93-24, November 1993.

[23] Herman, Robert, and Potts, R. B., "Single-Lane *Traffic Theory* and *Experiment - Theory of Traffic Flow,* " Elsevier Publishing Co., New York, 1961.

[24] Hurtig, J.K, Yurkovich, S., Passino, K.M., Littlejohn, D., "Torque Regulation with the General Motors ABS VI Electric Brake System," in *the Proceedings of the American Control Conference,* 1994.

[25] Khan, Y., Kulkarni, P., and Youcef-Toumi, K., "Modeling, Experimentation and Simulation of a Brake Apply Systems," American Control *Conference,* pp. 226-230, 1992.

[26] Ioannou, P., Chien, C.C. and Hauser, J., " Autonomous Intelligent Cruise Control," *IVHS* America, *May* 1992.

[27] Ioannou, P., Xu, Z., " Throttle and Brake Control Systems for Automatic Vehicle Following," *IVHS Journal,* Vol. 1, No. 4, pp. 345-377, 1994.

[28] Levine, J., and Athans, M., " On the optimal error regulation of a string of moving vehicles," *IEEE Transactions of Automatic Control,* Vol. 11, Nov. 1966, pp. 355-361.

[29] Peppard, Lloyd E., " String Stability of Relative motion PID vehicle control systems," *IEEE Transactions on Automatic Control,* Vol. 19-3:6, pp.529-531, Oct. 1974.

[30] Maciuca, D.B., Gerdes, J.C., Hedrick, J.K., "Automatic Braking Control for IVHS," *Proceedings of the International Symposium on Vehicle Control,"* 1994.

[31] McMahon, D.H., "Robust Nonlinear Control of Uncertain Systems : An Application to Intelligent Vehicle Highway Systems (IVHS)," *Ph. D Dissertation,* Vehicle Dynamics Lab., U. C. Berkeley, May 1994.

[32] McMahon, D.H., Hedrick, J.K., Shladover, S.E., "Vehicle Modelling and Control for Automated Highway Systems," In *Proceedings of the 1990 American Control Conference, San Diego, CA.*

[33] McMahon, D. H., Narendran, V. K., Swaroop, D., Hedrick, J. K., Chang, K. S., Devlin, P. E., "Longitudinal Vehicle Controllers for IVHS : Theory and Experiment ," In *Proceedings of the American Control* Conference, pp. 1753-1757, 1992.

[34] Mohanty, N., 'Signal Processing - Signals, Filtering and Detection," Van Nostrand Reinhold Company, 1987.

[35] Motor Auto Repair Manual, Volumes 1 and 2, 55th Edition, 1991.

[36] Motor Imported Car Repair Manual, Volumes 1 and 2, 13th Edition, 1991.

[37] Nash, Roscoe, "Brake Integrated Hydraulic Actuation System Master Cylinder, *SAE Paper No. 830412,* 1983.

[38] Perronne, J.-M., Renner, M., Gissinger, G.L.,"Dynamic Aspects of a Calliper Brake System," *Proceedings of the International Symposium on Vehicle Control,"* 1994.

[39] Puhn, F., *"Brake Handbook,"* Price Stern Sloan Inc., Los Angeles, CA 1985.

[40] Radlinski, R.W., "The Effect of Aftermarket Linings on Light Vehicle Braking Performance," U. S. Department of Transportation, NHTSA, Final Report, DOT HS 807 835, July 1991.

[41] Ren, W., Green, D., "Continuous Platooning: A New Evolutionary and Operating Concept for Automated Highway Systems", In *Proceedings of the American Control Control Conference,* Vol.1, July 1994, pp. 21-25.

[42] Rizzuti, C.D., Swaroop, Hedrick, J.K., " Effect of Sampling on String Stability of vehicle platoons," *Working paper,* Vehicle Dynamics Lab, September 1994.

[43] Raghavan, S., "Observers and Compensators for Nonlinear systems, with application to flexible joint robots," Ph. D. Dissertation, University of California, Berkeley, 1992.

[44] Sheikholeslam, S., and Desoer, C. A., "Longitudinal Control of a platoon of a platoon of vehicles,", In *Proceedings of the American Control Conference,* Vol. 1, May 1990, pp. 291-297.

[45] Shladover, S. E., " Vehicle Follower control for dynamic entrainment of Automated Guideway Transit Vehicles," *Transactions of ASME,* Vol. 101, pp. 313-320, December 1979.

[46] Shladover, S. E., "Longitudinal control of automotive vehicles in close-vehicle formation platoons," *Transportation Research,* Vol. 14A, No.2, pp. 63-81, April 1980.

[47] Slotine, J-J. E., Li, W., *"Applied Nonlinear Control,* Prentice-Hall, Inc., Englewood Cliffs, NJ, 1991.

[48] Slotine, J-J, E., Sastry, S. S., "Tracking Control of Nonlinear Systems Using Sliding Surfaces with Applications to Robot Manipulators," *In*ternational *Journal of Control,* 39,2, 1982.

[49] Swaroop, D. "String Stability of Interconnected Systems- An Application to Automated Highway Systems," Ph. D. Dissertation, University of California at Berkeley, December 1994.

[50] Swaroop, D., Hedrick, J.K., "Direct Adaptive Longitudinal Control of Vehicle Platoons," presented at *the* Conference *on Decision and Control,* Orlando, Dec. 1994.

[51] Swaroop, D., Hedrick, J.K, Chien, C.C., Ioannou, P. " A Comparison of Spacing and Headway Control Strategy for Automatically Controlled Vehicles," submitted to *Vehicle System Dynamics Journal.*

[52] Swaroop, D., Rizzuti, C. D., and Hedrick, J. K., "Limitations of Alternative Platoon Control Strategies," presented at *the ASME* Winter *Annual Meeting,* Chicago, Nov. 1994.

[53] Varaiya, P. P., " Smart Vehicles on Smart Roads - Problems of Control ," *IEEE Transactions on Automatic Control,* Vol. 38, No. 2, February 1993.

[54] Vidyasagar, M., and Vanelli, A., "New Relationships between Input-Output and Lyapunov Stability," *IEEE Transactions on Automatic Control,* Vol. 27, No.2, April 1982, pp. 481-483.

[55] White, J. E., Speyer, J. L., " Detection Filter Design : Spectral theory and algorithms," *IEEE Transactions on Automatic Control,* pp. 593-603, Vol. AC-32, No. 7, July 1987.

[56] Wong, J. Y., "Ground Vehicle Dynamics," *John Wiley* and sons, 1979.